MULTIWAVELENGTH OBSERVATIONS OF THE BLACK HOLE CANDIDATE 1E 1740.7-2942

Thesis by

William Adams Heindl

In Partial Fulfillment of the Requirements

for the Degree of

Doctor of Philosophy

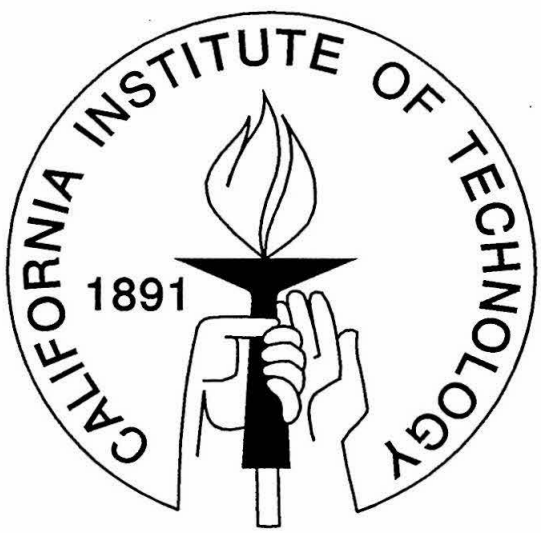

California Institute of Technology

Pasadena, California

1994

(Submitted February 8, 1994)

Acknowledgements

Many heartfelt thanks to all of you who have made contributions to this thesis, either directly or indirectly. I wish to express special gratitude to the following people, whose help in various forms has been particularly important to me.

Thank you, Tom, for being a truly thoughtful advisor. You and Charlene have been good friends through these last six and a half years, both the good ones and the bad ones.

John, thanks for the good advice, the unflagging support, and the airplane rides. I hope your career as an astronaut brings you all you hope for.

Steve and Rick, you made GRIP work and taught me an awful lot about doing science that I will use for the rest of my life. Thank you.

The rest of you GRIPPERS who've made the whole thing fly. David, Chris, Jeff, Jill, Dan, and Jim.

Doug and Andrea, we got each other through those first few years, and our friendships have continued to support me through the rest. I'm the last, but we've finally all made it. I wish you both success in all that you attempt.

Brad, thanks for showing me Neptune's Net and the rest of Southern California that's not Caltech! I plan to hike Mt. Langley on your birthday for many years to come, so you'd better keep in shape.

Stinson and the other Otters, including the Master of Heat, Cold, and Sound. A guy could have worse office mates. Thanks for the company, the conversations, and the general zaniness in Downs 219 since 1987.

RanCosmo, I'm sure I would have made it through to the end without those all important breaks at the malt shop, but it wouldn't have been much fun. I wish you each a speedy exit.

PDR and HMQ — Thanks for the grub. Remember Erice! (Don't worry, I won't let you forget.) By the way, I let you win that darts game, and you need to eat more limes.

Fiona, Julia would be proud. Don't stress (excessively, anyway).

Louise, Debby, Sharon, Deeby, and Donna without you I never would have flown to the right cities, had hotels to stay in, submitted proposals on time, nor navigated the Caltech administration successfully. All your help is much appreciated.

The NASA Graduate Student Researchers Program for feeding me and paying me to study such fascinating stuff. This work has been partially supported by NASA grants NGT-50804 and NAGW-1919.

Mom, Dad, Jo, Ray, Dan, Auntie, and the Ottawa gang. I didn't pick you, but I couldn't have done better if I had a choice. Thanks for making this a wonderful life!

Abstract

Observations of the Galactic center region black hole candidate 1E 1740.7–2942 have been carried out using the Caltech Gamma-Ray Imaging Payload (GRIP), the *Röntgensatellit* (*ROSAT*) and the Very Large Array (VLA). These multiwavelength observations have helped to establish the association between a bright emitter of hard X–rays and soft γ-rays, the compact core of a double radio jet source, and the X–ray source, 1E 1740.7–2942. They have also provided information on the X–ray and hard X–ray spectrum.

The Galactic center region was observed by GRIP during balloon flights from Alice Springs, NT, Australia on 1988 April 12 and 1989 April 3. These observations revealed that 1E 1740.7–2942 was the strongest source of hard X–rays within $\sim 10^\circ$ of the Galactic center. The source spectrum from each flight is well fit by a single power law in the energy range 35–200 keV. The best-fit photon indices and 100 keV normalizations are: $\gamma = (2.05 \pm 0.15)$ and $K_{100} = (8.5 \pm 0.5) \times 10^{-5}\,\mathrm{cm^{-2}\,s^{-1}\,keV^{-1}}$ and $\gamma = (2.2 \pm 0.3)$ and $K_{100} = (7.0 \pm 0.7) \times 10^{-5}\,\mathrm{cm^{-2}\,s^{-1}\,keV^{-1}}$ for the 1988 and 1989 observations respectively. No flux above 200 keV was detected during either observation. These values are consistent with a constant spectrum and indicate that 1E 1740.7–2942 was in its normal hard X–ray emission state. A search on one hour time scales showed no evidence for variability.

The *ROSAT* HRI observed 1E 1740.7–2942 during the period 1991 March 20–24. An improved source location has been derived from this observation. The best fit coordinates (J2000) are: Right Ascension = $17^h43^m54^s.9$, Declination = $-29^\circ44'45''.3$, with a 90% confidence error circle of radius $8''.5$. The PSPC observation was split between periods from 1992 September 28 – October 4 and 1993 March 23–28. A thermal bremsstrahlung model fit to the data yields a column density of $N_H = 1.12^{+1.51}_{-0.18} \times 10^{23}$ cm^{-2}, consistent with earlier X–ray measurements.

We observed the region of the *Einstein* IPC error circle for 1E 1740.7–2942 with the VLA at 1.5 and 4.9 GHz on 1989 March 2. The 4.9 GHz observation revealed two sources. Source 'A', which is the core of a double aligned radio jet source (Mirabel

et al. 1992), lies within our *ROSAT* error circle, further strengthening its identification with 1E 1740.7–2942.

Contents

List of Figures

List of Tables

Chapter 1

Introduction

The mid-1960s saw the first flights of balloon-borne hard X–ray[1] telescopes and with them, the first detection of hard X–rays from the direction of the Galactic center region. From that time to the present, the Galactic center has been one of the most frequent targets of high energy observations. One motivation for this has been a search for hard emission from the Galactic nucleus which could indicate the presence of a massive black hole like those seen in distant active galactic nuclei. While a few sources were identified by these early efforts, the rather coarse angular resolutions of the instruments made it impossible to derive a clear picture of the region and answer whether there was in fact a source of hard X–rays and γ-rays at the center of the Milky Way.

This remained the case until the mid-1980s when a new type of hard X–ray telescope was developed and came into use. With degree or better spatial resolution, very good flux sensitivity, and energy resolution similar to previous scintillator-based experiments, coded-aperture telescopes have painted an entirely new picture of the central portion of the Milky Way. Rather than speculating about contributions to spectra and light curves of a field that includes multiple, unresolved point sources,

[1] I will refer to photons with energies above ~10–20 keV as "hard X–rays" or "soft γ-rays." X–rays or "soft X–rays" have energies below this range. The distinction is made largely on the basis of the observational techniques used as opposed to the physical processes at the source: soft X–rays may still be collected using grazing incidence mirrors, while hard X–rays can no longer be practically focussed.

we can now make specific studies about the several variable sources of hard emission that populate the sky in the central 100 square degrees of the Galactic center. Thus, for the first time, we are capable of determining whether a powerful γ-ray source lies at the Galactic center.

This dissertation discusses one of the first of these telescopes sensitive to energies above 30 keV, the Caltech Gamma-Ray Imaging Payload (GRIP), and its identification and characterization of the brightest of the Galactic center sources, 1E 1740.7–2942. It also describes observations made at X–ray energies from 0.5 to 2.5 keV and at radio wavelengths undertaken as part of a multiwavelength campaign aimed at discovering the nature of this unique source.

The following sections recount some of the important instruments and observations that have led to the current state of understanding of the high energy emission from the Galactic center region. They are intended as perspective for the observations and analyses described in the body of this dissertation, not as a comprehensive history of the field.

1.1 The First Hard X-Ray Observations

Groups from the University of California, San Diego (UCSD) (Peterson *et al.* 1968), the Massachusetts Institute of Technology (MIT) (Clark, Lewin, and Smith 1968), the NASA Goddard Space Flight Center and the University of Maryland (GSFC/UM) (Riegler, Boldt, and Serlemitsos 1968), the University of New Hampshire (UNH) (Guo, Webber, and Damle 1973), Rice University (Haymes *et al.* 1968), and the University of Adelaide (Buselli *et al.* 1968) began observing the sky at energies above 10 keV as early as 1965. Their efforts followed the success of Geiger and proportional counters carried on sounding rockets which opened an observational window at energies up to $\sim$10 keV (see, for example, Friedman, Byram, and Chubb, 1967), and revealed a sky rich with previously unknown sources. The Galactic center region in particular contains well over twenty X–ray sources within a 10° radius (Trümper 1992).

The new hard X–ray instruments employed inorganic scintillation detec-

tors such as sodium iodide doped with thallium (NaI(Tl)) to detect hard X–rays during balloon flights at altitudes as great as 150,000 feet. In order to reduce atmospheric and internal backgrounds, the primary detectors were shielded either actively (by additional scintillators in anticoincidence) or passively. The fields of view (FOVs) were large, typically $\gtrsim 10°$ full width at half maximum (FWHM). With no innate imaging capabilities, these instruments simply summed the emission from all sources within the FOV. In order to achieve some spatial resolution, the UCSD, MIT, GSFC/UM, UNH, and Adelaide instruments employed a scanning technique. The MIT and GSFC/UM detectors were continuously rotated in azimuth at fixed elevation and the UNH instrument panned back and forth in azimuth, again at fixed elevation. The UCSD and Adelaide instruments were maintained at a fixed pointing direction while the sky moved through the FOV. The effect of these techniques is to provide temporal modulation of the detected flux as sources pass in and out of the FOV. Each scan therefore provides some information on the source distribution along the scan axis. The Rice instrument, having the widest FOV (24° FWHM), alternated source-on and source-off measurements for the purpose of background subtraction, rather than implementing a scanning technique.

The MIT, GSFC/UM, UNH, Rice, and Adelaide instruments looked in the direction of the Galactic center region, and all detected hard X–ray emission. However, their wide fields of view prevented firm identifications with sources known from soft X–ray observations. The spectrum of hard photons from the region was seen to be consistent with a power law ($dN/dE = K \times E^{-\gamma}\,\mathrm{cm}^{-2}\,\mathrm{s}^{-1}\,\mathrm{keV}^{-1}$) with a photon index, γ, between 2 and 3. The normalization varied by a factor of as much as 4 between measurements, suggesting variability of a source or sources in the region. In addition to power law emission, the Rice instrument detected a spectral feature near 500 keV during two balloon flights (Johnson, Harnden, and Haymes 1972; Haymes *et al.* 1975) which would prove to be the first γ-ray spectral line from a celestial source (see §1.4).

In 1970, the MIT group flew the first instrument capable of localizing sources at the degree level. This instrument featured an asymmetrically collimated FOV — a slit $1°.5 \times 13°$ FWHM. Scans perpendicular to the long axis of the slit placed sources

to better than $\sim 1^\circ$ in one axis. A pair of crossed scans would place the source in both axes. Using this method, the MIT instrument discovered the X–ray pulsar GX1+4 and identified it with a known soft X–ray source, 3U 1728-24 (Lewin, Ricker, and McClintock 1971; Ricker *et al.* 1976) 5 degrees from the Galactic center. No source was detected at the Galactic nucleus. In 1972 April, a second balloon flight of the same instrument detected GX1+4 during a single scan (Ricker *et al.* 1976). Its hard X–ray flux had increased by more than a factor of 3 above the 1970 observation to a level of $\sim 8 \times 10^{-4}$ $\mathrm{cm^{-2}\,s^{-1}\,keV^{-1}}$ at 50 keV. This sort of strong variability is now known to be a property of all the Galactic center hard X–ray sources, a fact that makes nonimaging observations especially problematic.

1.2 Hard X-Rays from the Galactic Center?

The next set of instruments to make important contributions to our picture of the Galactic center region did not have the resolving power of the MIT slit scanner, but benefited from either a large collecting area or satellite platforms from which to make their observations. In 1975, the *Ariel 5* satellite's scintillation telescope observed hard emission from the Galactic center region during an observation spanning 3 days. Although scans with its 8° FWHM aperture could not locate sources precisely, Coe *et al.* (1981) suggested that GX3+1 and a source at the Galactic center were active during this time and that the Galactic center source was responsible for $\sim 50\%$ of the high energy emission. They found that their data above 60 keV, where they felt the Galactic center source was dominant, were well fit by a power law with a photon index of $\gamma = 1.6 \pm 1.0$.

In November 1977, a group from the Naval Research Laboratory (NRL) flew a balloon-borne γ-ray telescope with a collecting area of 765 $\mathrm{cm^2}$— more than 10 times larger than most earlier instruments (Knight *et al.* 1985). This telescope's pointing system also gave it the ability to scan both along and perpendicular to the Galactic plane. Even with a 5° FWHM aperture, the instrument detected 5 sources associated with objects known from 2–10 keV observations. One of these sources, A1742-294, lies within $0^\circ.5$ of the Galactic nucleus. However, the statistics of the fit

were also consistent with an origin at the Galactic center. Knight *et al.* (1985) find a photon index of 1.88 ± 0.43 and a strength of $\sim 6 \times 10^{-5}$ $\mathrm{cm^{-2}\,s^{-1}\,keV^{-1}}$ at 100 keV for the hard emission.

The *OSO-8* (Orbiting Solar Observatory 8) also detected a source consistent with the Galactic nucleus during scans through the region a year later in 1978 September (Dennis *et al.* 1980). The γ-ray detector on *OSO-8* consisted of a 5° FWHM field of view scintillation telescope aligned 5° from the spacecraft spin axis. With the spacecraft spin axis pointing at Galactic coordinates, $l \sim 5°$and $b \sim 1°$, the telescope scanned through the Galactic center region every 10s during the 5 day observation. Fits to the counting rate as a function of scan angle required two sources—one consistent with the location of GX1+4, and a second near the Galactic nucleus. Figure 1.1 shows the 95% confidence contour for the position of the hard source together with the error region from the NRL balloon observation. Counting rates in four energy bands clearly showed that the near Galactic center source had a much harder spectrum than the X–ray pulsar GX1+4. A spectral fit assuming a source at the best fit location found a photon index, $\gamma = 2.3 \pm 0.3$ and flux density at 100 keV of $\sim 1 \times 10^{-4}\,\mathrm{cm^{-2}\,s^{-1}\,keV^{-1}}$, in reasonable agreement with the NRL result.

The UCSD/MIT instrument on board the first *High Energy Astronomy Observatory* (the *HEAO-1* satellite) made the last set of observations with fine enough collimation to provide useful information on the source distribution in the Galactic center region before the advent of true imaging at hard X–ray and γ-ray energies. The *HEAO-1* A4 instrument (Matteson 1978; Bradt, Ohashi, and Pounds 1992) consisted of two scintillation detectors with narrowly collimated ($1°.5 \times 20°$) fields of view. The spacecraft rotated with a 30 minute period on an axis along the Earth-Sun line. Thus, the field of view of the instruments scanned great circles 90° from the Sun, covering the whole sky every six months. *HEAO-1* observed the Galactic center in 1978 September and March and 1979 September (Levine *et al.* 1984; Matteson 1982). More than 10 sources appeared in the scans. Most of these were identified with sources known in the 1 – 10 keV band. However, the detections included a source within $\sim 0°.5$ of the Galactic center. The three observations found that this was the hardest source in the region, with photon indices of 2.1, 2.6, and 2.1. Its strength varied by

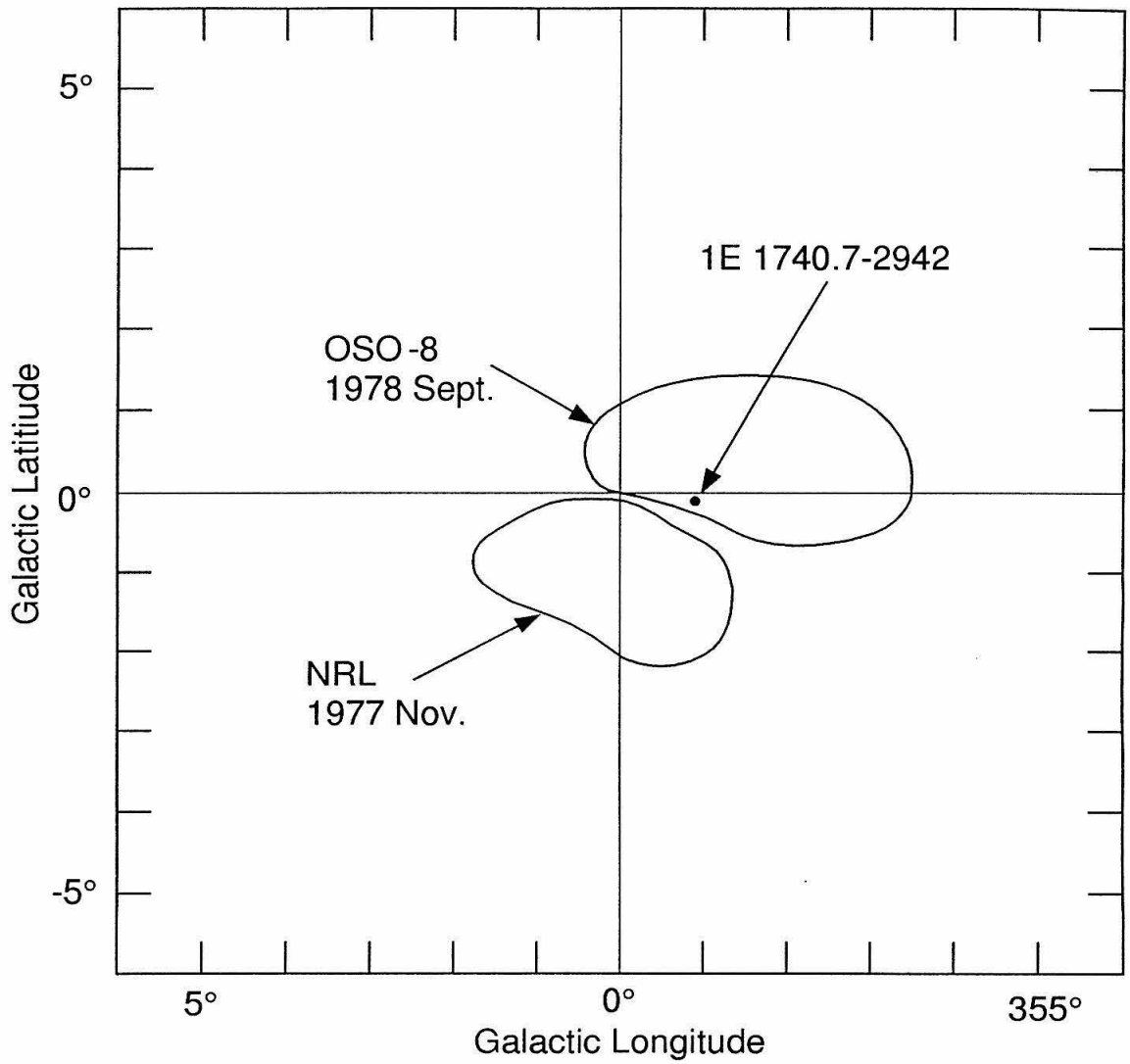

Figure 1.1: Error regions (95% confidence) for the near Galactic center hard X–ray source(s) from the NRL balloon experiment (Knight *et al.* 1985) and the *OSO-8* satellite (Dennis *et al.* 1980). Also shown is the position of 1E 1740.7–2942, which was likely the source detected by these observations.

as much as a factor of 3 on six month time scales, ranging from from $\sim 7 \times 10^{-5}$ to $\sim 2 \times 10^{-4}$ $\mathrm{cm^{-2}\,s^{-1}\,keV^{-1}}$ at 100 keV.

The NRL, *OSO-8*, and *HEAO-1* observations seemed to indicate the presence of a strong source of hard X–rays at the Galactic center. The source was even named "GCX" after the diffuse Galactic center X–ray source. Because of its unique nature in the region, its high luminosity (which is similar to Cyg X-1 assuming a distance of 10 kpc), and the fact that black hole powered active galaxies show hard emission, it was thought that this was perhaps a black hole at the center of the Milky Way. We will see in the next section, however, that these observations were consistent with emission from 1E 1740.7–2942, located $\sim 0°.8$ from the Galactic center.

1.3 Hard X-Ray Images of the Galactic Center

In 1985, the first true hard X–ray images of the Galactic center were obtained by the coded-aperture telescope on the Spacelab 2 mission (Skinner *et al.* 1987). A coded-aperture telescope works on the same principle as a pinhole camera, but uses many holes to increase throughput of source photons. The overlapping images detected by a position sensitive photon detector are then unfolded using mathematical techniques. For a more in depth discussion, see §2.1.1. Spacelab 2 was a free flying instrument released from the space shuttle for observations and then retrieved and returned to Earth. Its images spanned an energy range from 2.5–32.5 keV with angular resolutions of $12'$ and $3'$ corresponding to the two independent telescopes carried. Figure 1.2 shows images in four energy bands of the central 40 square degrees of the Galaxy. The low energy images are consistent with earlier high resolution images from the *Einstein* X–ray observatory. They show a complex of sources within $1°$ of the Galactic center, including a source coincident with the Galactic nucleus compact radio source, Sgr A*. However, due to the soft spectra of most of the sources, only two are detected at energies above 20 keV: A1742-294 and 1E 1740.7–2942, with 1E 1740.7–2942 the much brighter of the two. This led Skinner *et al.* (1987) to suggest that 1E 1740.7–2942 was the most likely source of the near Galactic center hard emission seen by *Ariel 5*, the NRL balloon telescope, *HEAO-1* and other wide

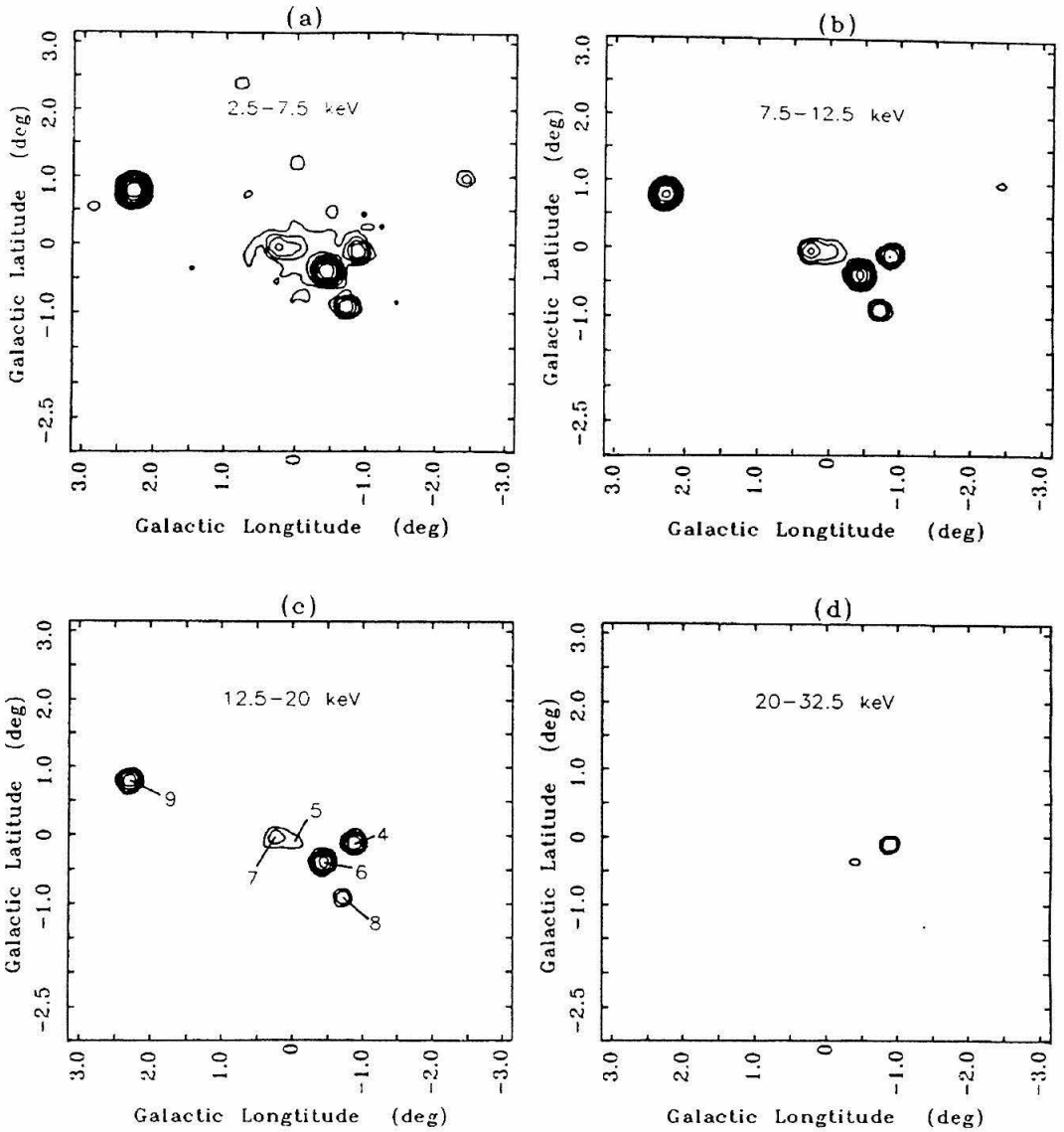

Figure 1.2: Spacelab 2 images of the Galactic center region in four energy bands from Skinner *et al.* (1989). While the region is crowded at low energies, only A1742-294 and 1E 1740.7–2942 are visible above 20 keV. Labeled sources are: (4) 1E 1740.7–2942, (5) Sgr A*, (6) A1742-294, (7) 1E1743.1-2843, (8) SLX1744-299 and SLX1744-300, and (9) GX3+1.

FOV instruments.

Three years later, in 1988 April, Caltech's GRIP telescope flew from Alice Springs, Northern Territory, Australia. Also a coded-aperture instrument, GRIP has a 5 cm thick NaI(Tl) detector which achieves sensitivity in an energy range extending from 30 keV to 10 MeV (Althouse *et al.* 1985). GRIP is described in Chapter 2. Our observation revealed a single bright source of hard X–rays located $\sim 0°.8$ from the Galactic nucleus (see Figure 1.3) (Cook *et al.* 1991a; Cook *et al.* 1991b). The position of this source was shown to be consistent with 1E 1740.7–2942 and only marginally consistent with any other source detected by Skinner *et al.* (1987). A comparison of the GRIP and Spacelab 2 spectra showed that the > 30 keV flux matched well with the lower energy emission, further confirming the association of the hard X–ray source with 1E 1740.7–2942. From these data, we measured a power law spectrum with a photon index of $\gamma = 2.05 \pm 0.15$ and a strength at 100 keV of $(8.5 \pm 0.5) \times 10^{-5}$ $\mathrm{cm^{-2}\,s^{-1}\,keV^{-1}}$, in reasonable agreement with the earlier nonimaging results.

1.4 Positron Annihilation Radiation

A second puzzle regarding the Galactic center has in some ways paralleled the mystery of the source of hard continuum emission. This puzzle, however, has yet to be solved. During balloon flights in 1970, 1971, and 1974, the Rice γ-ray spectrometer observed a line in the Galactic center spectrum near 500 keV (Johnson, Harnden, and Haymes 1972; Johnson and Haymes 1973; Haymes *et al.* 1975). The line was interpreted as most likely due to the annihilation of positron-electron pairs which produces characteristic 511 keV γ-rays. However, the line appeared red-shifted in the first two flights and blue-shifted in the third. The apparent red-shift may have been caused by three photon ortho-positronium annihilation continuum included in the line flux due to the energy resolution of the instrument (Leventhal 1973). An asymmetric line profile in the last observation led the authors to suggest that the true line energy was 511 keV (Haymes *et al.* 1975). In 1977, a group from Bell Laboratories and Sandia National Laboratory flew a high resolution germanium telescope which showed that the feature was indeed a narrow line at 510.7 ± 0.5 keV — the result of

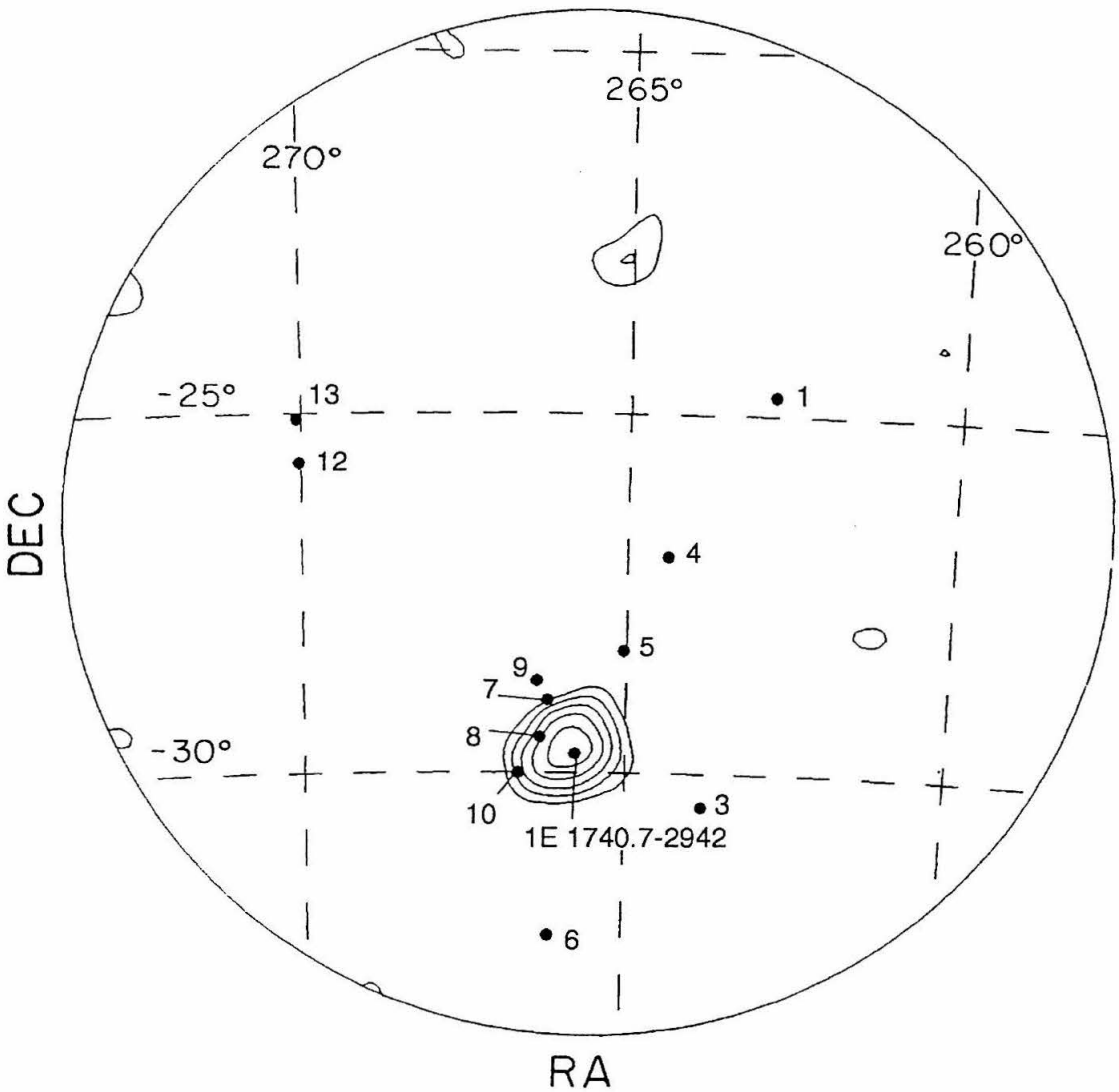

Figure 1.3: From Cook *et al.* (1991a). Image of the Galactic center region in the 35-200 keV energy band from one hour of the GRIP 1988 observation. The single hard X-ray source detected was shown to be 1E 1740.7–2942. Other hard X-ray sources are numbered as in Figure 4.1.

positron annihilation (Leventhal, MacCallum, and Stang 1978). The strength of the line was $\sim 1.2 \times 10^{-3}$ cm^{-2}s^{-1}.

Interest in the line grew enormously when an observation in spring 1980 with the germanium spectrometer on the *HEAO-3* satellite detected a factor of three decrease in the line strength (from $(1.85 \pm 0.21) \times 10^{-3}$ to $(0.65 \pm 0.27) \times 10^{-3}$ cm^{-2}s^{-1}) compared to the fall 1979 measurement which had been consistent with the Bell/Sandia measurement (Riegler *et al.* 1981). This variability implied a source region of less than 0.5 light years and was possible evidence for a massive black hole at the Galactic center. These data have since been reanalyzed and the significance of the variation reduced (Mahoney 1988). However, further high resolution observations by the Bell/Sandia group and others failed to detect the annihilation line through 1985, suggesting that the decrease was real (Leventhal *et al.* 1982; Leventhal *et al.* 1986; Paciesas *et al.* 1982). During this period and continuing to the present, the NaI γ-ray spectrometer on the *Solar Maximum Mission* annually observed the region and consistently detected the annihilation line at a level of $\sim 2 \times 10^{-3}$ cm^{-2}s^{-1}. (Share *et al.* 1988). The rather high value seen by this wide FOV (130° FWHM) instrument while narrower aperture instruments detected no emission suggests that there is a distributed source of 511 keV radiation.

Since 1988, the new, more sensitive balloon-borne germanium telescopes GRIS, from the GSFC, and HEXAGONE, from the UCSD/France collaboration, as well as the Oriented Scintillation Spectrometer Experiment (OSSE) on the *Compton Gamma-Ray Observatory* (*CGRO*) have again detected the annihilation line (Tueller 1993 and references therein). The germanium spectrometers with fields of view of $\sim 20°$ detected flux at a level of $\sim 1 \times 10^{-3}$ cm^{-2}s^{-1}, while OSSE, with a $4° \times 11°$ FOV, sees a lower level of $(2.5 \pm 0.3) \times 10^{-4}$ cm^{-2}s^{-1} (Purcell *et al.* 1993). This dependence of the flux on the FOV further indication of a distributed source along the Galactic plane. These instruments have yet to confirm time variability.

The best fit models to all the observations now require a compact source to provide variability, as well as a distributed source to explain the observed dependence on FOV. It is the compact source which may eventually be identified by a coded-aperture telescope. In fact, a strong candidate has already been identi-

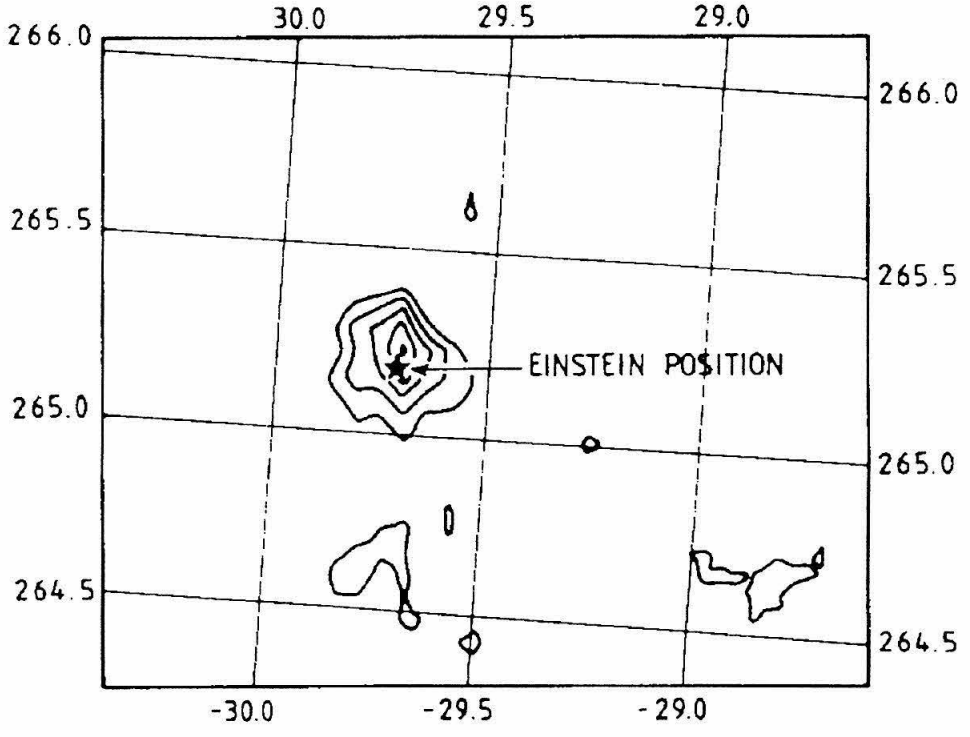

Figure 1.4: From Bouchet *et al.* (1991). SIGMA image of the Galactic center region from 330-570 keV on 1990 October 13–14. The star indicates the *Einstein* position of 1E 1740.7–2942. This outburst, which lasted between 18 and 70 hr is suggestive that 1E 1740.7–2942 is a source of positron annihilation radiation.

fied: 1E 1740.7–2942. In 1990 October, SIGMA, the coded-aperture telescope on the *GRANAT* observatory, detected an outburst of emission from 1E 1740.7–2942 between 200 – 600 keV (see Figure 1.4). This spectral "hump" has been interpreted as the emission from positron annihilations in a hot plasma. While no narrow 511 keV line was detected in this episode, 1E 1740.7–2942 is now a prime candidate for a source of positrons which may escape to annihilate in the interstellar medium, producing the variable component to the Galactic center 511 keV emission.

After twenty years of nonimaging hard X–ray observations, coded-aperture

telescopes have answered one of the most important questions about our galaxy: Is the nucleus of the Milky Way a persistent strong source of hard X–ray and soft γ-ray emission? The answer is, "No." In so doing, however, they have identified a new and exciting high energy source and touched off a flurry of observations intended to discover the nature of this powerful emitter of hard X–rays and γ-rays. Observations of 1E 1740.7–2942 have also provided a major clue (or perhaps red herring?) in the longstanding mystery of the Galactic 511 keV emission.

1.5 The Structure of this Dissertation

The background presented here has demonstrated the importance of the imaging capabilities provided by coded-aperture telescopes for the Galactic center and any other crowded region of the hard X–ray sky. It has also provided a setting for the studies of 1E 1740.7–2942 which are described in the body of this thesis. The rest of this dissertation details the analysis of the observations of 1E 1740.7–2942 performed with the GRIP telescope in 1988 April and 1989 April, taking as a starting point the hard X–ray identification of 1E 1740.7–2942. It also describes X–ray observations made with *ROSAT* and radio observations made at the Very Large Array which have played an important role in extending our understanding of this very interesting source.

This dissertation is built around three papers which have been published or accepted for publication in *The Astrophysical Journal.* They appear here unmodified except in typesetting. The figures and tables have been renumbered to conform to the overall document scheme and the bibliographies have been incorporated in the overall thesis bibliography. Chapters 3 and 4 are in depth discussions and analyses of the GRIP observations, and Chapter 5 covers the *ROSAT* and VLA observations and results. Chapter 3 appeared originally as a *Letter* in *The Astrophysical Journal* (Cook *et al.* 1991b). This paper marks the beginning of my study of the Galactic center region in general and 1E 1740.7–2942 in particular. In 1993, Chapter 4 appeared as a paper in *The Astrophysical Journal* (Heindl *et al.* 1993). Finally, Chapter 5 will appear in *The Astrophysical Journal* in 1994 August (Heindl, Prince, and Grunsfeld

1994).

The remainder of the chapters fill in details to supplement the published chapters. Chapter 2 provides a description of the coded-aperture technique and its application in the GRIP telescope as well as the observations made of the Galactic center region. Chapter 6 updates the high energy observations of 1E 1740.7–2942 made by SIGMA since the 1989 GRIP flight. Chapter 7 summarizes the results of searches for a companion at optical and infrared wavelengths. Chapter 8 contains the conclusions of this work.

Chapter 2

Gamma-Ray Instrumentation and Observations

The γ-ray observations of 1E 1740.7–2942, performed with the Caltech Gamma-Ray Imaging Payload (GRIP) form the central focus of this dissertation. GRIP is described briefly here, and other brief descriptions are included in Chapters 3 and 4, as part of works which previously appeared in *The Astrophysical Journal* and *The Astrophysical Journal Letters*. This chapter is intentionally terse, because my main involvement with GRIP has been in its use as an astronomical observatory, rather than in the development of the instrument itself. Also, GRIP has been described in the literature (Althouse *et al.* 1985) and extensively in two previous theses (Finger 1987; Palmer 1992). I did, however, participate in the 1989 field campaign which obtained the data discussed in Chapter 4. I have also been heavily involved in the development of the new detector system which has been built for the second generation GRIP telescope, GRIP-2 (see Chapter 8).

In addition to the hard X–ray and γ-ray observations, we observed 1E 1740.7–2942 at X–ray and radio wavelengths using the *Röntgensatellit* (*ROSAT*) (Trümper 1984) and the Very Large Array (VLA) (Bridle 1986) respectively. These observations are detailed in Chapter 5.

2.1 GRIP

GRIP is a balloon-borne γ-ray telescope which forms images and spectra in the energy range 30 keV – 10 MeV. GRIP uses the coded-aperture technique to produce sky maps at energies where mirrors and lenses are no longer effective. For complete discussions of the technique, the GRIP instrument, and its performance, see Skinner (1984), Althouse *et al.* (1985), Finger (1987), and Palmer (1992).

2.1.1 The Coded-Aperture Technique

A coded-aperture telescope requires two primary components: a "mask" and a position sensitive photon detector. The mask is a pattern of opaque and transparent regions which spatially modulates the sky flux incident on the photon detector. Each source in the field of view casts a γ-ray shadow of the mask pattern on the detector. Providing that this pattern is well chosen, the detected shadow can be deconvolved to form a sky image. A set of optimal patterns for γ-ray astronomy are those built on skew Hadamard uniformly redundant arrays (URAs) (Finger and Prince 1985). Two properties of URAs make them well suited to coded-aperture imaging. First, apart from effects due to finite cell sizes, their auto-correlation functions are a constant baseline with a single narrow peak. This is the "uniformly redundant" feature, and it guarantees that deconvolving the shadow pattern produces a unique sky map without artifacts. Second, these URAs are nearly half open and half closed. At any time, half the detector measures source plus background flux, while the other half measures background alone. This is statistically optimal for γ-ray astronomy, which is strongly background dominated for nearly all sources.

2.1.2 The Detector System

Figure 2.1 shows the elements of the imaging system and Table 2.1 lists its important parameters. The primary detector is a 41 cm diameter, 5 cm thick NaI(Tl) disk. Scintillation photons are detected by nineteen 3″ photomultiplier tubes (PMTs) which are optically coupled to a glass window at the rear of the detector. A

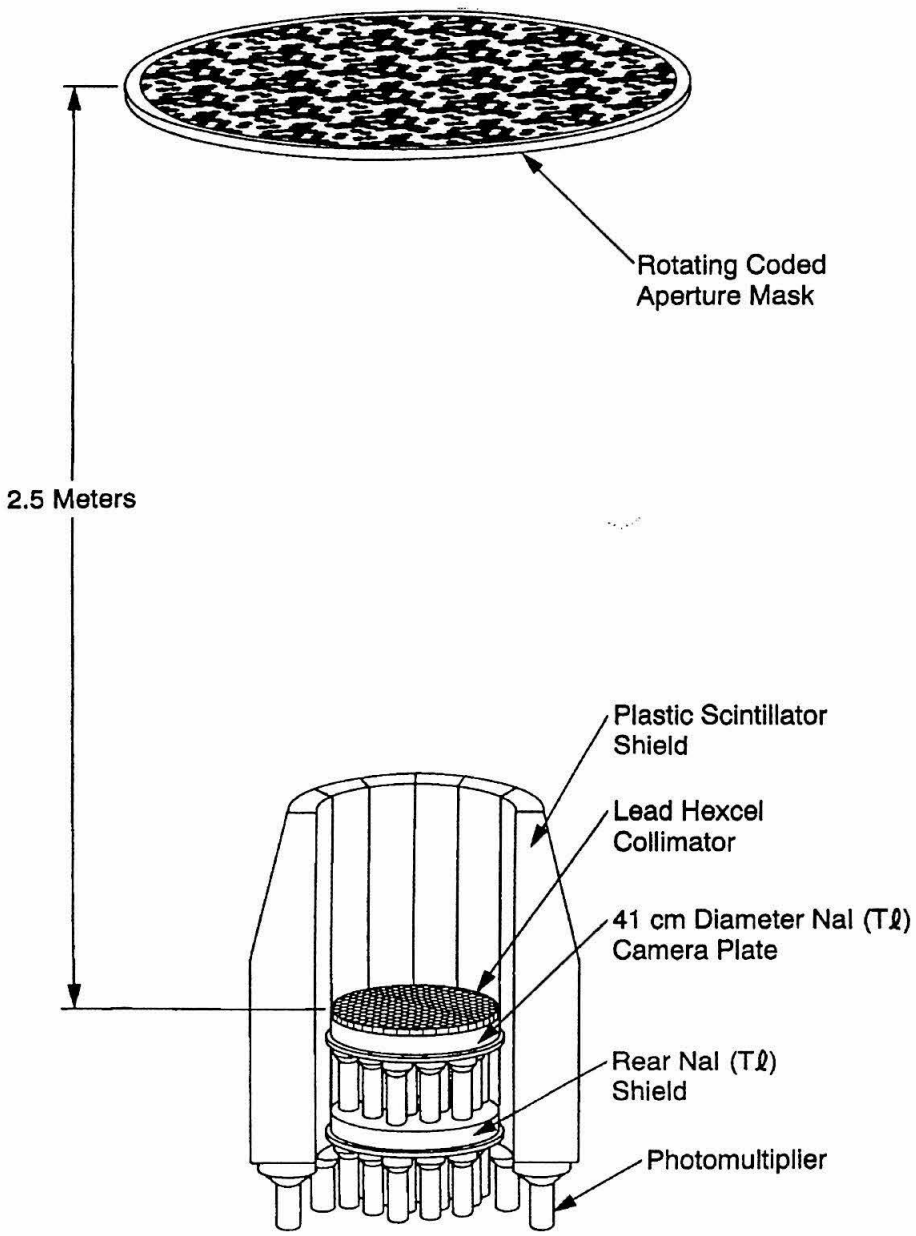

Figure 2.1: The GRIP detector system.

TABLE 2.1

Key parameters of the GRIP telescope and gondola.

Energy Range	30keV – 10MeV
Energy Resolution (FWHM)	23% @ 60 keV 6% @ 1 MeV
Field of View	14° FWHM
Angular Resolution	1.°1 FWHM
Primary Detector Useful Area	41 cm × 5 cm NaI(Tl) 645 cm^2
Shields	Rear: 5 cm NaI(Tl) Sides: 16 cm Plastic Scintillator Front: 14° FWHM Pb collimator
Mask	Rotating (1 rpm) HURA Cells: 4.8 cm flat-flat/2.8 cm Pb, 0.8mm Sn 2.5m above detector
Detector Position Resolution (FWHM)	1.3 cm @ 122keV 1.0 cm @ 662keV
Altitude	120,000 ft
Balloon	23/28 MCF
Duration	$\lesssim$ 40 hr

maximum likelihood algorithm is used to compute event locations in three dimensions from the distribution of detected light, and deposited energies are computed from the sum of the 19 PMT signals. The position resolution—which determines how sharply the shadow is detected—is 1.2 cm FWHM at 122 keV and 1.0 cm at 662 keV. The detector energy resolution is 25% FWHM at 60 keV and 7% at 1 MeV.

The camera plate is shielded at the rear and the sides by active anticoincidence detectors. A second NaI(Tl) camera plate (which does not record event positions) forms the rear shield, while a thick ($\sim$16 cm) plastic scintillator surrounds the periphery of the detector. The active shield system reduces several components of the background. These include atmospheric γ-rays, γ-rays from celestial sources outside the coded FOV, source photons and internally produced background photons which Compton scatter and leave the camera plate, and events which produce 29 keV iodine escape photons. A passive lead collimator with a 14° aperture (FWHM) reduces the diffuse component of background within the field of view.

2.1.3 The Mask

The particular URAs employed in GRIP are built on a hexagonal lattice and are therefore called hexagonal uniformly redundant arrays (HURAs) (Finger and Prince 1985). HURAs have the additional property of being nearly anti-symmetric upon 60 degree rotation, with only the central cell remaining unchanged. Because of this antisymmetry, subtracting the detected photon distribution (shadow pattern) accumulated with the mask rotated by 60 degrees from that accumulated with the unrotated mask provides a point by point background subtraction in the detector. We call the patterns resulting from these antisymmetric orientations, "mask" and "antimask" patterns. This mask/anti-mask background subtraction is achieved with GRIP through a continuous rotation of the mask during flight. Because the mask consists of a unit pattern repeated several times, a single point source produces a lattice of peaks in the sky map — one for each repetition. Rotation breaks the translational symmetry of the mask and restores the unique nature of the deconvolved sky map. For a complete discussion of the use of HURAs for coded-aperture imaging,

see Cook *et al.* (1984) and Finger and Prince (1985).

The mask pattern used for the observations described here is shown in Figure 2.3. Each opaque cell is a right hexagonal cylinder 4.8 cm flat-to-flat. Dividing 4.8 cm by the 250 cm mask to detector separation yields GRIP's 1°.1 resolution. The opaque cells are made of 2.8 cm of lead on top of 0.8 mm of tin. The tin absorbs lead fluorescence photons (several lines of $\sim$ 80 keV) which would otherwise contribute to the instrumental background. The blocks are mounted on an aluminum hexcel platform which serves as the turntable for mask rotation.

2.1.4 Effective Area

Figure 2.3 is a plot of the instrumental effective area as a function of energy. The effective area is given by

$$A_{eff} = \epsilon\sqrt{\eta}A_{geom}. \tag{2.1}$$

The factors ϵ and η are both functions of energy, while $A_{geom} = 645$ cm^2 is the (constant) geometric detector area used for analysis. ϵ, the instrument efficiency, is the fraction of incident photons which deposit their full energy in the detector. It includes the effects of attenuation in passive instrument materials, the on-axis blockage of the collimator, and the full-energy efficiency of the detector itself. The imaging factor, η, (of order unity) describes the loss of sensitivity caused by the spreading of the detected mask shadow due to the finite size of the detector point spread function. The step at 300 keV is due to a cut applied to events below 300 keV. At these energies, events in the rear half of the detector are preferentially background photons and are therefore rejected.

2.1.5 The Pointing Platform

Figure 2.4 is a diagram of the full telescope and gondola. The telescope is mounted in an altitude-azimuth pointing platform. Elevation is maintained by a stepper motor driven ballscrew assembly. Azimuthal pointing is maintained through a

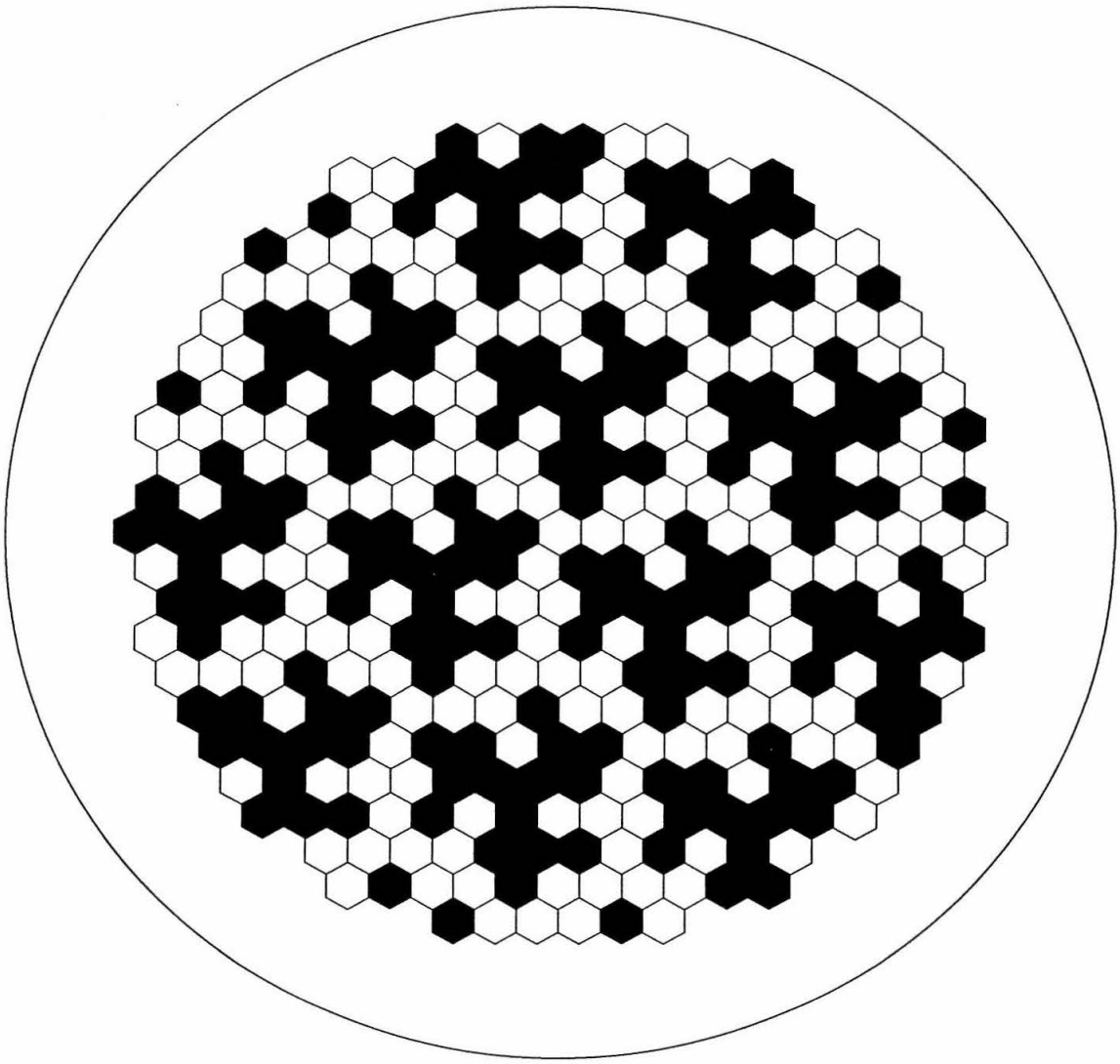

Figure 2.2: The GRIP mask pattern. Black and white cells indicate opaque and transparent regions respectively. The cells are 4.8 cm flat-to-flat.

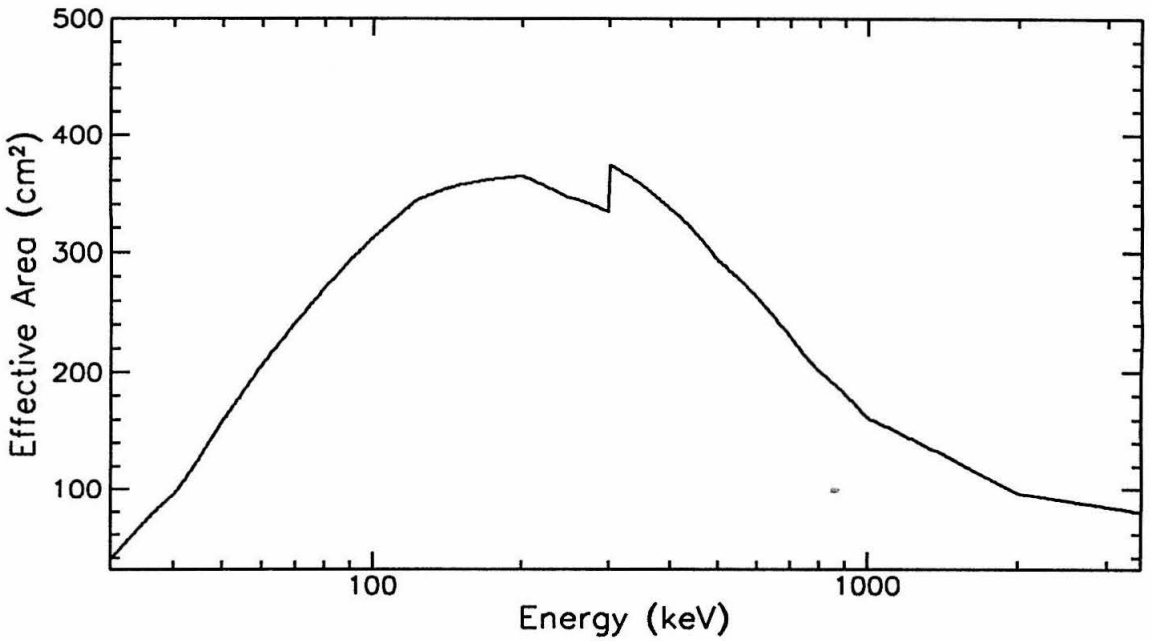

Figure 2.3: The GRIP effective area. The curve includes the full energy detection efficiency, attenuation in passive instrument materials, the collimator blockage for on-axis sources, and the imaging factor. The step at 300 keV results from a depth dependent event cut employed at energies below 300 keV.

feedback system based on a magnetometer arranged in a flux nulling mode. The magnetometer is mounted on a rotation stage which is oriented to zero the flux through the magnetometer when the telescope is at the desired azimuth. Any deviation gives rise to differential flux in the magnetometer producing an error signal which drives the azimuthal control motor to correct for the error. Both the elevation drive motors and the magnetometer rotation stage are controlled by an on-board microprocessor which calculates the required hardware parameters (motor steps and stage rotation) to track a given right ascension and declination. Because tilts of the pointing platform can directly affect the telescope elevation and the nulling of the magnetometer, a pair of inclinometers with orthogonal sensitive axes are mounted on the gondola frame. These are not used for real time pointing, but provide corrections to detected photon positions which are applied *ex post facto* in the image reconstruction process.

Achieved aspect solutions, including corrections from the inclinometer and magnetometer error signals, are typically accurate to better than $\sim 0^\circ.5$ (Palmer 1992). However, this is insufficient to identify sources in confused fields. In particular, the Galactic center field is known to be crowded at X–ray energies on the sub-degree level. For this reason, GRIP has an optical aspect sensing system. Two CCD star cameras, one of which is image intensified, are mounted on the telescope body (see Figure 2.4). During nighttime pointings, positions of detected stars provide accurate information on deviations of the telescope from the desired pointing direction. The use of these cameras for aspect determination is described in Chapters 3 and 4.

2.2 Observations

The city of Alice Springs in Australia's Northern Territory is ideally located for balloon-borne observations of the Galactic center region. At its latitude of 24°42' S, the Galactic center transits nearly overhead, providing long observations with low atmospheric overburden. It is also far from any densely populated area, so that balloon flights have little chance of injuring persons or property.

As part of the NASA's SN1987A observational campaign, we flew GRIP four times from Alice Springs between 1987 May and 1989 April. During two of these

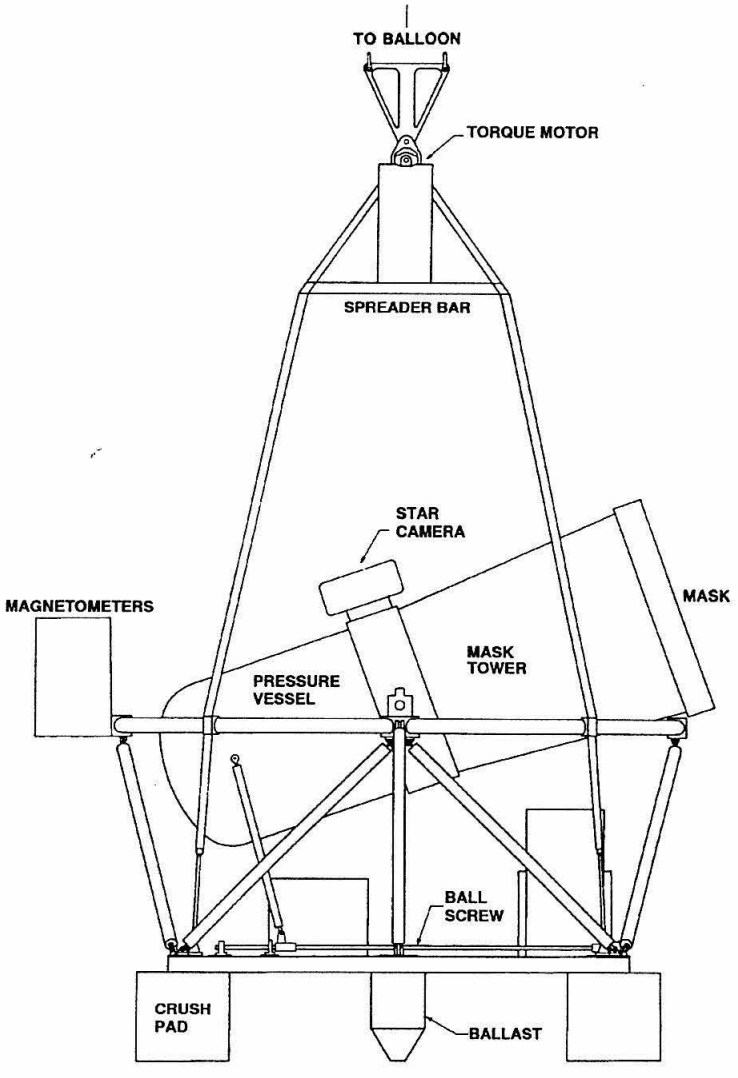

Figure 2.4: The GRIP gondola.

TABLE 2.2

GRIP observations of the Galactic center region.

Date	livetime (hr)	Atmospheric Depth[a] (g/cm^2)
1988 April 12	6.2	6.2
1989 April 3–4	11.7	6.6

[a]Time average value. Includes effect of telescope zenith angle.

flights, we observed the Galactic center region. Table 2.2 summarizes the Galactic center observations.

During 1988 April, the Galactic center region was observed during a single transit. In 1989 April, a long flight (~40 hr) allowed observations to be made during two transits.

Chapter 3

GRIP Results, 1988

Originally appeared in
The Astrophysical Journal, volume 372, pages L75–L78, 1991 May 10

CODED-APERTURE IMAGING OF THE GALACTIC CENTER REGION AT GAMMA RAY ENERGIES

WALTER R. COOK, JOHN M. GRUNSFELD, WILLIAM A. HEINDL, DAVID M. PALMER, THOMAS A. PRINCE, STEPHEN M. SCHINDLER, AND EDWARD C. STONE
Division of Physics, Mathematics, and Astronomy, California Institute of Technology, M.S. 220-47, Pasadena, CA 91125

ABSTRACT

The first coded-aperture images of the Galactic center region at energies above 30 keV have revealed two strong γ-ray sources. One source has been identified with the X-ray source 1E 1740.7–2942, located 0.°8 away from the nucleus. If this source is at the distance of the Galactic center, it is one of the most luminous objects in the galaxy at energies from 35 to 200 keV. The second source is consistent in location with the X-ray source GX354+0 (MXB1728-34). In addition, γ-ray flux from the location of GX1+4 was marginally detected at a level consistent with other post-1980 measurements. No significant hard X-ray or γ-ray flux was detected from the direction of the Galactic nucleus (Sgr A*), or from the direction of the recently discovered γ-ray source GRS1758-258.

Subject headings: galaxies: The Galaxy gamma rays: general X-rays: sources

3.1 Introduction

Observations from Spacelab 2 (Skinner *et al.* 1987) and Spartan-1 (Kawai *et al.* 1988) between 1 and 30 keV, together with earlier results from the *Einstein* observatory between 0.9 and 4 keV (Watson *et al.* 1981; Hertz and Grindlay 1984), identified several point sources within approximately 1° of the Galactic nucleus, including a point source at the nucleus itself. At higher energies, observations by nonimaging instruments with wide fields of view (FWHM > 15°) detected 0.511 MeV positron annihilation line radiation and hard continuum emission extending above

1 MeV from the general direction of the Galactic center (e.g., Riegler et al. 1981; Leventhal et al. 1982; Riegler et al. 1985; and Leventhal et al. 1989) . Both line and continuum components were found to vary in intensity on time scales as short as six months. The compact source size required by the time variability, and the unusual γ-ray spectrum, have stimulated considerable speculation on the nature of the source of emission.

In this paper, we report γ-ray flux measurements based on the first coded-aperture imaging observations of the Galactic center region at γ-ray energies (30 keV - 7 MeV). The initial report of these observations (Cook *et al.* 1989) discussed the detection of a strong γ-ray source that was tentatively identified as the X-ray source 1E 1740.7–2942 (Hertz and Grindlay 1984), consistent with the Spacelab 2 observation of this source as dominant in the region at 19-30 keV (Skinner *et al.* 1987). Further analysis of our data confirmed 1E 1740.7–2942 as the source of the primary γ-ray emission, and in addition revealed a second source, consistent in location with the X-ray burst source GX354+0 (Cook *et al.* 1990). Here we present improved γ-ray flux measurements for 1E 1740.7–2942 and GX354+0.

3.2 Observations

The observations were performed with the Caltech Gamma-Ray Imaging Payload (GRIP), a balloon borne coded-aperture telescope sensitive to photons in the energy range from 30 keV to 10 MeV (Althouse *et al.* 1985). The instrument employs a rotating hexagonal-celled uniformly redundant array (HURA) and a position-sensitive NaI(Tl) scintillation detector to image a 14° diameter field of view with 1.1° angular resolution.

The Galactic center region was observed for two 4-hour periods during the interval 1988 April 12.62 to 13.00 UT, as part of a 30 hour balloon flight of the instrument from Alice Springs, NT, Australia. The data were processed in seven segments of somewhat more than one hour each. For each segment a single strong point source of γ-ray emission was detected at energies between 35 and 200 keV. Data was available from an on-board CCD star camera to determine the absolute

position of the source emission in four of the seven observation periods, leading to the identification of the strong γ-ray source as 1E 1740.7–2942 (Cook *et al.* 1990). The remaining three observation periods occurred during daylight when no stars were visible in the CCD camera.

We used the strong source, identified as 1E 1740.7–2942 as a pointing reference to co-align images from all the separate 1 hr segments. This procedure reduced possible blurring effects resulting from pointing uncertainties and allowed images from all the segments, including the last three which lacked star camera data, to be combined in a search for weaker sources. A second source was detected in the energy range from 23 to 122 keV, as shown in Figure 3.1 (where the primary peak has been aligned with 1E 1740.7–2942). The presence of the second peak, consistent in location with the known X-ray source, GX354+0, further supported the identification of the primary peak with 1E 1740.7–2942.

Flux measurements and upper limits for 1E 1740.7–2942 and GX354+0, are presented in Table 3.1 and Figure 3.2. The flux values were computed as weighted averages of values obtained in each of the seven one-hour segments, with weights chosen to minimize the statistical error. The use of detailed instrument calibrations, including laboratory measurements of photon attenuation in passive instrument material, and the angular response of the lead collimator, has improved the accuracy of the present measurements, compared with those presented previously (Cook *et al.* 1989; Cook *et al.* 1990). Flux measurements for the Crab Nebula and Pulsar, also made during the 1988 April flight, agree with previous measurements (Jung 1989 and references therein) within approximately 10% at energies from 35 keV to 200 keV (Cook *et al.* 1991a). Details on the processing of coded-aperture images to obtain source flux measurements are given in Cook et al. 1984, Finger 1987, and Palmer et al. 1991 .

Table 3.1 also includes results for three other sources: the Galactic nucleus radio source Sgr A*, the X-ray binary pulsar GX1+4, and the recently discovered γ-ray source GRS1758-258.

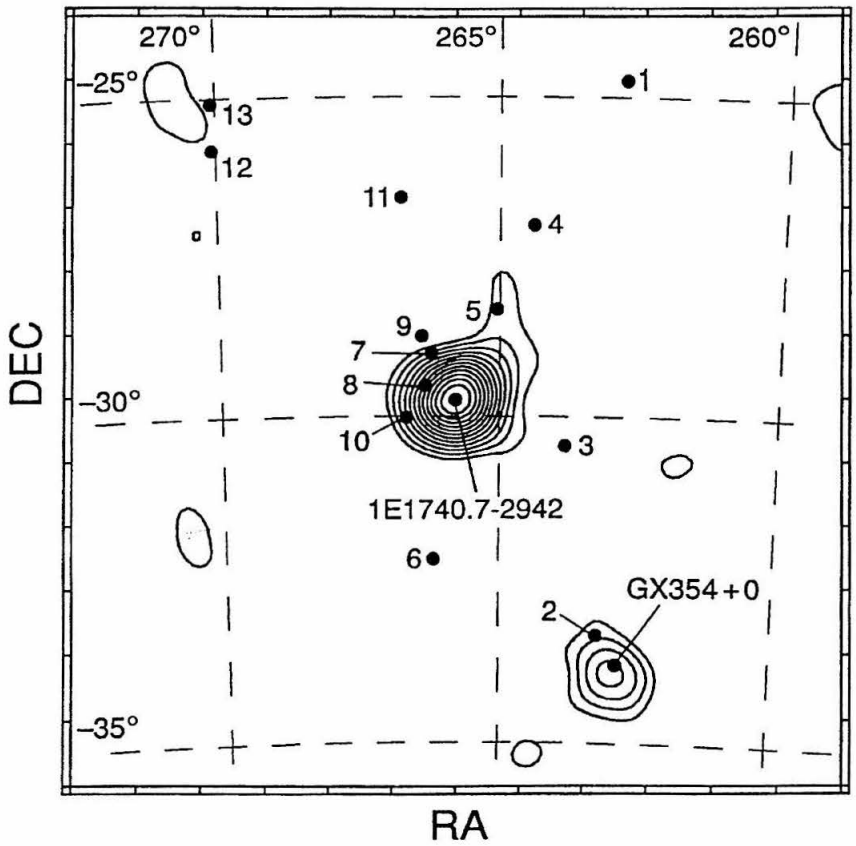

Figure 3.1: Image of the Galactic center region from 23 to 122 keV. Right ascension (*vertical lines*) and declination (*horizontal lines*) are indicated for epoch 1988.3. The contours indicate the number of excess counts in a given direction, calibrated in units of the statistical significance of the excess, with contours beginning at the 2σ level and spaced by 1σ. Sources 1E 1740.7–2942 and GX354+0 are labeled by name, while other known hard X-ray sources (Bradt and McClintock 1983; Levine *et al.* 1984; Skinner *et al.* 1987) are numbered as follows: (1) GX1+4, (2) MXB1730-335 ("Rapid Burster"), (3) SLX1732-304, (4) SLX1735-269, (5) SLX1737-282, (6) A1743-322, (7) Sgr A* (8) A1742-294, (9) 1E1743.1-2843, (10) SLX1744-299, (11) GX3+1, (12) GRS1758-258, and (13) GX5-1.

TABLE 3.1

Galactic Center Region Source Flux Values [a]

ENERGY	DIFFERENTIAL FLUX (10^{-5} cm^{-2} s^{-1} keV^{-1})				INTEGRAL FLUX (10^{-4} cm^{-2} s^{-1})	
INTERVAL	35–58 keV	58–122 keV	122-270 keV	270–490 keV	511 keV[b]	545-2150 keV
1E 1740.7–2942	40.6 ± 5.5	12.2 ± 1.0	1.96 ± 0.35	< 0.47	< 6.8	< 46.1
($\alpha = 2.05$)	(47)	(84)	(178)	(378)		
GX 354+0	38.6 ± 10.8	6.12 ± 2.03	< 1.94	< 0.92	< 7.1	< 18.0
($\alpha = 3.37$)	(46)	(79)	(199)	(378)		
GX 1+4	17.9 ± 7.5	< 4.1	< 0.82	< 0.69	< 3.7	< 27.0
($\alpha = 1.9$)	(48)	(93)	(199)	(378)		
Sgr A*[c]	...	...	...	< 0.65	< 11.7	< 52.1
				(378)		
GRS 1758-258	< 19.9	< 3.1	< 1.1	< 0.89	< 7.8	< 22.8
	(50)	(93)	(199)	(378)		

[a]Differential flux values correspond to a power law ($dJ/dE = KE^{-\alpha}$) evaluated at the mean energy (keV), listed in parenthesis below the corresponding flux value. The exponent, α, is given below the source name. Upper limits are quoted at 95% confidence, and assume a flat power law ($\alpha = 0$).

[b]The flux upper limits for a narrow line at 511 keV were derived by dividing the integral flux limits for a 55 keV wide energy interval by the fraction (0.87) of 511 keV photons which would be detected in that interval.

[c]Fluxes and upper limits are not given for the three lowest energy ranges. This is due to contamination from the nearby bright source 1E 1740.7–2942

3.3 Discussion

1E 1740.7–2942.— The identification of the strong, central γ-ray source (Fig. 3.1) as 1E 1740.7–2942 (Cook *et al.* 1990) is consistent with the earlier imaging results from Spacelab 2 at energies below 30 keV (Skinner *et al.* 1987). At energies above 30 keV, the recent imaging results from SIGMA confirm our identification of 1E 1740.7–2942 as the primary hard X-ray source (Mandrou 1990). This source has not yet been identified at other than X-ray and γ-ray wavelengths.

Our spectral results for 1E 1740.7–2942 and the earlier results from Spacelab 2 (Skinner *et al.* 1989) are shown together in Figure 3.2. The hard spectrum, which distinguished 1E 1740.7–2942 from other nearby sources viewed by Spacelab 2, is seen to continue to approximately 200 keV. In the energy range from 35 to 200 keV the spectrum is well fit by a power law, $dJ/dE = K(E/100\ keV)^{-\alpha}$, with spectral index $\alpha = 2.05 \pm 0.15$, and flux normalization, $K = 8.5 \pm 0.5 \times 10^{-5}$ cm^{-2} s^{-1} keV^{-1}.

Our results for 1E 1740.7–2942 may also be compared to earlier nonimaging measurements. Our measured spectrum falls near the lower envelope of previous flux measurements for the Galactic center region obtained at energies from about 50 keV to 1 MeV with nonimaging, wide aperture ($> 10°$ FWHM) instruments (Matteson 1982). The higher fluxes obtained with these instruments at energies below 100 keV are probably due to the inclusion of other (possibly time-variable) hard X-ray sources such as GX354+0 (see below) located within 10° of the Galactic center. Several instruments (Dennis *et al.* 1980; Matteson 1982; Levine *et al.* 1984; Knight *et al.* 1985) with relatively narrow apertures (1.5° to 5° FWHM) have observed a source (or sources) near the Galactic center with flux at 100 keV ranging from 0.5×10^{-4} to 2.0×10^{-4} cm^{-2} s^{-1} keV^{-1}, comparable to that shown in Figure 3.2. Our observations strongly support the suggestion by Skinner *et al.* (1987) that 1E 1740.7–2942 was the source of the high energy flux seen in these earlier observations.

One possibility is that 1E 1740.7–2942 is a system similar to the black hole candidate Cyg X-1 with several states of emission, one of which produces the spectrum shown in Figure 3.2, and another which yields hard MeV continuum and 0.511 MeV emission. Indeed, our measured spectrum for 1E 1740.7–2942 is similar in absolute

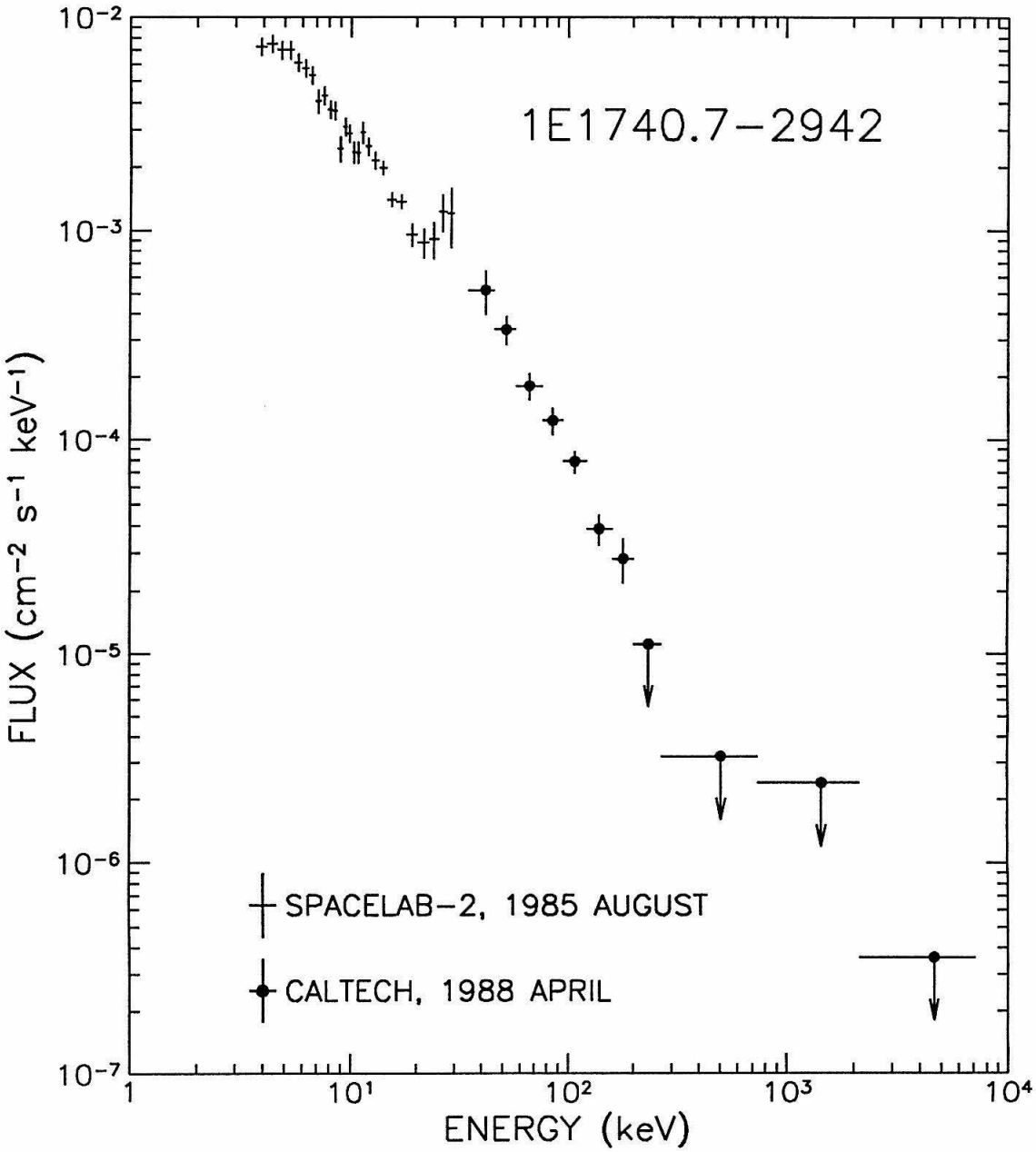

Figure 3.2: Gamma-ray differential energy spectrum measurements for the source 1E 1740.7–2942. Error bars are $\pm 1\sigma$, while upper limits are at the 95% confidence level.

intensity and spectral shape to the γ_3 state of Cyg X-1, as measured by the HEAO A-3 experiment in 1979 (Ling *et al.* 1987). Our measurements for 1E 1740.7–2942 yield a 35-200 keV luminosity of 2.1×10^{37} ergs s^{-1} (at an assumed distance of 8.5 kpc), comparable to the 50-400 keV luminosity measured for Cyg X-1 in its γ_3 state of 2.3×10^{37} ergs s^{-1} (Ling *et al.* 1987). Further, the spectrum of Cyg X-1 in its γ_1 state has similarities to the Galactic center spectrum measured in 1979, showing a hard excess of emission above 0.511 MeV with comparable luminosity (Lingenfelter and Ramaty 1989). Recently, a time variable hard shoulder of emission from 1E 1740.7–2942 extending from 250-600 keV, has been reported by Mandrou *et al.* (1990).

GX354+0.— The X-ray burster GX354+0 is a source of both persistent and transient X-ray emissions (e.g., Basinska et al. 1984; Hoffman et al. 1976; Hoffman et al. 1977). The X–ray intensity of the persistent source is known to vary by over a factor of ~ 5 (Basinska *et al.* 1984; Forman *et al.* 1978). The *Einstein* observatory measured the most intense and hot non-burst spectrum to date, and found it to be consistent with a thermal bremsstrahlung model having a temperature of kT=17.7 keV (Grindlay and Hertz 1981).

Our flux measurements for GX354+0, averaged over the entire 8 hour observation, are presented in Table 3.1. Comparison between our data and an extrapolation of the 17.7 keV thermal bremsstrahlung spectrum, measured by the *Einstein* observatory, yields approximate agreement, suggesting that the source may have been near its maximum non-burst brightness during our observation. From our data, the best fit temperature, with estimated 1 σ errors, is kT = 31 (+23, -10) keV.

GX1+4.— Observations of the X-ray binary pulsar GX1+4, in the decade following its discovery by Lewin, Ricker, and McClintock (1971), showed the source to be one of the brightest hard X-ray sources in the Galactic center region, and to have an unusually large monotonic spin up rate of approximately 2 percent per year (Elsner *et al.* 1985). In contrast, during the 1980's the source was observed to be in a "low" state of emission (Makishima *et al.* 1988; Manchanda 1988; Sakao *et al.* 1990) accompanied by a halt in the rapid spin up of the pulsar. Recent observations show the pulsar spinning down (Makishima *et al.* 1988; Gilfanov *et al.* 1989; Sunyaev

and the *GRANAT* team 1990). McClintock and Leventhal (1989), have proposed GX1+4 as a candidate for the compact source of Galactic center 0.511 MeV emission, since this emission may have decreased in approximate correlation with the shift in observational properties of GX1+4.

While emission from GX1+4 is not apparent in the 22-122 keV image of Figure 3.1, a greater than 2σ flux measurement was obtained in the 35-58 keV interval as listed in Table 3.1. This flux corresponds to 67 ± 28 mCrab at 50 keV and is in agreement with the recent measurements of Mony *et al.* (1989) and Sharma *et al.* (1990).

GRS1758-258.— This source was recently discovered by the ART-P and SIGMA coded-aperture instruments aboard the *GRANAT* space observatory (Mandrou 1990). Our 95% confidence upper limit for the flux in the energy interval from 35 to 58 keV corresponds to 78 mCrab, and is consistent with the ART-P result of 90 ± 20 mCrab for 20 to 40 keV.

0.511 MeV *Line and MeV Continuum Upper Limits.*— Our 1988 April imaging observations of the Galactic center have yielded no positive detection of either 0.511 MeV line emission, or continuum emission at higher energies. Table 3.1 lists 95% confidence flux upper limits for the 0.511 MeV line, and for a broad continuum band from 0.55 to 2.1 MeV, as obtained for 1E 1740.7–2942 Sgr A*, GX1+4, GX354+0, and GRS1758-258.

Sgr A*, the compact Galactic nucleus radio source, and more recently 1E 1740.7–2942 and GX1+4, have been suggested as candidates for the source of the variable Galactic center positron annihilation line and hard MeV continuum emission (Lingenfelter & Ramaty 1982, Skinner et al. 1987, McClintock & Leventhal 1989) . This emission was seen to turn off or decrease between the *HEAO 3* observations of 1979 fall and 1980 spring (Riegler *et al.* 1985). The flux decrease was most dramatic at energies near 1 MeV, where the continuum level dropped by a factor of 20 or more. The 0.511 MeV radiation has recently been reported to have turned on again in 1988 (Leventhal *et al.* 1989; Gehrels *et al.* 1990), then off again by 1989 May (Matteson *et al.* 1989).

Our 95% confidence flux upper limits for the 0.54 – 2.1 MeV interval range

from 1.8×10^{-3} to 5.2×10^{-3} $cm^{-2} s^{-1}$, and are all well below the 1979 Fall *HEAO 3* spectrum (Riegler *et al.* 1985), which, when integrated over the same energy range, gives $1.0 \pm 0.2 \times 10^{-2}$ $cm^{-2} s^{-1}$.

Our 0.511 MeV upper limits may be compared to recent Galactic center 0.511 MeV line flux measurements made with nonimaging Ge spectrometers during 1988 May and October (Gehrels *et al.* 1991), and 1989 May (Matteson *et al.* 1989). These observations yielded values of 7.5 ± 1.7, 11.8 ± 1.6, and $6.5 \pm 1.9 \times 10^{-4}$ $cm^{-2} s^{-1}$ respectively. Our 0.511 MeV upper limits do not conflict with the 1988 May measurement (made only 18 days after our flight), since our limits apply for isolated points in our field of view and are relatively immune to the presence of diffuse flux. After adjustment for the diffuse 0.511 MeV flux measured by *SMM* (Share *et al.* 1988), the portion of the May 1988 measurement which might be attributed to a compact source is only $2.8 \pm 1.7 \times 10^{-4}$ $cm^{-2} s^{-1}$(Gehrels *et al.* 1990).

In summary, we see no evidence of 0.511 MeV line emission from 1E 1740.7–2942 Sgr A*, GX1+4, GX354+0, or GRS1758-258. We also did not observe a continuum excess in the energy range 250-600 keV like that reported by SIGMA (Mandrou *et al.* 1990) for 1E 1740.7–2942. However, the recent SIGMA observation provides evidence that transient positron annihilation may be important in 1E 1740.7–2942 strengthening the possibility that this was indeed the source of narrow positron annihilation radiation seen in observations during the 1970's and late 1980's.

We acknowledge the important contributions to the development of the GRIP telescope made by W. Althouse, D. Burke, A. Cummings, M. Finger, C. Starr, J. Weger and the personnel of the Central Engineering Services at Caltech. We thank the personnel of the National Scientific Balloon Facility and the NASA Wallops Flight Facility for their excellent balloon launch support. This work was supported in part by NASA grants NGR 05-002-160 and NAGW-1919.

Note added in proof.—A recent report by Paul et al. (in Proc. Internat. Symp. on Gamma-Ray Line Astrophysics, Paris-Saclay, in press [1991]), based on SIGMA observations of the 1990 October 13 high-energy flare (250–600 keV) from 1E 1740.7–2942 (Mandrou *et al.* 1990), strengthens the interpretation of the event as

being associated with an electron-positron pair plasma.

Chapter 4

GRIP Results, 1989

Originally appeared in
The Astrophysical Journal, volume 408, pages 507–513, 1993 May 10

AN OBSERVATION OF THE GALACTIC CENTER HARD X-RAY SOURCE, 1E 1740.7-2942, WITH THE CALTECH CODED-APERTURE TELESCOPE

WILLIAM A. HEINDL, WALTER R. COOK, JOHN M. GRUNSFELD[1], DAVID M. PALMER[2], THOMAS A. PRINCE, STEPHEN M. SCHINDLER, AND EDWARD C. STONE
Division of Physics, Mathematics, and Astronomy, California Institute of Technology, M.S. 220-47, Pasadena, CA 91125

ABSTRACT

The Galactic center region hard X-ray source 1E 1740.7–2942 has been observed with the Caltech Gamma-Ray Imaging Payload (GRIP) from Alice Springs, Australia on 1988 April 12 and on 1989 April 3 and 4. We report here results from the 1989 measurements based on 14 hours of observation of the Galactic center region. The observations showed 1E 1740.7–2942 to be in its normal state, having a spectrum between 35 and 200 keV characterized by a power law with an exponent of (2.2 ± 0.3) and flux at 100 keV of $(7.0 \pm 0.7) \times 10^{-5}\,\mathrm{cm^{-2}\,s^{-1}\,keV^{-1}}$. No flux was detected above 200 keV. A search for time variability in the spectrum of 1E 1740.7–2942 on one hour time scales showed no evidence for variability.

Subject headings: black holes galaxies: The Galaxy gamma rays: general X-rays: sources

4.1 Introduction

The source 1E 1740.7–2942 was discovered in soft X-rays (0.9 to 4 keV) with the *EINSTEIN* observatory in 1979 (Hertz and Grindlay 1984). In 1985, it was again observed in soft X-rays by Spartan 1 (Kawai *et al.* 1988) between 1 and 5 keV. The first hard X-ray identification, made using the coded mask telescope (SL2-XRT) on the Spacelab 2 mission (Skinner *et al.* 1987; Skinner *et al.* 1989), showed 1E 1740.7–2942 to be the dominant source within the central few degrees of the galaxy in the 20–30

[1]Current Address: JSC
[2]Current Address: NASA Goddard Space Flight Center, Code 661, Greenbelt, MD 20771

keV band. Between 35 and 200 keV, 1E 1740.7–2942 was identified by the Caltech balloon-borne coded-aperture instrument, GRIP, in 1988 (Cook *et al.* 1989; Cook *et al.* 1990; Cook *et al.* 1991b). In these observations, 1E 1740.7–2942 was found to be the brightest Galactic center hard X-ray source, having a strong power law spectrum extending up to 200 keV. GRIP again observed 1E 1740.7–2942 on 1989 April 3–4 (Grunsfeld *et al.* 1991). The results of this observation are presented here.

The Galactic center region has also been observed at hard X-ray energies by the balloon-borne telescope EXITE (approximately 1 month after the 1989 GRIP observation) (Covault, Manandhar, and Grindlay 1990), the HEXE and TTM instruments on *MIR* (Skinner *et al.* 1991), and the ART-P and SIGMA instruments aboard the *GRANAT* spacecraft (Sunyaev *et al.* 1991a; Sunyaev *et al.* 1991b; Paul *et al.* 1991; Bouchet *et al.* 1991). With the exception of a subset of the SIGMA observations (see below), all of these instruments found the energy spectrum of 1E 1740.7–2942 to be similar to the GRIP 1988 spectrum, defining a 'normal' state of the source. The SIGMA observations showed that in addition to this normal state, 1E 1740.7–2942 has both a 'hard' and a 'low' emission state (Sunyaev *et al.* 1991b).

The 'hard' spectrum (Bouchet *et al.* 1991) is characterized by the normal power law spectrum below 200 keV, but exhibits a rising continuum spectrum above 200 keV, peaking near 500 keV, and cutting off above 700 keV. This state was seen by SIGMA only during an observation on 1990 October 13–14. A probable source of this feature is e^+e^- annihilations in a hot pair plasma (Bouchet *et al.* 1991). Observations by SIGMA on 11 and 15 October 1990 found 1E 1740.7–2942 in its normal emission state, indicating that the hard state lasted between 18 and 70 hr. This variability on a time scale of a few days or less limits the emission region to a size of a few $\times 10^{15}$cm. Although no narrow line annihilation radiation has been reported for this period, the fact that the feature is centered near the positron annihilation energy makes 1E 1740.7–2942 a likely candidate for the compact source of positron annihilation radiation near the Galactic center required by the observed time variable 511 keV flux (Riegler *et al.* 1981; Lingenfelter and Ramaty 1989; Gehrels 1991).

The 'low' emission state of 1E 1740.7–2942 (Sunyaev *et al.* 1991b) is characterized by emission in the power law region (30–200 keV) about 20% or less of

that observed in the normal state, with no detectable emission above 200 keV. Between the 1990 October and 1991 February SIGMA Galactic center observations, 1E 1740.7–2942 entered this state and apparently remained at a low flux level until at least 1991 April (Sunyaev *et al.* 1991b). It has also been reported (Bazzano *et al.* 1992) that the narrow (1°.9 FWHM) field of view (FOV) balloon-borne instrument, POKER, detected 1E 1740.7–2942 in this low state just 6 weeks after the 1989 GRIP observations and 2 weeks after the EXITE observations.

Observations made with the Very Large Array (VLA) (Prince *et al.* 1991b) have revealed a weak radio source (source 'A') within the 12 arcsec radius X-ray error circle for 1E 1740.7–2942, as determined by TTM (Skinner *et al.* 1991). Furthermore, a preliminary 5 arcsec radius error circle for 1E 1740.7–2942 based on a *ROSAT* high resolution imager (HRI) observation at 0.1–2 keV includes source 'A' (Prince *et al.* 1991a). Recent VLA observations (Mirabel *et al.* 1992) have found that source 'A' lies at the center of an aligned double radio jet. Millimeter wavelength observations have recently shown a molecular cloud in line of sight coincidence with 1E 1740.7–2942, suggesting a possible association (Bally and Leventhal 1991; Mirabel *et al.* 1991) with the resulting possibility that Bondi-Hoyle accretion onto a black hole moving through interstellar gas could be the source of the hard X-ray luminosity.

In this paper, we discuss our 1989 observations of 1E 1740.7–2942 in the energy range 30 keV to 7.5 MeV. We present a measurement of the hard X-ray spectrum as well as a search for time variability of the spectrum in the power law region, 35-200 keV, and the 'bump' region, 300-600 keV. Preliminary results of this analysis were presented in Grunsfeld *et al.* (1991).

4.2 Observations

The observations reported here were performed with the Caltech Gamma-Ray Imaging Payload (GRIP), a balloon-borne coded-aperture telescope sensitive to photons in the energy range 30 keV to 10 MeV (Althouse *et al.* 1985). The detector system consists of a rotating hexagonal uniformly redundant array (HURA) which modulates the sky flux incident on an actively shielded, position-sensitive NaI(Tl)

scintillation detector. A lead hexcel collimator (added since Althouse *et al.* (1985)) reduces the contribution of the diffuse aperture flux to the background. For these observations, GRIP was configured for 1°.1 angular resolution over a 14° FOV. An image-intensified CCD star camera and a second CCD camera for viewing bright stars and planets are employed to obtain precise aspect solutions for observations made during nighttime hours. During daylight conditions, telescope orientation is determined from a set of inclinometers and magnetometers. An on-board altimeter and the OMEGA radio navigation system give the physical location of the gondola.

GRIP observed the Galactic center region for 16.3 hours during a 42 hour flight beginning 1989 April 3 from Alice Springs, NT, Australia. Because 1E 1740.7–2942 may have been obscured by the gondola suspension during the Galactic center transit, 2.3 hours of data have not been used in this analysis. Thus, the results from a total observation time on the Galactic center region of 14.0 hours are presented here. Approximately half of the observation occurred during the night, when precise pointing aspect is determined from the star camera system. Because of the failure of a trigger circuit which provides event tags for the decay photons from an on-board calibration source, data in the energy range 46 to 71 keV were contaminated with 60 keV ^{241}Am line photons and have not been used in the analysis.

4.3 Analysis

4.3.1 Aspect Determination

The two CCD star cameras described above have FOVs which are offset from the γ-ray telescope axis. This allows them to provide useful data even when the γ-ray telescope points through the balloon. Analysis of images from the two cameras determines an axis of the CCD camera platform which is nearly parallel to the imaging axis of the γ-ray telescope. The offset between these axes is calibrated through in-flight observations of the Crab Nebula and Pulsar and verified through observations of Cygnus X-1. For the Galactic center observations, offsets determined from the camera system were used in post-flight analysis to correct images for errors in

the real-time pointing. The primary source of error in aspect determination using the camera system is the statistical uncertainty in the location of the Crab in the γ-ray image used to calibrate the camera system offset. The resulting one dimensional rms uncertainty in image positions is about 4 arcmin. Any detected source will have an additional position uncertainty due to the location statistics of its image peak.

During daylight hours, when no star camera data were available, the γ-ray data were divided into time periods using two approaches. For analysis of the overall spectrum, the periods were chosen such that in each period an image source peak was detected at a significance of at least 5σ in the energy range 35 to 200 keV. The source flux was then determined from the image value at the peak location (see §3.2). Calculating the flux based on the image value at the peak, rather than at the nominal source location, introduces a systematic flux overestimate in these periods of less than 5%, but is insensitive to residual pointing errors which may be present in the daytime data. These periods varied in length between 0.5 and 1.7 hr. For the time variability analyses, where the choice of time periods by measured source peak significance may bias the overall measurement, locations were determined from images incorporating approximately 2 hr of data. These data were then divided into 0.9-1.3 hr periods, and fluxes were calculated at the previously determined source locations.

4.3.2 Flux Determination

A detailed treatment of the method by which source fluxes in individual energy bins are determined is given in the Appendix. A brief summary of the method used is given here.

Source fluxes are determined using a modification of the trial spectrum method described by Fenimore, Klebesadel, and Laros (1983). In this technique, a model spectral form is integrated with the instrument response function in order to derive a predicted count spectrum. In analysis of data from a coded-aperture instrument, the predicted and measured count spectra are replaced by predicted and measured "image values." The set of image values is analogous to the count spectrum in a non-imaging instrument, but also includes effects due to the imaging properties

of the coded-aperture instrument. A goodness of fit parameter (e.g., χ^2) is employed to determine which of several trial model spectra best fits the data. The best fit model spectrum is then used to derive flux values in individual energy bins.

In the analyses described here, two input spectral forms were used. The first was a standard power law form. The second, which was used to search for emission from 1E 1740.7–2942 between 300 and 600 keV, was the Gaussian line profile (mean = 480 keV, FWHM = 240 keV) given by Bouchet *et al.* (1991).

4.4 Results

4.4.1 Imaging

Figure 4.1 shows an image of the Galactic center region for the energy range 35-200 keV obtained using the 7.4 hr of data for which a complete aspect solution was available from the star camera system.

A single bright hard X-ray source is visible, located 8 arcmin from the expected location of 1E 1740.7–2942. Figure 4.2 is an expanded view of the source region, showing the 90% confidence error circle for the location of the source. The error circle is approximately 24 arcmin in diameter and includes uncertainties arising from the aspect determination (cf. §3.1) and source peak location statistics. The error circle excludes all other known hard X-ray sources.

It should be noted that in Figure 4.1, a peak of greater than 2σ significance appears at the expected location of GRS 1758-258. During these observations GRS 1758-258 was well off the collimator axis (14° FWHM) and was therefore observed with reduced sensitivity. Although the peak in Figure 4.1 is too small to provide a firm detection, a measurement of the flux from the location of GRS 1758-258 incorporating all 14.0 hr of Galactic center data yields a 3.6σ result in the energy range 35 to 200 keV. It therefore seems likely that this peak is due to GRS 1758-258. Assuming an E^{-2} power law spectrum (Sunyaev *et al.* 1991a), the 100 keV source flux

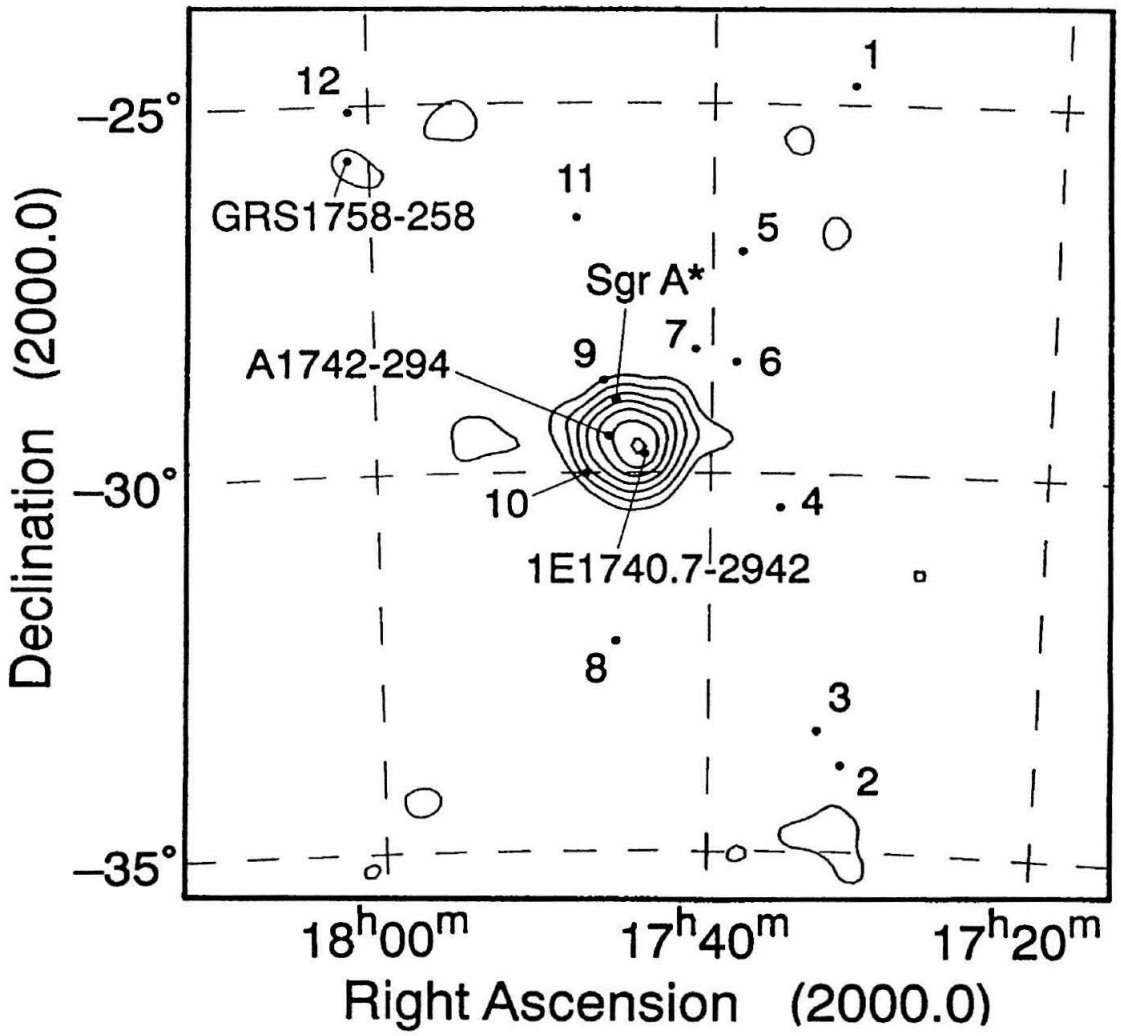

Figure 4.1: GRIP image of the Galactic center region from 35 to 200 keV on 1989 April 3, 4. the contours indicate the number of excess counts in a given direction, calibrated in units of the statistical significance of the excess, with contours beginning at the 2 σ level and spaced by 1 σ. Known hard X–ray sources (Levine *et al.* 1984; Skinner *et al.* 1987; Paul *et al.* 1991; Cook *et al.* 1991a) are (1) GX 1+4, (2) GX 354+0 (3) MXB 1730-335 ("Rapid Burster"), (4) SLX 1732-304, (5) SLX 1735-269, (6) GX 359+2 (7) SLX 1737-282, (8) A1743-322, (9) 1E 1743.1-2843, (10) SLX 1744-299, (11) GX 3+1, (12) GX 5-1.

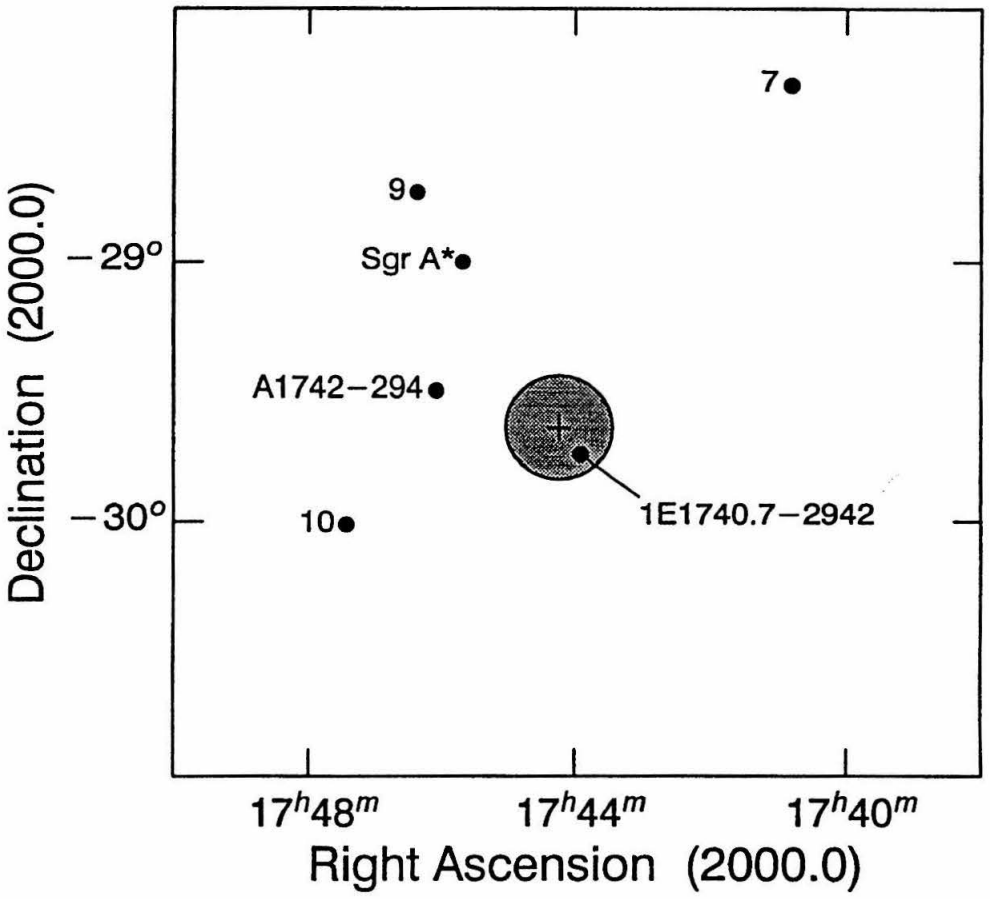

Figure 4.2: Expanded view of the source region showing the 90% confidence error circle for the location of the γ-ray source. Only 1E 1740.7–2942 appears within the error circle. Known hard X–ray sources are numbered as in Fig. 4.1.

for GRS 1758-258 would be $(2.6 \pm 0.7) \times 10^{-5}\,\mathrm{cm^{-2}\,s^{-1}\,keV^{-1}}$. This value is somewhat lower than the 100 keV flux of $(4.8 \pm 0.3) \times 10^{-5}\,\mathrm{cm^{-2}\,s^{-1}\,keV^{-1}}$ derived from SIGMA observations of 1990 March-April and September-October (Sunyaev *et al.* 1991a); however, the difference is not surprising given the observed variability of GRS 1758-258 (Cordier *et al.* 1991).

Also in the FOV during these observations was the burst source GX354+0. In 1988, GRIP detected GX354+0 near its maximum nonburst brightness (Cook *et al.* 1991b; Cook *et al.* 1991a), having a flux of approximately 100 mCrab between 35 and 122 keV. It has recently been seen by SIGMA at a flux level of 75 mCrab (Gilfanov *et al.* 1992). GX354+0 was not detected in the 1989 GRIP observations. Employing a flat input spectrum (a power law with an exponent of zero) yields a 95% confidence upper limit to the flux from GX354+0 of $1.8 \times 10^{-5}\,\mathrm{cm^{-2}\,s^{-1}\,keV^{-1}}$ (approximately 10 mCrab) in an energy band from 35 to 122 keV.

4.4.2 Spectrum

The photon number spectrum for 1E 1740.7–2942, based on all 14.0 hours of data (both daytime and nighttime periods), is shown in Figure 4.3. Above 200 keV, no significant flux was detected from 1E 1740.7–2942, and upper limits at the 95% confidence level for energy bands above 200 keV are given in Figure 4.3. A flux measurement made in a 90 keV wide energy band centered near 511 keV, with a narrow positron annihilation line input spectrum, gives a 95% confidence upper limit to the 2γ positron annihilation radiation flux from 1E 1740.7–2942 of $3.7 \times 10^{-4}\,\mathrm{cm^{-2}\,s^{-1}}$.

Between 35 and 200 keV, the data are well fit (cf. Equation A2) by a single power law ($dJ/dE = K(E/100keV)^{-\gamma}$), with a spectral slope of $\gamma = 2.2 \pm 0.3$ and flux normalization of $K = (7.0 \pm 0.7) \times 10^{-5}\,\mathrm{cm^{-2}\,s^{-1}\,keV^{-1}}$. Parameter errors are defined by an increase of 2.3 in χ^2, appropriate for a two parameter fit and 68% confidence (Lampton, Margon, and Bowyer 1976; Avni 1976). Figure 4.4 shows confidence regions for this fit at the ${\chi^2}_{min} + 1$ and ${\chi^2}_{min} + 2.3$ levels.

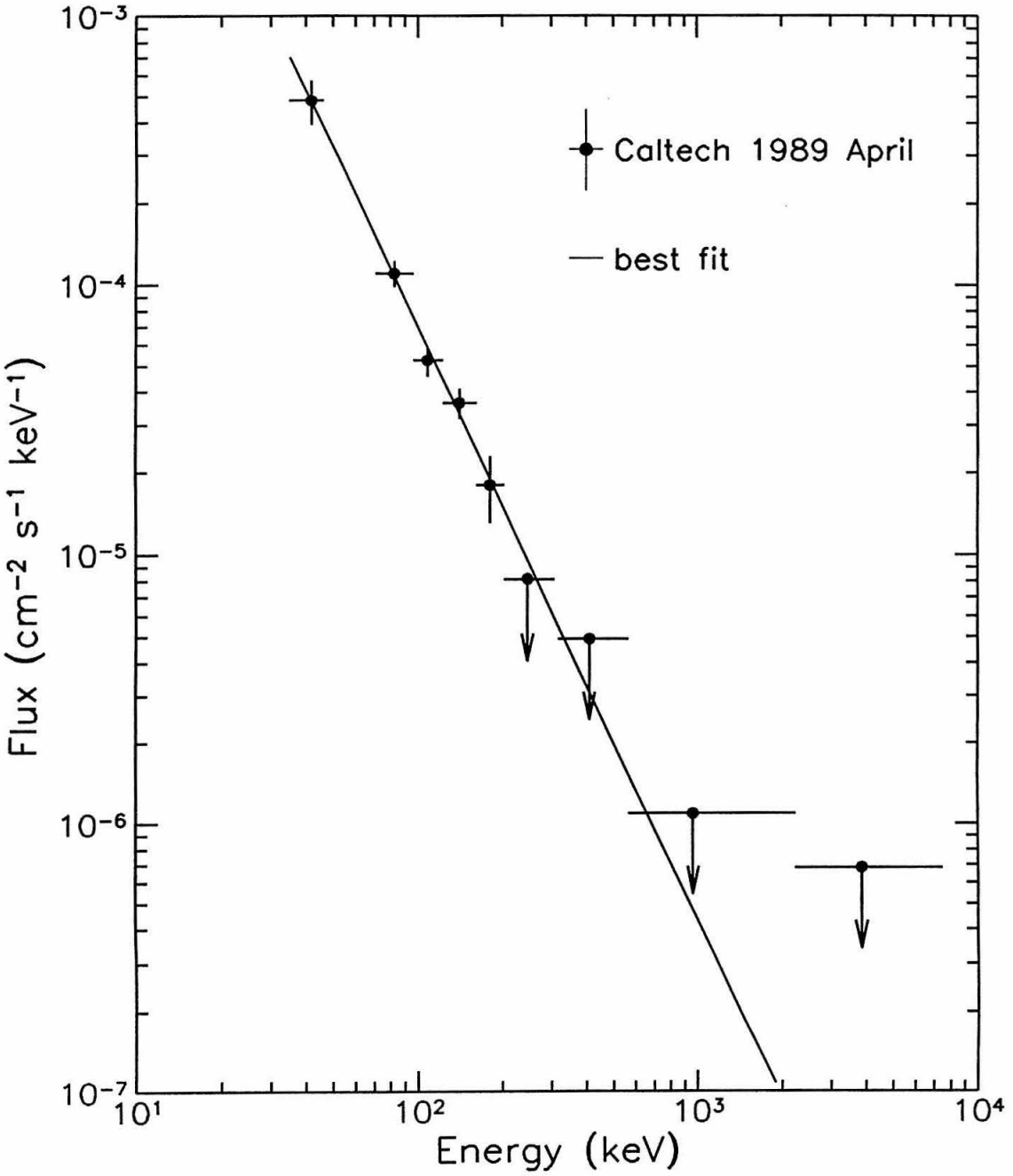

Figure 4.3: Photon number spectrum of 1E 1740.7–2942. Upper limits are at the 95% confidence level. Also shown is the best fit power-law spectrum [$dJ/dE = K(E/100\ keV)^{-\gamma}$]: $K = (7.0 \pm 0.7) \times 10^{-5}$ cm^{-2}s^{-1}keV^{-1}, $\gamma = 2.2 \pm 0.3$.

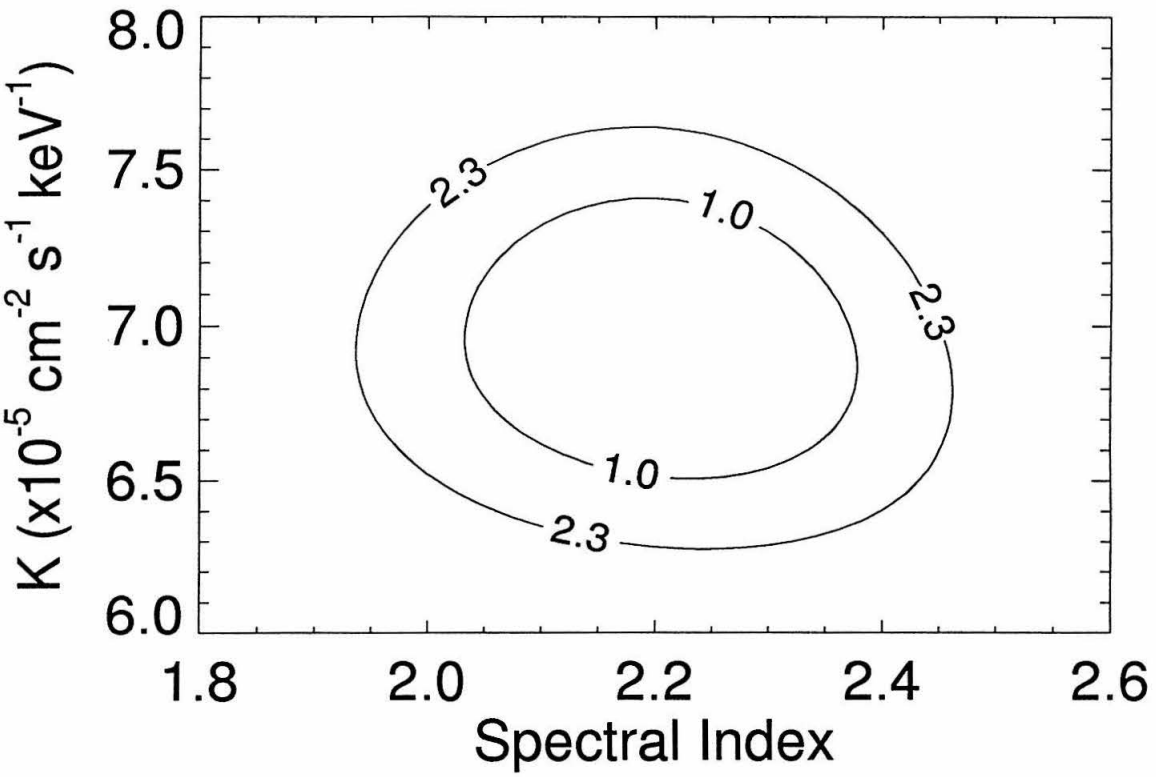

Figure 4.4: χ^2 contours for the power-law fit in Fig. 4.3. Contours are at $\chi^2_{min}+1$ and $\chi^2_{min}+2.3$, where χ^2_{min} is the value for the best-fit parameters. These levels give 68% confidence regions for one and two parameter fits, respectively. The reduced χ^2 of the two parameter fit is 1.0 for 58 d.o.f.

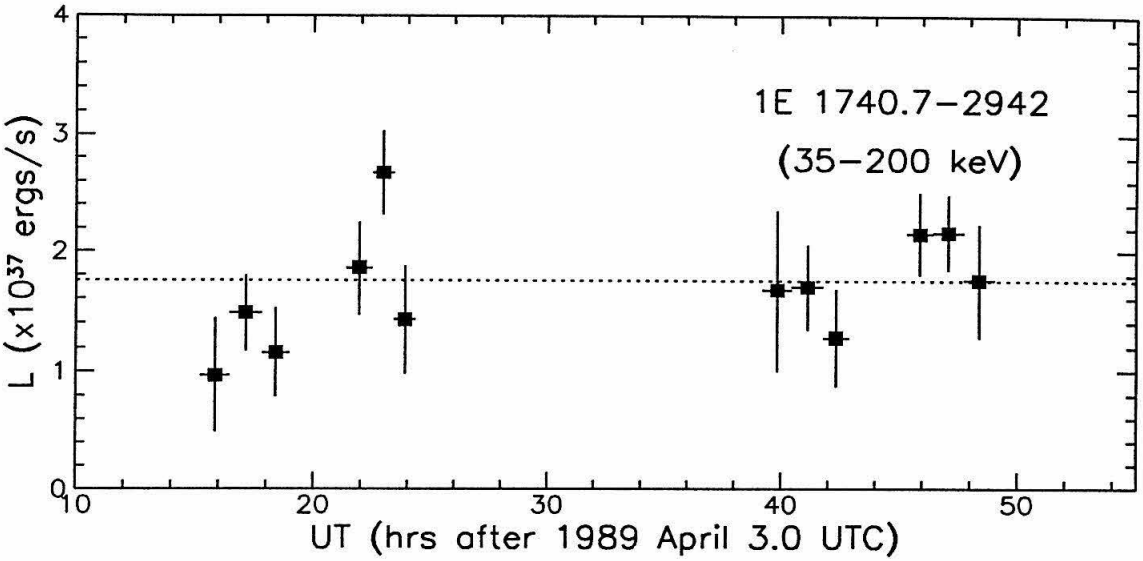

Figure 4.5: Time history of the 35–200 keV luminosity of 1E 1740.7–2942, assuming a source distance of 8.5 kpc. The best-fit flux level is indicated by the dashed line and has a reduced χ^2 of 1.61 for 11 d.o.f.

Figure 4.5 shows the time history of the 35 to 200 keV luminosity, calculated from the integral of the $E^{-2.2}$ power law fit and assuming a source distance of 8.5 kpc. Fitting the measurements to a single luminosity yields a value of $(1.7 \pm 0.1) \times 10^{37}$ ergs cm^{-2} s^{-1}, with a reduced χ^2 of 1.61 with 11 degrees of freedom. The probability of exceeding this χ^2 is 9%, giving no strong evidence for variability on these time scales.

The sensitivity of GRIP makes it possible to search on hour time scales for the presence of a feature such as the 300-600 keV excess observed by SIGMA. The 95% confidence level upper limits to the flux in the 300-600 keV region are shown in Figure 4.6. Variations in the upper limits are due to the time-variable atmospheric depth of the observations and statistical fluctuations in the images. Also shown in Figure 6 is the combined upper limit from the entire observation and the flux level from the SIGMA 1990 October measurement. It is apparent that on hour time scales during the GRIP observation, the 300-600 keV excess was not present at the level seen by SIGMA.

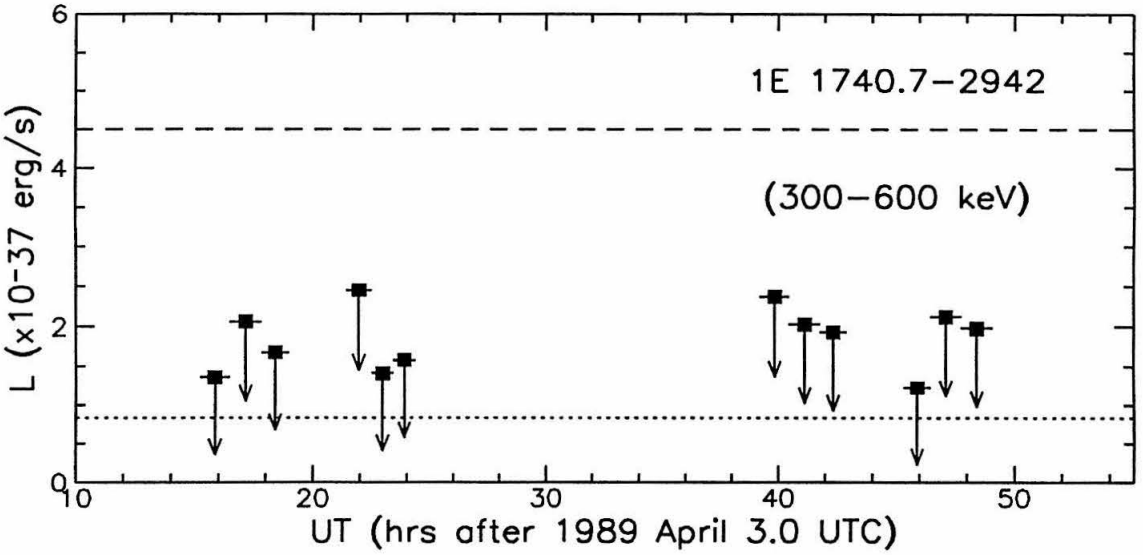

Figure 4.6: 95% confidence upper limits to the 300–600 keV luminosity of 1E 1740.7–2942 as a function of time, assuming a source distance of 8.5 kpc. The dashed line is the flux level seen by SIGMA on 1991 October 13–14 (Sunyaev *et al.* 1991b). Integrating the SIGMA "bump" spectrum from Bouchet *et al.* (1991) gives a somewhat higher value for the 300–600 keV luminosity. The dotted line shows the overall limit for the entire GRIP observation.

4.5 Discussion

The GRIP 1989 April spectrum for 1E 1740.7–2942 is very similar to those measured by GRIP in 1988 April (Cook *et al.* 1989; Cook *et al.* 1990; Cook *et al.* 1991b), EXITE in 1989 May (Covault, Manandhar, and Grindlay 1990), SIGMA in 1990 March, April, and September (Sunyaev *et al.* 1991a; Sunyaev *et al.* 1991b; Paul *et al.* 1991; Bouchet *et al.* 1991; Schmitz-Fraysse *et al.* 1992), and by HEXE in 1989 March (Skinner *et al.* 1991) (see Figure 4.7, discussed below). The consistency of these measured spectra in the period 1988-1990 serves to define the 'normal' emission state and suggests that this state was predominant over a period of years. No variability was reported for 1E 1740.7–2942 prior to the discovery of the hard state by SIGMA. Recently, however, Bazzano *et al.* (1992) reported that on 1989 May 9, just six weeks after the GRIP observation, 1E 1740.7–2942 was in the low state. The time scale of this variability implies a size of $< 4 \times 10^{17}$ cm for the hard X-ray emission region. A stronger limit of $< 10^{17}$ cm is set using the EXITE observation which occurred 4 weeks after the GRIP observation. This can be compared with the upper limit from the SIGMA observations of a few times 10^{15} cm for the region responsible for the excess hard state emission. Although these limits differ by almost two orders of magnitude, they cannot rule out a single region for both the normal and hard state emissions.

The spectra from imaging and narrow FOV ($< 2°$) hard X-ray observations of 1E 1740.7–2942 prior to 1990 October are shown together in Figure 4.7. The close agreement between the normal state measurements, made with several different instruments, is notable. The normal state spectrum between 35 and 200 keV is similar to the γ_2 and γ_3 states of Cygnus X-1 (Ling *et al.* 1987; Cook *et al.* 1991b) both in spectral shape and total luminosity. Because of these similarities, it is natural to speculate that similar processes are at work in both systems. Cygnus X-1 is believed to be a stellar mass black hole accreting from its blue supergiant companion. Its spectrum has been well fit using a Comptonized model (Liang and Dermer 1988; Sunyaev and Titarchuk 1980). Fitting a Sunyaev and Titarchuk (1980) Comptonized

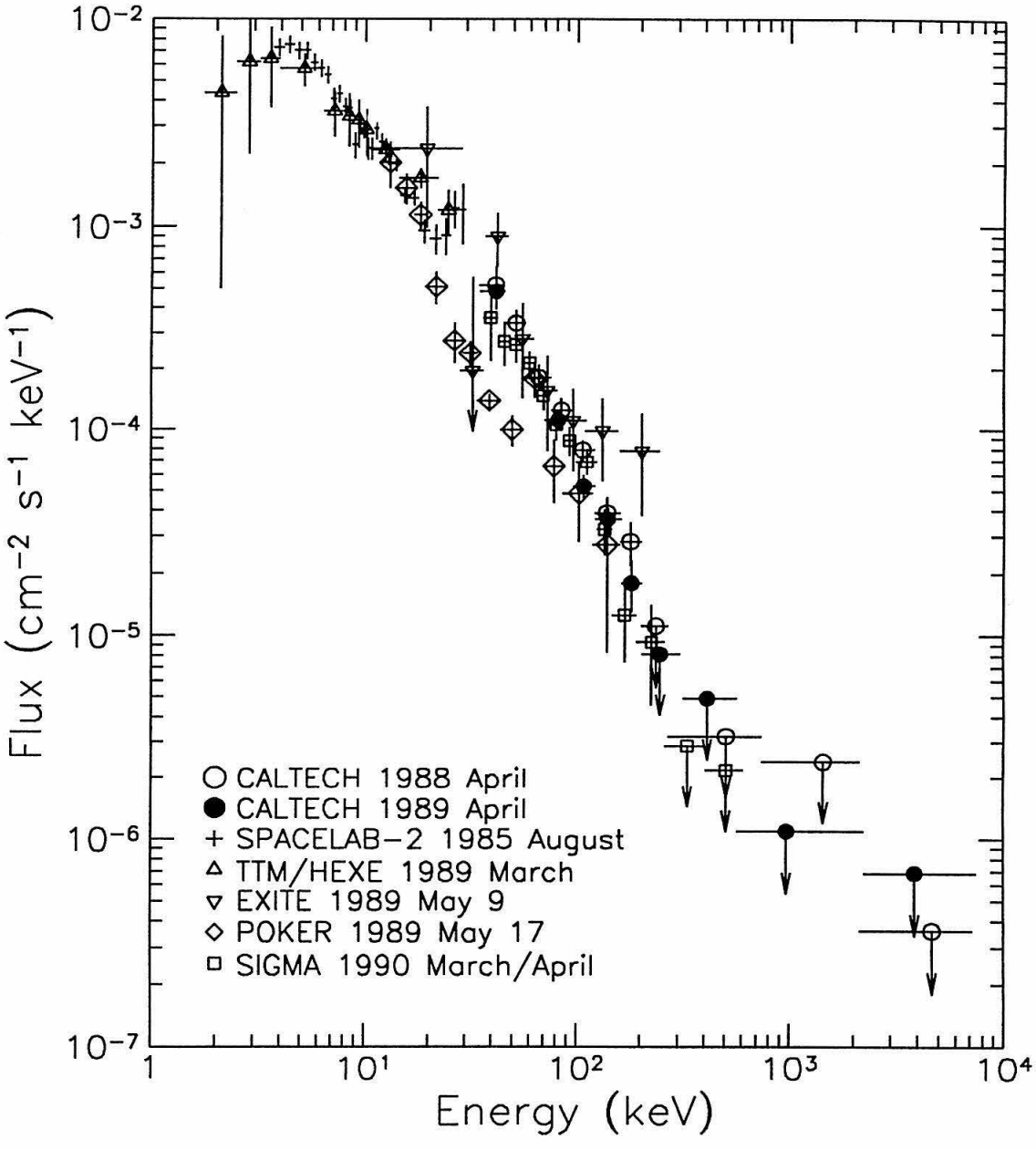

Figure 4.7: Comparison of 1E 1740.7–2942 imaging and narrow FOV spectra. Shown are spectra from all hard X–ray and $< 2°$ FOV observations made prior to 1990 October (Cook *et al.* 1991b; Skinner *et al.* 1991; Skinner *et al.* 1989; Covault, Manandhar, and Grindlay 1990; Bazzano *et al.* 1992; Bouchet *et al.* 1991). With the exception of Bazzano *et al.* (1992), all these observations found 1E 1740.7–2942 to be in its "normal" state.

spectrum to the derived fluxes in Figure 4.3 yields an electron temperature of kT $\approx$ 50 keV and an optical depth of 2. Because of the energy range of the GRIP flux measurements, these values are not well constrained, although they are consistent with those measured by SIGMA (Sunyaev *et al.* 1991b) and HEXE (Skinner *et al.* 1991).

Although the normal state of 1E 1740.7–2942 appears to have been stable on long time scales, it is interesting to ask if this apparent long-term stability of the power law continuum might overlie variability on shorter time scales, as seen in Cygnus X-1. While the results shown in Figure 4.5 may appear to give some indication of variability, they do not strongly contradict a constant flux. We conclude that the power law spectrum was relatively stable on hour time scales during the GRIP observation. This is in agreement with the HEXE result (Skinner *et al.* 1991), which reported no variability in 1E 1740.7–2942 on time scales from minutes to months.

An intriguing observational question concerning the Galactic center region is the nature of the time variable positron annihilation radiation seen there. The first evidence of variability came from observations made with the *HEAO-3* satellite, which showed a significant decrease in 511 keV emission from the Galactic center region between the fall of 1979 and spring of 1980 (Riegler *et al.* 1985; Riegler *et al.* 1981). Between 1988 May and October, the GRIS balloon-borne germanium spectrometer detected an increase in 511 keV line radiation, finding fluxes inconsistent with a constant value at the 95% confidence level (Gehrels *et al.* 1991). A measurement with another balloon-borne germanium spectrometer, the UCSD/France instrument HEXAGONE, in 1989 May (Chapuis *et al.* 1991), only 7 weeks after the GRIP flight, showed the line flux to again have decreased to a level consistent with known diffuse Galactic plane emission (Gehrels 1991). The SIGMA 'bump' emission, which is likely the result of e^+e^- annihilations in a hot pair plasma (Bouchet *et al.* 1991), seems to be another signature of the action of positrons, this time from a definite source: 1E 1740.7–2942. In fact, such direct evidence of the presence of positrons associated with 1E 1740.7–2942 makes it a very strong candidate for the variable 511 keV source. However, the lack of narrow line emission prevents a positive identification. Thus, the identification of the 511 keV source awaits an imaging experiment to detect the

direct annihilation photons.

The GRIP 95% confidence upper limit of $3.7 \times 10^{-4}\,\mathrm{cm}^{-2}\,\mathrm{s}^{-1}$ for 511 keV line flux from 1E 1740.7–2942 is significantly lower than the limit of $6.8 \times 10^{-4}\,\mathrm{cm}^{-2}\,\mathrm{s}^{-1}$ obtained by GRIP for 1E 1740.7–2942 in 1988 (Cook *et al.* 1991b). Gehrels (1991) derived a compact source strength of $(3.9 \pm 2.7) \times 10^{-4}\,\mathrm{cm}^{-2}\,\mathrm{s}^{-1}$ from the HEXAGONE measurement by subtracting a contribution based on a model of the diffuse Galactic plane 511 keV emission having a flat distribution and a strength of $1.2 \times 10^{-3} cm^{-2} s^{-1} rad^{-1}$. This is in agreement with the GRIP upper limit, and both measurements are below the level of $(7.8 \pm 1.6) \times 10^{-4}\,\mathrm{cm}^{-2}\,\mathrm{s}^{-1}$ derived for the GRIS 1988 October measurement Gehrels (1991). Therefore, if 1E 1740.7–2942 were the compact source of annihilation photons seen by GRIS, it subsequently entered a low or off state.

We acknowledge the important contributions to the development of the GRIP telescope made by W. Althouse, D. Burke, A. Cummings, M. Finger, C. Starr, J. Weger, and the personnel of the Central Engineering Services at Caltech. We thank the personnel of the National Scientific Balloon Facility and the NASA Wallops Flight Facility for their excellent balloon launch support. This work was supported in part by NASA grant NAGW-1919. W. Heindl is supported under the NASA GSRP, NGT-50804.

4.6 Appendix: Source Flux Determination

In X-ray and gamma-ray astronomy it is desirable to give the detector count spectrum as well as the deconvolved source flux spectrum. The former gives a model independent representation, but can have a strong instrumental signature. The latter gives a model dependent estimate of the actual source spectrum, removing to a large extent the instrumental signature by taking into account the instrument response matrix. In the case of GRIP, it is not possible to give a simple instrument count spectrum, because parameters such as line of sight atmospheric depth and collimator transmission for a given source direction vary over the duration of an observation. Therefore we give source flux values for individual energy bins which are as model

independent as possible.

In an instrument with perfect energy resolution (i.e., a source photon of energy E is always detected with energy E, or equivalently, the instrument response matrix is diagonal), the determination of the photon flux in a given energy bin is independent of the true spectral shape of the source. Because only photons with energies in a particular bin contribute to that bin, the source flux may be directly determined from the count spectrum and the (diagonal) detector response matrix.

However, for an instrument with finite energy resolution, the nature of the source spectrum affects the determination of fluxes through the off-diagonal terms in the response matrix. For example, for a source with a steep spectrum, photons with energies below a given energy bin may contribute significantly to the counting rate in that bin. At the same time, photons with energies within that bin will be lost to nearby bins. Therefore, in order to account for these effects, the determination of fluxes in individual energy bins must make some assumption about the true nature of the source spectrum. Because our aim is to produce a model independent flux spectrum, it is desirable that these assumptions have a minimal effect on the derived fluxes. Our approach is to employ the best fit spectral shape, as determined from the full set of energy bins, to the derivation of fluxes in individual energy bins. We then verify that varying the assumed spectral shape has only a small effect on the resultant flux values. When no positive flux is detected in a given energy bin, a flat spectrum (i.e., a power law with a spectral index of 0) is assumed for the purpose of setting upper limits.

As mentioned in §3.2., the source flux values are estimated using a forward convolution method. The data are first divided into time periods over which variations in parameters such as atmospheric depth and source attenuation due to the collimator are small. For each period, an image is produced for each energy bin of interest. These images, derived from disjoint data sets, are statistically independent.

The image values at the source location in the individual images are designated $i_{\alpha n}$, where α denotes the time period and n the energy bin. A spectral class, $dJ/dE(\psi, E)$, with N adjustable parameters, $\psi = (\psi_0, \psi_1, ...)$, is then chosen as a set of model spectra. As applied here, one of the parameters is an overall normalization,

while the others (e.g., the spectral index in a power law) determine the spectral shape.

The parameters, ψ, are varied over a physically reasonable range, with each set of values corresponding to a separate model spectrum. To determine χ^2 for a given model, the model spectrum is integrated with the instrument response function, $R_{\alpha n}(E)$, appropriate for each time period and energy bin. The response function includes the time-dependent effects of varying atmospheric depth and collimator attenuation, as well as energy-dependent effects such as attenuation in passive instrument material, the energy resolution and position resolution of the detector, and the overall imaging properties of the instrument. This integration produces a set of predicted image values, $\hat{i}_{\alpha n}(\psi)$, corresponding to the measured image values $i_{\alpha n}$.

$$\hat{i}_{\alpha n}(\psi) = \int_0^\infty \frac{dJ}{dE}(\psi, E) R_{\alpha n}(E) dE; \tag{4.1}$$

χ^2 is then given by

$$\chi^2 = \sum_\alpha \sum_n \left\{ \frac{[i_{\alpha n} - \hat{i}_{\alpha n}(\psi)]^2}{{\sigma_{\alpha n}}^2} \right\} \tag{4.2}$$

where $\sigma_{\alpha n}$ is the standard deviation in the measured image value and depends only on the energy bin, n, and the number of events contributing to the image. Because almost all GRIP observations are background dominated with a large number of events contributing to each image, $\sigma_{\alpha n}$ is model independent, and may be determined from the measured number of counts contributing to the image. The model parameters which minimize χ^2define the best fit spectral shape and are denoted ψ^*, with ψ_0^* as the overall normalization.

Once a spectral shape has been determined, the source fluxes in individual energy bins may be determined. This is done by integrating the best fit spectral shape, employing unit normalization ($\psi_0^* = 1$), with the instrument response function to get a second set of predicted image values, $\hat{i}_{\alpha n}(\psi^*; \psi_0^* = 1)$. The flux normalization in a given energy bin for a specific time period is then:

$$\kappa_{\alpha n} = \frac{i_{\alpha n}}{\hat{i}_{\alpha n}(\psi^*; \psi_0^* = 1)}, \tag{4.3}$$

with the statistical uncertainty in $\kappa_{\alpha n}$ given by:

$$\sigma_{\kappa_{\alpha n}} = \frac{\sigma_{\alpha n}}{\hat{i}_{\alpha n}(\psi^*; \psi_0^* = 1)}. \tag{4.4}$$

A weighted average of the $\kappa_{\alpha n}$ over the time periods, α, then gives the flux normalization for the energy bin n:

$$\overline{\kappa}_n = \left(\frac{\sum_\alpha \kappa_{\alpha n}/\sigma^2_{\kappa_{\alpha n}}}{\sum_\alpha 1/\sigma^2_{\kappa_{\alpha n}}} \right). \tag{4.5}$$

The flux, $F_n(\overline{E}_n)$, is then given by:

$$F_n = \overline{\kappa}_n \times \frac{dJ}{dE}(\psi^*; \psi_0^* = 1; E = \overline{E}_n) \tag{4.6}$$

where $\overline{E}_n$ is the mean energy in bin n.

It is through relation (4.6) that the fluxes derived for individual energy bins depend on the chosen spectral shape, and thus on the data in all energy bins and time periods used in the determination of χ^2. However, it is the case for GRIP that the fluxes derived in this fashion are relatively insensitive to changes in the input spectrum, and these systematic errors are small compared to the statistical errors. For the case of 1E 1740.7–2942, varying the spectral index between 0 and 4 resulted in changes in the derived fluxes of less than 12%.

In order to search for time variability, the average in equation (4.5) is taken over energy bins rather than time periods. This method provides a measurement of the flux normalization for each time period. The product of this normalization and the spectral shape (cf. eq. [4.6])) is then integrated over energy to determine integral fluxes.

Chapter 5

ROSAT and VLA Observations

To appear in
The Astrophysical Journal, August 1, 1994

OBSERVATIONS OF 1E 1740.7-2942 WITH *ROSAT* AND THE VLA

WILLIAM A. HEINDL, THOMAS A. PRINCE, AND
JOHN M. GRUNSFELD[1]
Division of Physics, Mathematics, and Astronomy, California Institute of Technology, M.S. 220-47, Pasadena, CA 91125

ABSTRACT

We have observed the Galactic black hole candidate 1E 1740.7–2942 in X–rays with both the *ROSAT* HRI and PSPC and at 1.5 and 4.9 GHz with the VLA. From the HRI observation we derive a position for 1E 1740.7–2942 of Right Ascension $= 17^h43^m54^s.9$, Declination $= -29°44'45''.3$ (J2000), with a 90% confidence error circle of radius $8''.5$. Thermal bremsstrahlung fits to the PSPC data yield a column density of $1.12^{+1.51}_{-0.18} \times 10^{23}$ cm^{-2}, consistent with earlier X–ray measurements. The VLA observation at 4.9 GHz revealed two sources. Source 'A', which is the core of a double aligned radio jet source (Mirabel *et al.* 1992), lies within the *ROSAT* error circle, further confirming its identification with 1E 1740.7–2942.

Subject headings: Black Holes — X-Rays: sources — Radio Sources: Identifications

5.1 Introduction

Since 1985, observations in the hard X–ray and soft γ-ray energy bands have shown 1E 1740.7–2942 to be the dominant source in the central few degrees of the Galactic center region (Skinner *et al.* 1987; Cook *et al.* 1991b). This fact and the observation by SIGMA (Bouchet *et al.* 1991) of a transient hard excess in the spectrum suggestive of positron annihilation motivated a campaign of multi-wavelength observations aimed at discovering the nature of this unusual source. The search for counterparts has been carried out at radio (Prince *et al.* 1991b; Mirabel *et al.* 1992; Gray, Cram, and Ekers 1992; Mirabel *et al.* 1993), millimeter (Mirabel *et al.* 1991; Bally and Leventhal 1991), infrared (Prince *et al.* 1991b; Mirabel and

[1]Current address: NASA Johnson Space Center, Code CB, Houston, TX 77058.

Duc 1992; Djorgovski, Thompson, and Mazzarella 1992), and optical (Skinner *et al.* 1991; Mereghetti *et al.* 1992; Leahy, Langill, and Kwok 1992; Bignami, Caraveo, and Mereghetti 1993) wavelengths. The radio observations have shown that the compact central core of a double radio jet lies within the X–ray error circle, and the millimeter observations reveal a line of sight alignment with a dense molecular cloud. If this molecular cloud is associated with 1E 1740.7–2942, it might provide a source of material for accretion as well as a medium for the slowing and annihilation of positrons present in the radio jets (Mirabel *et al.* 1991). It is therefore important to determine whether 1E 1740.7–2942 lies within the molecular cloud. The X–ray spectrum is a sensitive diagnostic of the source column depth, N_H, and so can shed light on the relationship of 1E 1740.7–2942 and the molecular cloud. Knowledge of the column depth is also important to the interpretation of optical and infrared data, as the level of extinction limits the sensitivity of counterpart searches at these wavelengths.

We report here the results of observations of 1E 1740.7–2942 at X–ray wavelengths using the high resolution imager (HRI) and position sensitive proportional counter (PSPC) on *ROSAT* and at 1.5 GHz and 4.9 GHz using the Very Large Array (VLA) in Socorro, New Mexico. Preliminary results of the HRI and VLA observations have been reported in Prince *et al.* (1991a) and Prince *et al.* (1991b) respectively.

5.2 Observations

The HRI observation was performed during the period 1991 March 20 – 24. It incorporates 11 observation intervals of between 850 and 2500 s duration for a total live time of 19900 s. While 1E 1740.7–2942 apparently remained in its normal state throughout 1990, observations by SIGMA (Mandrou *et al.* 1993) in 1991 February and March showed that 1E 1740.7–2942 entered a low state (hard X–ray luminosity of ~ 0.25 of normal) prior to our HRI observation.

The PSPC observation was split over two observing periods – the first between 1992 September 28 and October 4 (hereafter PSPC-I) and the second between 1993 March 23 and 28 (hereafter PSPC-II). PSPC-I encompassed 12 observation in-

tervals for a total livetime of 15160 s, and PSPC-II comprised 7 observation intervals with a total livetime of 13070 s. SIGMA observations prior to PSPC-I and spanning PSPC-II give an indication of the likely state of 1E 1740.7–2942 during the *ROSAT* pointings. In 1992 September, 1E 1740.7–2942 was seen to be in its normal state. By 1993 March it entered the "sub-luminous" state (Churazov *et al.* 1993b) described by Cordier *et al.* (1993c).

We observed the region of the *Einstein* IPC 1E 1740.7–2942 error circle (see Figure 5.2) with the VLA on 1989 March 2. The observations were made at 1.5 and 4.9 GHz for a duration of 4.5 hr each. The array was in the A/B configuration which provides a good point spread function for southern sources (Bridle 1986).

5.3 Analysis and Results

5.3.1 HRI Error Circle

The HRI observation revealed three sources near the center of the field of view (FOV) (see Figures 5.5 and 5.1). Only source "1" is consistent in location with previous error circles for 1E 1740.7–2942 (Hertz and Grindlay 1984; Skinner *et al.* 1987; Kawai *et al.* 1988; Skinner *et al.* 1991). In order to derive an HRI error circle, we applied corrections to the nominal image coordinates based on the HRI boresight offsets of Kürster and Hasinger (1992), who give errors in the HRI positions of 23 sources with known accurate locations. Using their data and discarding two sources with anomalously large errors, we found the average offsets for the remaining 21 sources. We then plotted the integral distribution of radial offsets in order to estimate the 90% confidence radius for any detected source. These boresight corrections dominate the final position uncertainty, resulting in a 90% confidence error circle of radius $8''.5$. The best fit coordinates (epoch J2000.0) to source "1" (= 1E 1740.7–2942), are: Right Ascension = $17^h43^m54^s.9$ and Declination = $-29°44'45''.3$.

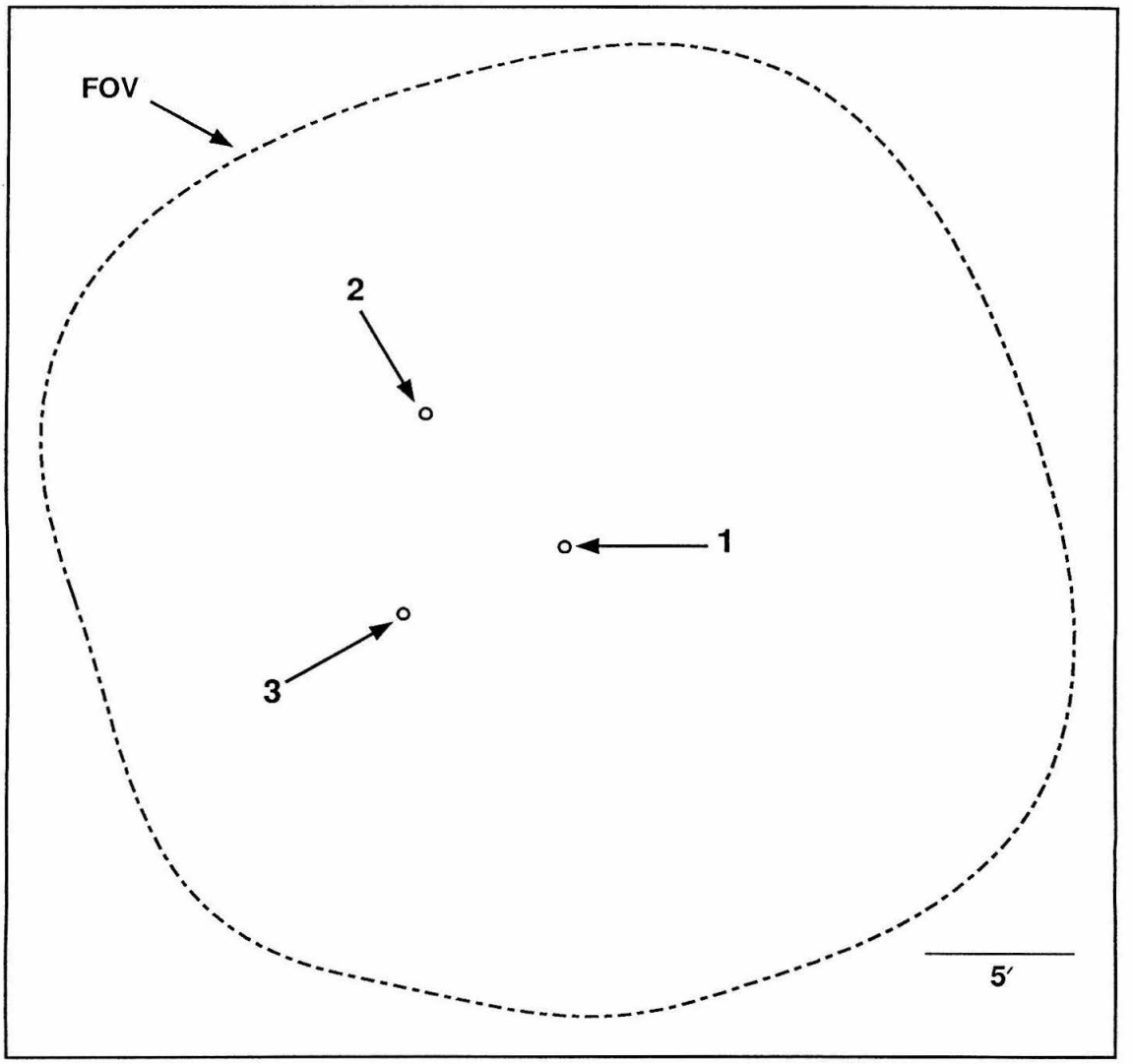

Figure 5.1: Diagram of the *ROSAT* HRI image of the 1E 1740.7–2942 field obtained during 1991 March 20 – 24. The actual image appears in Figure 5.5. Three sources were detected near the center of the field. Only source "1" is consistent with previous X–ray error circles for 1E 1740.7–2942. North is up and east is to the left.

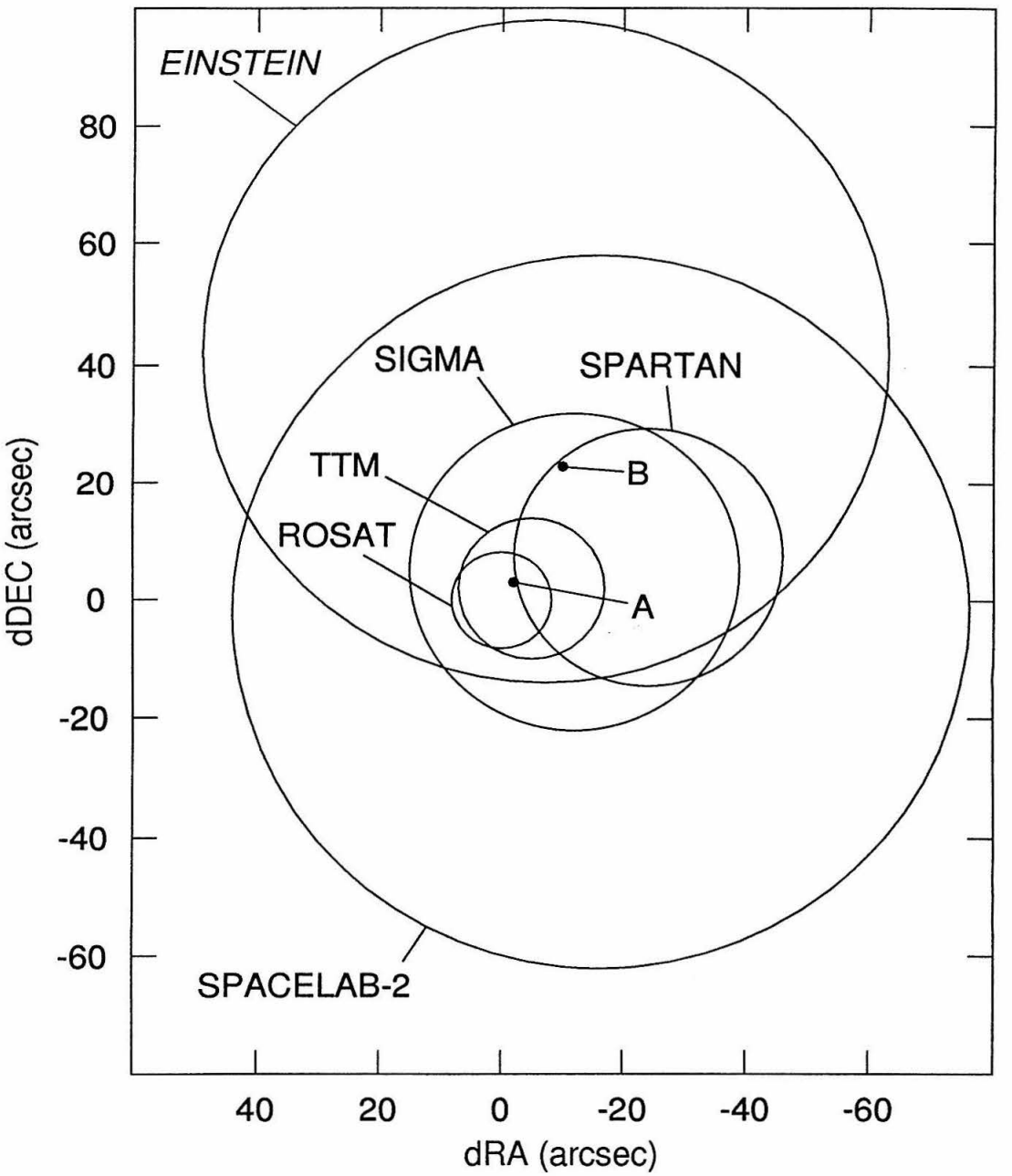

Figure 5.2: X–ray and hard X–ray error circles for 1E 1740.7–2942. Also shown are the positions of the VLA sources 'A' and 'B'. Offsets are relative to the HRI X–ray position: R.A. = $17^h43^m54^s.9$, Dec. = $-29°44'45''.3$ (J2000). References: *Einstein*, (Hertz and Grindlay 1984); Spacelab 2, (Skinner *et al.* 1987); SIGMA, (Cordier *et al.* 1993c); Spartan-1, (Kawai *et al.* 1988); TTM, (Skinner *et al.* 1991).

5.3.2 Spectrum

We analyzed the PSPC observations assuming both power law and thermal bremsstrahlung models. Model parameters were estimated using the likelihood ratio method (Cash 1979). PSPC-I and PSPC-II were treated individually and also summed to form a single measurement. Table 5.1 summarizes the results of the spectral fits. Because the nominal PSPC energy range extends only to 2.5 keV, the data do not place an upper bound on the source temperature, and no physical constraints on a power law index are obtained. Under the bremsstrahlung model, however, only a relatively narrow range of column densities are allowed for temperatures between 0.1 and 100 keV. In addition, models with temperatures below $\sim$0.5 keV resulted in significantly worse fits than temperatures above $\sim$1 keV. For these reasons, the thermal bremsstrahlung column densities and fluxes in Table 5.1 were calculated assuming $kT = 14.3$ keV, while the column densities for the power law model assumed a photon index of 2, both corresponding to the best fit values from the Spartan-1 measurement (Kawai *et al.* 1988). As a check on our spectral fits, we used the instrument response and spectral modeling software contained in the *ROSAT* Mission Information and Planning System (MIPS) to predict count rates for the best fit column depth and normalization, based on the thermal bremsstrahlung spectra in Table 5.1. The predicted rates were statistically consistent with the measured values. Figure 5.3 shows the measured source count spectrum together with a folded thermal bremsstrahlung spectrum ($kT = 14.3$ keV, $N_H = 1.12 \times 10^{23}$ cm^{-2}). We note that images produced from the pulse invariant energy channels > 256 (the limit of the current PSPC response matrix) show significant counts from 1E 1740.7–2942 and should provide improved fits when the response matrix is extended.

5.3.3 Other Sources

In addition to the HRI sources "2" and "3", several sources were detected in the PSPC. Figure 5.6 shows the central region of the PSPC image for the entire observation including both PSPC-I and PSPC-II. 1E 1740.7–2942 and the well-known source A1742-294 (=1E 1742.9-2929) (van Paradijs 1993) are labeled by name.

TABLE 5.1

Spectral fits to the *ROSAT* observations.

	1990 March HRI	1992 Sept.–Oct. PSPC-I	1993 Mar. PSPC-II	Combined PSPC
Rate $(10^{-3}\ s^{-1})$	1.9 ± 0.3	3.3 ± 0.7	2.0 ± 0.7	2.7 ± 0.5
Thermal Bremsstrahlung:				
N_H $(10^{23}\ cm^{-2})$ [a]	...	$1.26^{+1.72}_{-0.21}$	$0.92^{+1.58}_{-0.20}$	$1.12^{+1.51}_{-0.18}$
L_{2-10} (kT = 14.3 keV)	~ 3.9[b]	$2.6^{+3.1}_{-1.4}$	$0.44^{+0.57}_{-0.27}$	$1.3^{+1.2}_{-0.6}$
$(10^{36}$ ergs s^{-1} at 8.5 kpc)				
Power Law ($\gamma = 2$):				
N_H $(10^{23}\ cm^{-2})$	...	$1.32^{+0.24}_{-0.20}$	$0.98^{+0.25}_{-0.23}$	$1.18^{+0.17}_{-0.15}$
Flux at 1 keV	...	$0.11^{+0.13}_{-0.06}$	$0.02^{+0.03}_{-0.01}$	$0.05^{+0.04}_{-0.02}$
$(cm^{-2}\ s^{-1}\ keV^{-1})$				
Hard X–ray State (Mandrou *et al.* 1993)	low	normal	sub-luminous	...

[a] Best fit assumes $kT = 14.3$ keV (Kawai *et al.* 1988), errors are 68% confidence for 0.1 keV $< kT <$ 100 keV.

[b] Estimated by folding the combined PSPC spectrum through the HRI response.

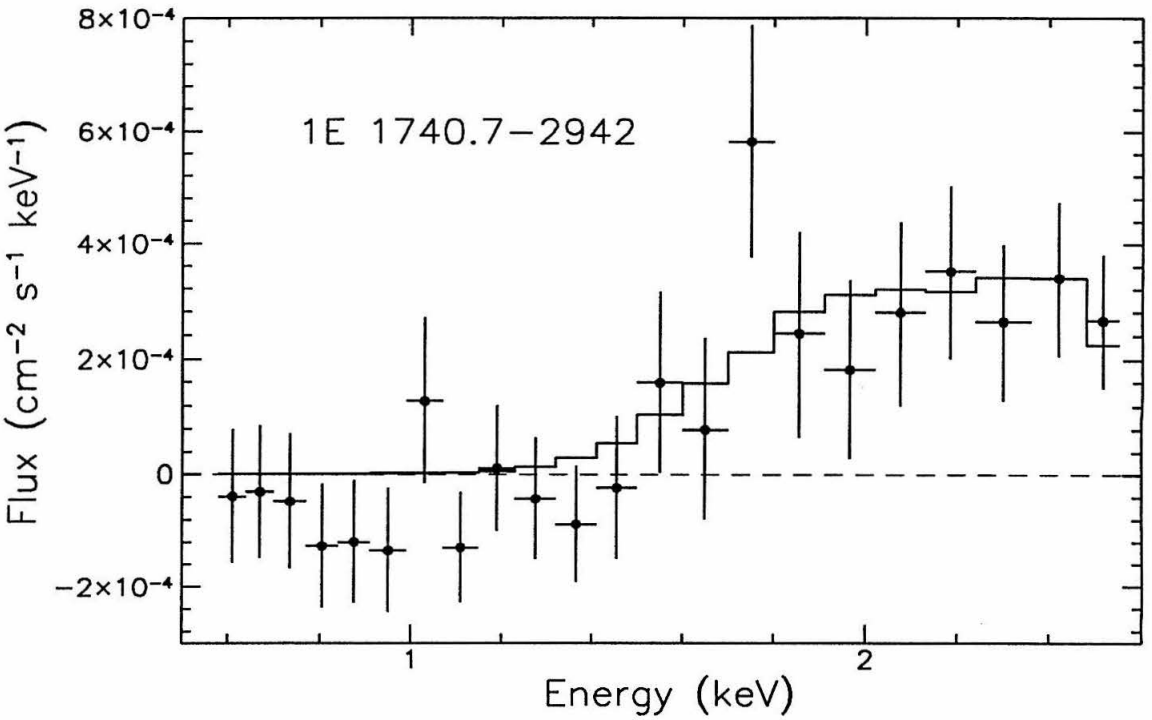

Figure 5.3: Background subtracted PSPC count spectrum of 1E 1740.7–2942 with folded thermal bremsstrahlung model. The model parameters are $kT = 14.3$ keV, $N_H = 1.12 \times 10^{23}$ cm^{-2}.

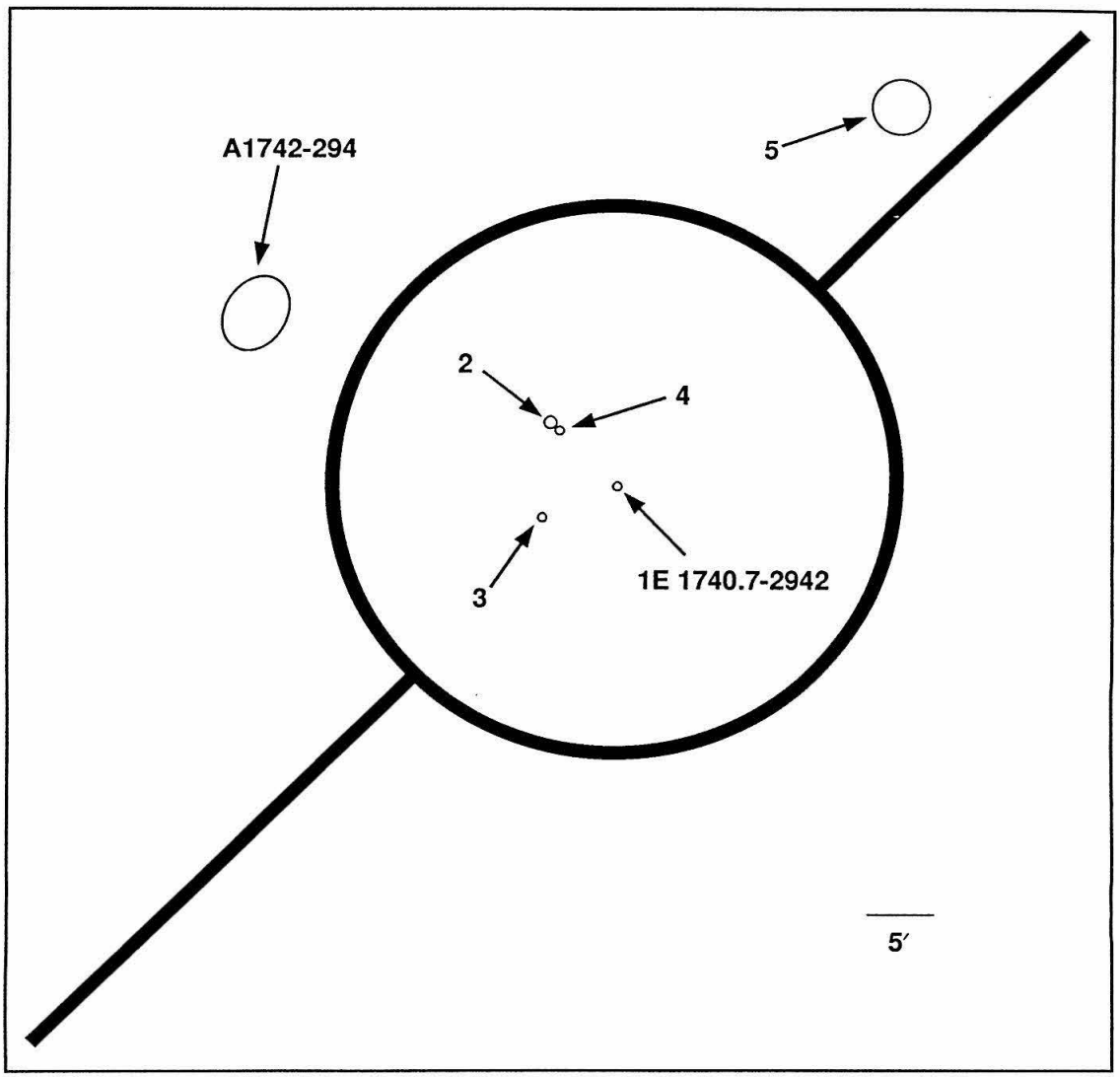

Figure 5.4: Diagram of the central region of the summed PSPC-I/II image. The actual image appears in Figure 5.6. Sources "2" and "3" are the same as in the HRI. Among other detected sources are the well-known X–ray source A1742-294 (van Paradijs 1993), a transient, "4", which appeared during a single 1400 s observation interval, and a source near the edge of the FOV, "5". The circle and diagonal lines indicate PSPC window supports. North is up and east is to the left.

TABLE 5.2

Coordinates (J2000) of the HRI and PSPC sources.

Source	Right Ascension	Declination	R_{90} ($''$)
1E 1740.7–2942	$17^h43^m54^s.9$	-29°44′45″.3	8.5
"2"	$17^h44^m17^s.7$	-29°39′45″.3	8.5
"3"	$17^h44^m21^s.5$	-29°47′17″.4	8.5
"4"	$17^h44^m15^s.4$	-29°40′14″.2	10
"5"	$17^h42^m16^s.3$	-29°15′08″.6	∼60

Sources "2" and "3" are the HRI sources. Source "4", located only ∼40″ from "2", is a transient which appeared only during a single observation interval lasting 1400 s. The small feature in the HRI image southwest of source "2" may also be due to this transient source. Table 5.2 gives coordinates for 1E 1740.7–2942 and "2," "3,", and "4" as well as 90% confidence error radii. The positions of "2" and "3" were determined in the same fashion as for 1E 1740.7–2942. The position of "4" was estimated from its offset from "2" in the PSPC image and the position of "5" was estimated from the PSPC image alone. We fit the spectrum of source "2" in order to cross check our spectral analysis technique for 1E 1740.7–2942. We find $kT = 0.77^{+0.81}_{-0.28}$ keV, $N_H = 4.7^{+2.0}_{-1.6} \times 10^{21}\mathrm{cm}^{-2}$ and photon index $\gamma = 3.7^{+1.4}_{-1.2}$ and $N_H = 6.4^{+3.0}_{-2.3} \times 10^{21}\mathrm{cm}^{-2}$ for thermal bremsstrahlung and power law models respectively. Both results are in good agreement with fits obtained using the XANADU/XSPEC (Shafer *et al.* 1990) package.

5.3.4 VLA Images

As reported in Prince *et al.* (1991b), two weak sources, 'A' and 'B', were detected in the *Einstein*/IPC error circle (see Figure 5.2). Only 'A' (R.A. = $17^h43^m54^s.75$, Dec. = -29°44′42″.7, epoch J2000.0) is consistent with the more recent X–ray error circles from HEXE/TTM (Skinner *et al.* 1991) and *ROSAT*. It has a flux of ~ 0.4 mJy at 4.9 GHz and is undetected at 1.5 GHz. Source 'B' (R.A. = $17^h43^m54^s.16$, Dec. = -29°44′42″.0, J2000), which lies outside of the new error circles, has a flux of ~ 0.25 mJy at 4.9 GHz and 1.5 mJy at 1.5 GHz and is possibly extended. As part

of their program of VLA monitoring of 1E 1740.7–2942, Mirabel *et al.* (1993) have analyzed the archival VLA data from these observations and presented coordinates and fluxes for 'A' and 'B' consistent with those given here.

5.4 Discussion

5.4.1 Association of the X–ray and Radio Sources

In Prince *et al.* (1991b), we suggested that the pointlike nature of 'A' at 4.9 GHz and the possible diffuse nature of 'B' made 'A' the more likely counterpart to 1E 1740.7–2942. Shown in Figure 5.2 is the current X–ray error circle together with those from earlier measurements and the positions of 'A' and 'B'. As was the case with the TTM error circle (Skinner *et al.* 1991), the location of 'A' is consistent with that of the X–ray source while 'B' lies outside of the error circle. Since our observations, Mirabel *et al.* (1992) have observed 1E 1740.7–2942 with the VLA in the C configuration which has increased sensitivity to low surface brightness objects. They found that source 'A' is compact, time variable, and located at the center of double radio jets, the brighter of which is source 'B'. They also estimated the probability that a random extragalactic source with a flux density of 0.4 mJy would fall in the 12″ TTM error circle to be 0.3% . The new *ROSAT* error circle is half as large and so bolsters the association by reducing the probability of a chance alignment by a further factor of two. The positional coincidence of the two sources together with correlated variability in the radio source and the hard X–rays from 1E 1740.7–2942 (Mirabel *et al.* 1992) make a strong case for the association.

5.4.2 Association with the Molecular Cloud

The column depth to 1E 1740.7–2942 has previously been measured by Spartan-1 (Kawai *et al.* 1988), ART-P and SIGMA on *GRANAT* (Sunyaev *et al.* 1991a), and TTM/HEXE on *MIR* (Skinner *et al.* 1991). Of these, the energy range of Spartan-1 (1 – 5 keV) was most appropriate, because it spans the X–ray cutoff

region. In 1985, Spartan-1 found column depths of $N_H = 1.45^{+0.26}_{-0.22} \times 10^{23}\mathrm{cm}^{-2}$ and $1.61^{+0.35}_{-0.29} \times 10^{23}\mathrm{cm}^{-2}$ assuming thermal bremsstrahlung and power law spectra respectively. The results from the other instruments ranged from $N_H \sim 0.4 \times 10^{23}\mathrm{cm}^{-2}$ to $> 3 \times 10^{23}\mathrm{cm}^{-2}$ with model dependent variations of up to a factor of ~ 10 (Chen, Gehrels, and Leventhal 1993; Kawai *et al.* 1988; Skinner *et al.* 1991; Sunyaev *et al.* 1991a), indicating that the higher energy ranges of these measurements were insufficient to accurately fit the turnover in the spectrum. Our value from the combined 1992 fall and 1993 spring observations of $N_H = 1.12^{+1.51}_{-0.18} \times 10^{23}$ cm^{-2} is consistent with the Spartan-1 result. Also, the individual observations are consistent with each other, offering no indication of variability in the column depth over the long ($\sim$6 yr) period spanning the observations.

The idea that 1E 1740.7–2942 lies within the dense molecular cloud observed by Bally and Leventhal (1991) and Mirabel et al. (1991) is based on circumstantial and theoretical evidence. Given the line of sight alignment, the association depends on both objects being at the same distance. The normal state hard X–ray luminosity of 1E 1740.7–2942 is similar to that of Cyg X-1, under the assumption that it lies at the distance (8.5 kpc) of the Galactic center. Furthermore, the cloud's Doppler shift and velocity width are consistent with a location near the Galactic center. These facts, taken with the observed alignment, are suggestive of an association, but are by no means conclusive. The column depth to 1E 1740.7–2942 is $\sim$2–3 times greater than that to the Galactic center (see above), indicating that 1E 1740.7–2942 is either absorbed at the source or lies behind additional material – possibly the molecular cloud. Our measurement is consistent with this picture, but does not favor it. Subtracting a Galactic center column depth of 7×10^{22} cm^{-2}, corresponding to $A_v = 30$ mag (Gorenstein 1975; Rieke and Lebofsky 1985), from a range of $(1-2) \times 10^{23}$ cm^{-2} leaves an additional column of $(0.3 - 1.3) \times 10^{23}$ cm^{-2}. An analysis by Churazov *et al.* (1993a), based on residual Compton scattering of hard X–rays from the molecular cloud (under the assumption that 1E 1740.7–2942 lies within the cloud) after a transition to the low state, sets a limit on the column depth due to the cloud of $N_H < 1.6 \times 10^{23}$ cm^{-2}. This is consistent with the excess column calculated above,

but is only an upper limit and so does not require that 1E 1740.7–2942 be located within the cloud.

From a theoretical standpoint, 1E 1740.7–2942's presence in the molecular cloud is attractive because it provides a plausible explanation for several phenomena. First, it could supply the extra column depth required by some measurements. Second, the cloud is a suitable medium for the slowing of energetic pairs present in the radio jets. The positrons, upon stopping, may rapidly annihilate in the relatively dense gas of the cloud, producing narrow 511 keV radiation (Bally and Leventhal 1991). Finally, it is possible that the cloud itself could be the source of matter which powers the hard X–ray luminosity (Bally and Leventhal 1991).

Because of the possibility that material not associated with the cloud might intervene between the source and the observer, the column depth alone cannot determine whether 1E 1740.7–2942 lies within the cloud. However, Bally and Leventhal (1991) estimate from the ^{12}CO emission that the total column depth along the line of sight in a 1′.5 region around the radio source is $\sim 6 \times 10^{23}\mathrm{cm}^{-2}$ ($N_{H_2} \sim 3 \times 10^{23}\mathrm{cm}^{-2}$). The higher resolution maps of HCO^+ from Mirabel *et al.* (1991) suggest that this value should be reasonably representative of the column depth to 1E 1740.7–2942 from which we conclude that 1E 1740.7–2942 is unlikely to be an extragalactic source. If it were, it would be obscured by this entire column and would exhibit much higher absorption of the X–ray spectrum than is observed. Although the column depth is very uncertain, only $\lesssim 3 \times 10^{23}\mathrm{cm}^{-2}$ is required to contradict the X–ray measurements. This strengthens the probabilistic argument that two such strong γ-ray emitters (1E 1740.7–2942 and GRS 1758-258), each associated with the core of a double radio jet source, are unlikely to be located near the center of the Galaxy and yet be extragalactic. If, however, the CO measurement significantly overestimates the column depth (due, for example, to density variations or the location of 1E 1740.7–2942 significantly away from the peak emission) it is still possible that 1E 1740.7–2942 lies behind the cloud.

5.4.3 Comparison with the Hard X–ray State

As mentioned in section 5.2, each of our *ROSAT* observations was preceded or spanned by hard X–ray observations from SIGMA (Cordier, Paul, and Hameury 1993; Mandrou *et al.* 1993; Churazov *et al.* 1993b). Although none of these observations was simultaneous with the *ROSAT* pointings, it is still interesting to look for correlations between the X–ray and hard X–ray fluxes. In order to compare the X–ray state during the HRI observation to that from the PSPC and SIGMA observations, we used MIPS to fold an absorbed thermal bremsstrahlung spectrum (kT = 14.3 keV, $N_H = 1.12 \times 10^{23}$ cm^{-2}, $F_x = 1.5 \times 10^{-10}$ ergs cm^{-2} s^{-1}) through the HRI response. This model predicts only 13 counts for the 1990 observation, $\sim$1/3 the $\sim$40 detected, suggesting that the X–ray luminosity was significantly greater than during the PSPC observations.

Table 5.1 lists 2–10 keV luminosities estimated for the PSPC by integrating a 14.3 keV bremsstrahlung spectrum and for the HRI by scaling from the MIPS predicted count rate. Source states determined from the nearest SIGMA observations are also given. Large uncertainties in the estimated luminosities prevent any strong statement regarding correlations between the X–rays and hard X–rays. However, the HRI and PSPC-I pointings are suggestive that the X–rays and hard X–rays are not strongly correlated. The high luminosity observed in the HRI coincided with the low state observed by SIGMA throughout 1991. PSPC-I also showed a relatively high X–ray flux, but 1E 1740.7–2942 was most likely in the normal state. The lowest observed luminosity was during PSPC-II, when 1E 1740.7–2942 was in the moderate luminosity sub-luminous hard X–ray state.

5.5 Conclusions

We have presented new measurements of the location and X–ray spectrum of 1E 1740.7–2942. The location of the compact core of the aligned radio jets reported by Mirabel *et al.* (1992) lies within the new error circle, strengthening the association of these objects. The column depth is consistent with the best previous measure-

ments. The new measurements cannot confirm the association of 1E 1740.7–2942 with a dense molecular cloud observed at millimeter wavelengths. They do, however, support arguments that 1E 1740.7–2942 must be a Galactic source and is not simply a background galaxy. A comparison of the X–ray luminosity to the hard X–ray state shows no evidence for a correlation between the fluxes in these two bands.

5.6 Acknowledgements

We acknowledge important contributions by Shri Kulkarni in several aspects of this work. This research was supported in part by NASA grants NAG5-1687 and NAGW-1919. W.A.H. is supported under the NASA GSRP, NGT-50804.

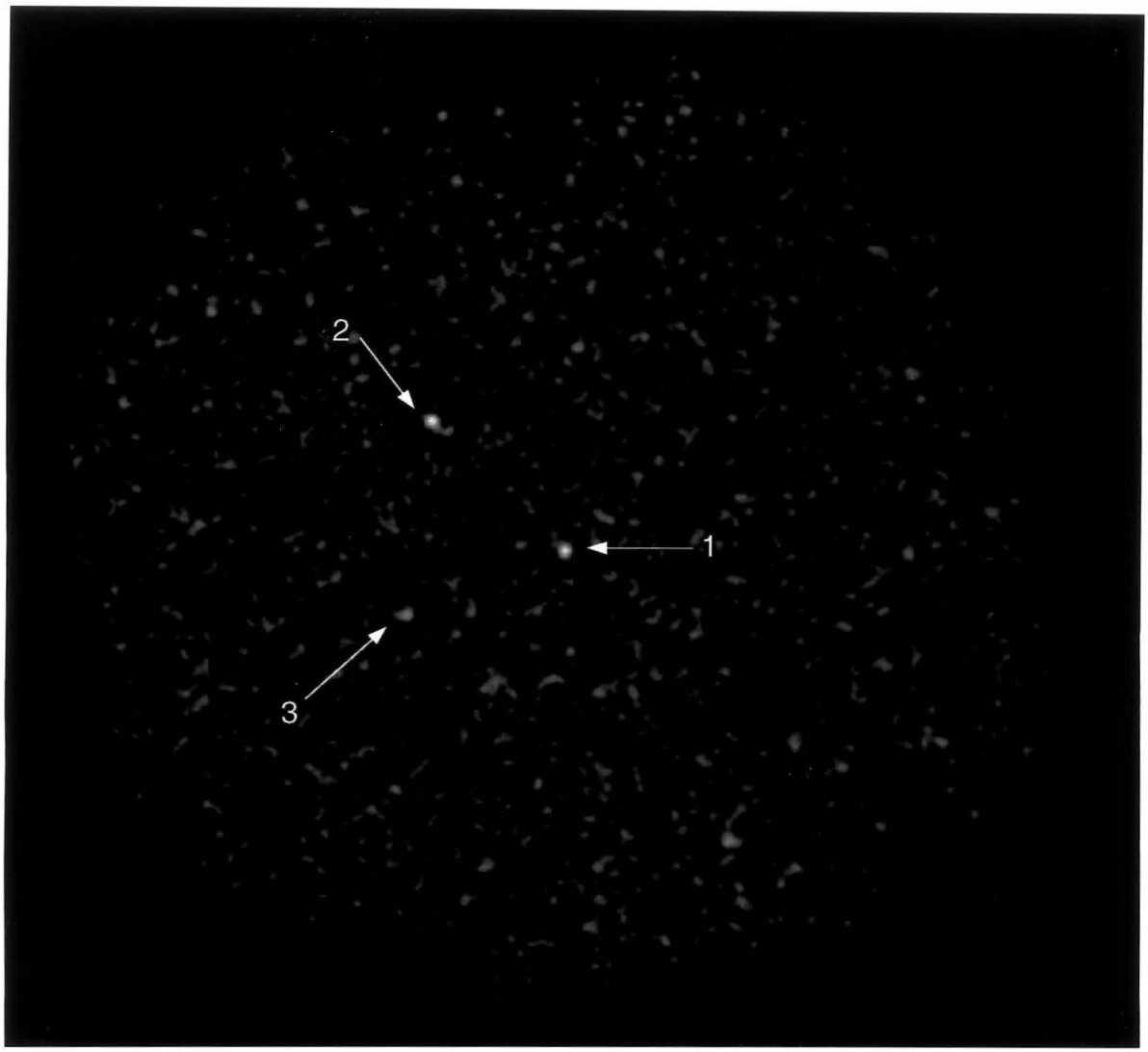

Figure 5.5: Grayscale representation of the *ROSAT* HRI image of 1E 1740.7–2942. Sources are labeled as in Figure 5.1. North is up and east is to the left.

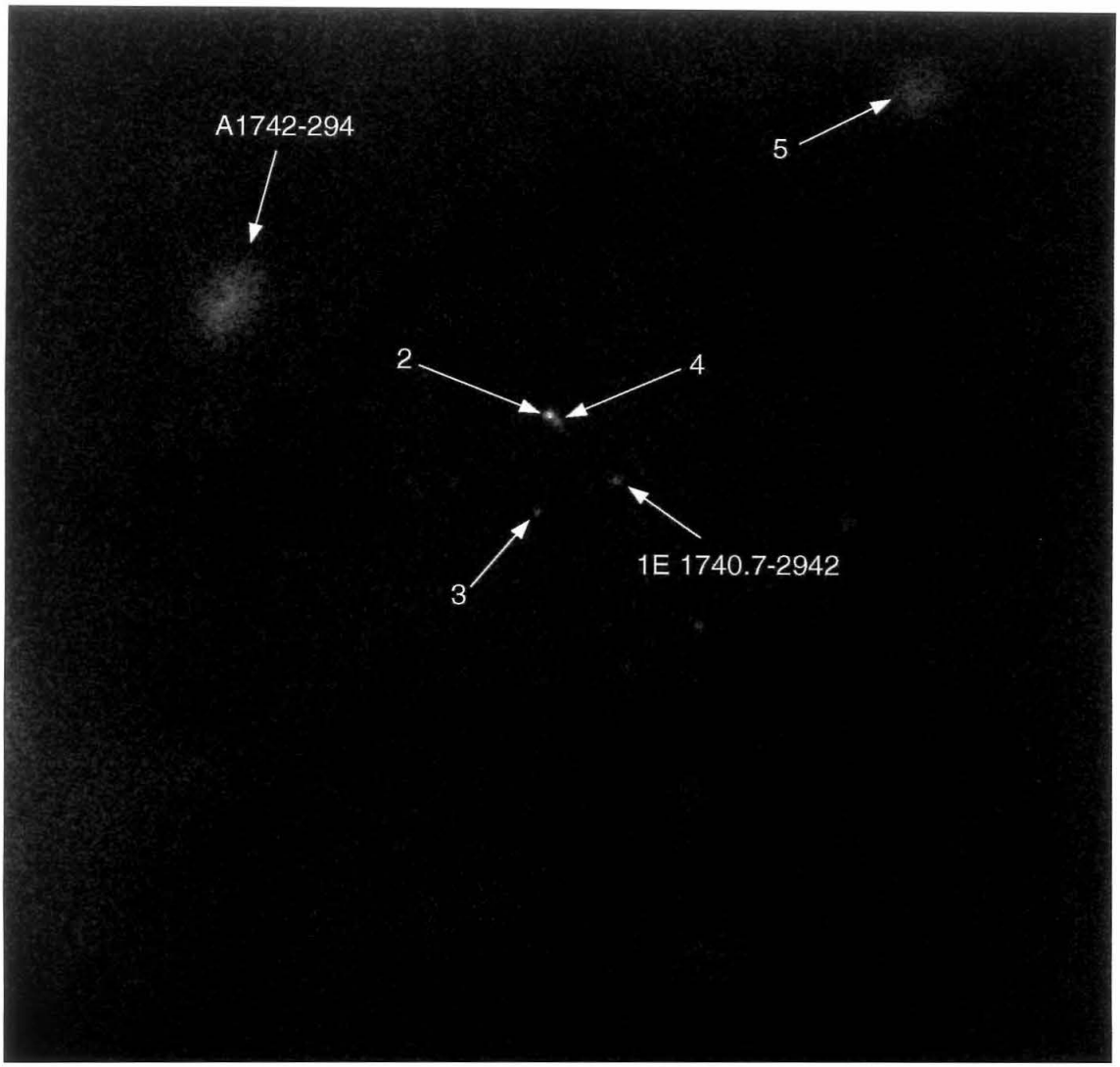

Figure 5.6: Grayscale image of the center of the PSPC field of view. Sources are labeled as in Figure 5.4. North is up and east is to the left.

Chapter 6

Recent γ-Ray Observations: Spectral States of 1E 1740.7-2942

6.1 Recent Observations

Since the NASA balloon campaign of 1989 April–May from Alice Springs, NT, Australia (see Chapter 4), the only imaging or narrow FOV observations of the region at hard X–ray and soft γ-ray energies have been made by the SIGMA and ART-P coded-aperture telescopes on the *GRANAT* spacecraft (e.g., Cordier *et al.* (1993a)) and with coarser resolution at lower sensitivity by BATSE on the *CGRO* (see §8.2.3) (Zhang *et al.* 1993a). Since its launch in 1989 December, *GRANAT* has made long observations during February–April and August–October of each year. These observing windows are set by spacecraft pointing constraints. Long term monitoring has enabled the *GRANAT* team to make in depth studies of the spectrum and temporal behavior of 1E 1740.7–2942. As of 1993 December, a total of five distinct spectral states have been cataloged as well as variability on time scales from days to months (Cordier *et al.* 1993a; Cordier *et al.* 1993c; Churazov *et al.* 1993a). In this chapter, I discuss these states and the 1E 1740.7–2942 flux history.

6.2 The States of 1E 1740.7-2942

In Chapter 4, I described three states of 1E 1740.7–2942. These were the "normal," "hard," and "low" states. The 30 to 200 keV spectrum of all these states varies only in luminosity and not spectral shape, which is always well fit by a Comptonized spectrum with an electron temperature $kT_e \approx 35$ keV and an optical depth $\tau \approx 2$. In the normal state, the 100 keV flux is $\sim 1 \times 10^{-4}\,\mathrm{cm^{-2}\,s^{-1}\,keV^{-1}}$. The low state luminosity is ~20% or less of the normal state. The hard state has 30–200 keV flux similar to the normal state, but is set apart by strong emission between 200 and 600 keV possibly due to e^+e^- annihilations in a hot plasma. In addition to these states, the SIGMA observations have now led to the identification of two new states — a "low-hard" state (Churazov *et al.* 1993c) and a "sub-luminous" state (Cordier *et al.* 1993c) (see table 6.1).

In the low-hard state, the 30–200 keV flux was similar to the low state, but, emission was once again seen at energies above 200 keV. The strength of the hard excess was, however, much lower than in the hard state. This state was relatively short-lived (~10–20 days), observed only during 1991 October 1 – 19, following observations of the low state during 1991 August 30 – September 25. Again, the 30–200 keV spectral shape was similar to that of the normal and low states.

The sub-luminous state appears identical to the normal state, but with 40–150 keV luminosity a factor of ~2.4 lower (Cordier *et al.* 1993c). While the low state luminosity is only ~20% or less of the normal state, often falling below the SIGMA detection limit, the sub-luminous state was consistently detected by SIGMA during 1992 February 17 – April 9 with no evidence of day to day variations apart from a possible slow, monotonic rise in flux.

In §4.1, the high state was described as a transient phenomena seen in only a single SIGMA observation. Since Chapter 4 appeared in *The Astrophysical Journal* (Heindl *et al.* 1993), a second high state outburst has been reported by Cordier *et al.* (1993b). During a 20 hr pointing on 1992 September 19 – 20, SIGMA detected enhanced emission between 200 and ~500 keV, consistent in shape with the 1990 October outburst. The hard X–ray flux between 30 and 200 keV was at the normal

TABLE 6.1

The states of 1E 1740.7–2942.

State		Approximate Luminosity ($\times 10^{37}$ ergs s^{-1})[a]	
SIGMA	Two-component[b]	30 – 200 keV	300 - 600 keV
Normal	Comptonized	2	< 0.6
Sub-luminous	Comptonized	0.8	< 0.6
Low	Comptonized	$\lesssim 0.3$	< 0.8
Hard	hard-excess	2	2 – 4
Low-Hard	hard-excess	0.4	1

[a] Assuming a distance of 8.5 kpc

[b] Classification according to two component source model (§6.3).

state level and was unchanged from measurements made during the week before and 2 days after the outburst. While the shape of the the hard excess was similar to the 1990 event, its flux was lower by about a factor of 2. Table 6.1 summarizes the observed states of 1E 1740.7–2942. Figure 6.1, from Churazov *et al.* (1993a), shows the 5 states of 1E 1740.7–2942 as observed by SIGMA and Figure 6.2 shows the light curve in the 40–150 keV band, with the various emission states indicated at the bottom.

6.3 Discussion

1E 1740.7–2942 was first suggested as a black hole candidate because of the similarity of its normal state spectrum to the γ_2 and γ_3 states of Cyg X-1 (Cook *et al.* 1991b; Sunyaev *et al.* 1991b), which is one of the best candidates for a high-mass Galactic black hole binary system. Not only are the spectra both well fit by a Comptonized spectrum with an electron temperature $kT_e \approx 50$ keV and optical depth $\tau \approx 2$; the hard X–ray luminosities are also very similar, assuming 1E 1740.7–2942 lies at the distance of the Galactic center. This sort of spectrum is not typical of neutron stars. Figure 6.3 shows the GRIP 1988 1E 1740.7–2942 spectrum plotted with the best fit Comptonized spectrum from the *HEAO-3* Cyg X-1 observations from 1979 November (Ling *et al.* 1987), scaled to a distance of 8.5 kpc. The similarity is

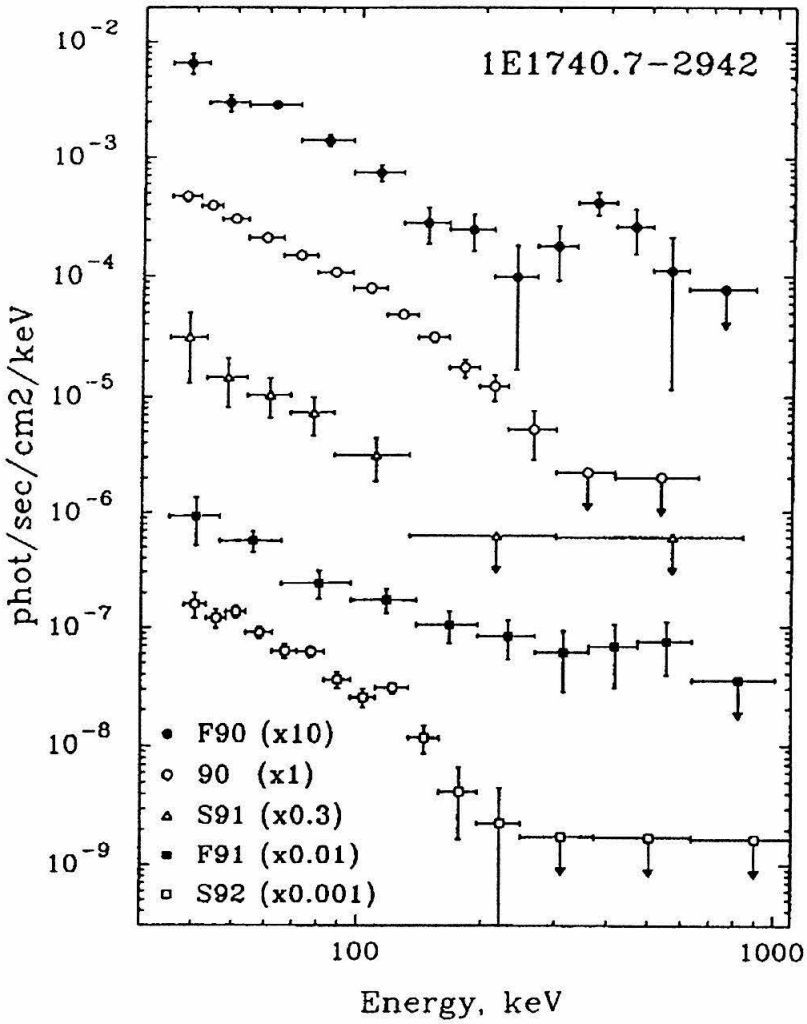

Figure 6.1: From Churazov *et al.* (1993a). Spectral states of 1E 1740.7–2942 as measured by SIGMA. The various states (multiplied by constant factors for clarity) are: "F90" – hard; "90" – normal; "S91" – low; "F91" – low-hard; and "S92" – sub-luminous.

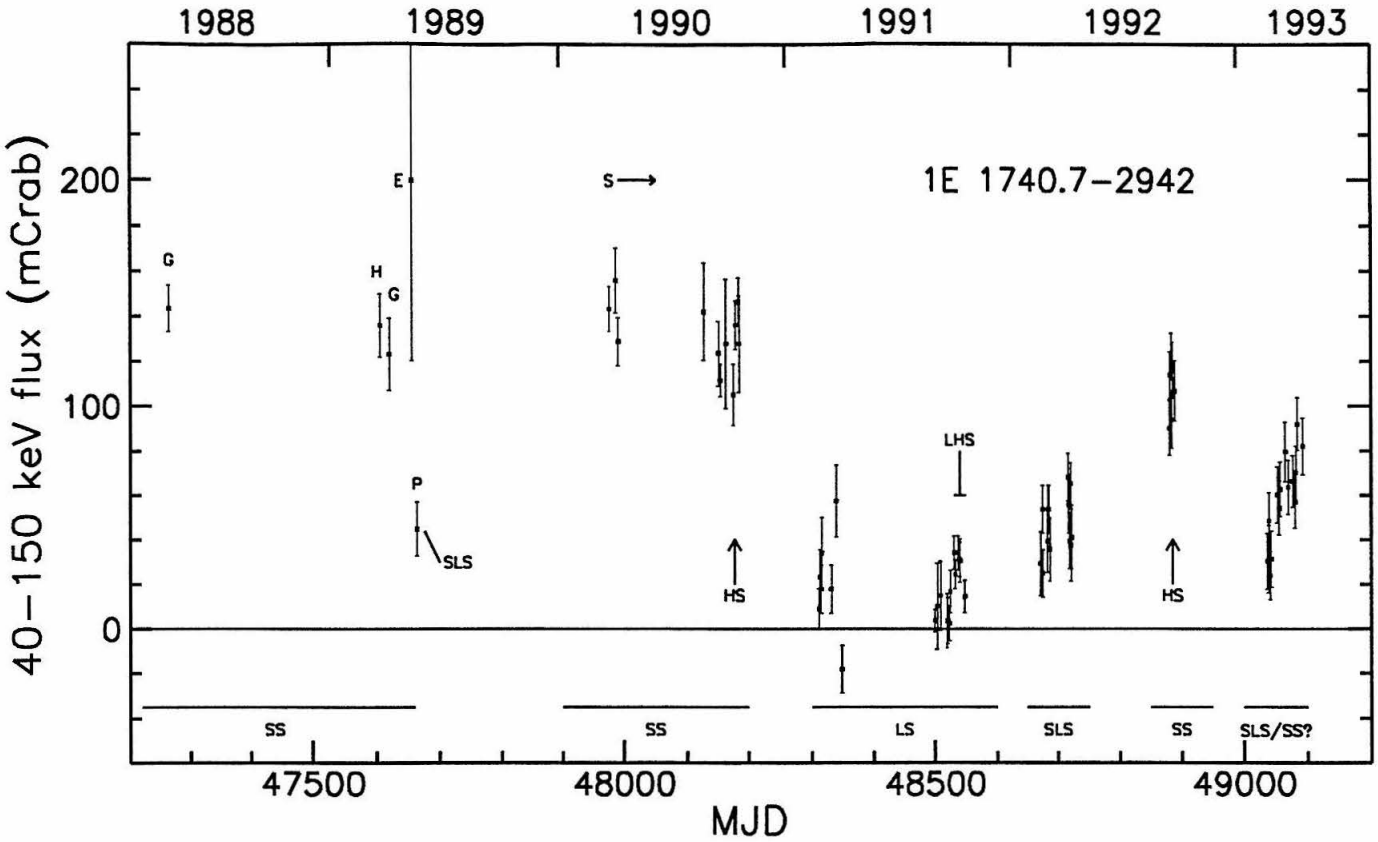

Figure 6.2: The hard X–ray light curve of 1E 1740.7–2942 since 1988. Observations before spring 1990 are: G – GRIP (Cook *et al.* 1991b; Heindl *et al.* 1993); H – HEXE (Skinner *et al.* 1991); and E – EXITE (Grindlay, Covault, and Manandhar 1993). Observations from 1990 on are from S – SIGMA (Churazov *et al.* 1993b; Churazov 1993; Cordier *et al.* 1993b). Different states are indicated by: SS – standard/normal; LS – low; HS – hard; SLS – sub-luminous; and LHS – low-hard. In the two component scheme (see §6.3), variations represent changes in luminosity of the "Comptonized" state rather than actual changes in the emission mechanism. Only the indicated HS and LHS periods represent a fundamental change in the emission.

remarkable, suggesting that the two sources have similar natures.

Both sources have also shown emission above the cutoff in their nominal Comptonized spectra. Because of this excess hard emission, the hard and low-hard states can be compared to the γ_1 state of Cyg X-1 which shows hard emission up to $\sim$2 MeV. Although the 1E 1740.7–2942 hard bump has only been seen to extend to $\sim$600 keV, both phenomena could still be due to e^+e^- annihilations with different plasma temperatures. Based on *HEAO-3* observations of the region in 1979 and 1980, it has been suggested that 1E 1740.7–2942 may also be a variable source of MeV continuum emission (Cook *et al.* 1991b; Laurent and Paul 1994). Because of time variability and the duty cycle and sensitivity of high energy observations, it is plausible that such emission has been missed. In particular, an MeV excess with similar luminosity to the Cyg X-1 γ_1 state would not be detectable by SIGMA (Churazov *et al.* 1993c).

Although 1E 1740.7–2942 and Cyg X-1 are similar in several ways, there are also significant differences. For example, the transitions between the Cyg X-1 states are marked by a pivoting of the spectrum near 400 keV, with the hard emission appearing at the expense of the softer flux (Ling *et al.* 1987). No such behavior is seen in 1E 1740.7–2942, where the 30 – 200 keV emission appears unaffected by the presence of a hard excess. Also, Cyg X-1 is not associated with the core of a radio jet source. The presence of such differences should be kept in mind when comparing 1E 1740.7–2942 to Cyg X-1.

As is the case for Cyg X-1, a two component source model is currently the most generally discussed picture for 1E 1740.7–2942 (Liang and Dermer 1988; Bouchet *et al.* 1991; Sunyaev *et al.* 1991b). In this model, the $<$ 200 keV emission is produced by Comptonization of soft photons by a hot accretion disk, while the hard emission results from e^+e^- annihilations in a hot plasma surrounding a central black hole. This picture suggests that the five spectral states of 1E 1740.7–2942 discussed above may result from independent variations of the two components, rather than changes in the nature of the emission mechanism. In fact, in all five observed states, the 30-200 keV spectral shape of 1E 1740.7–2942 is essentially unchanged. There appear to be only two distinct spectral *shapes* in the soft γ-ray energy band—

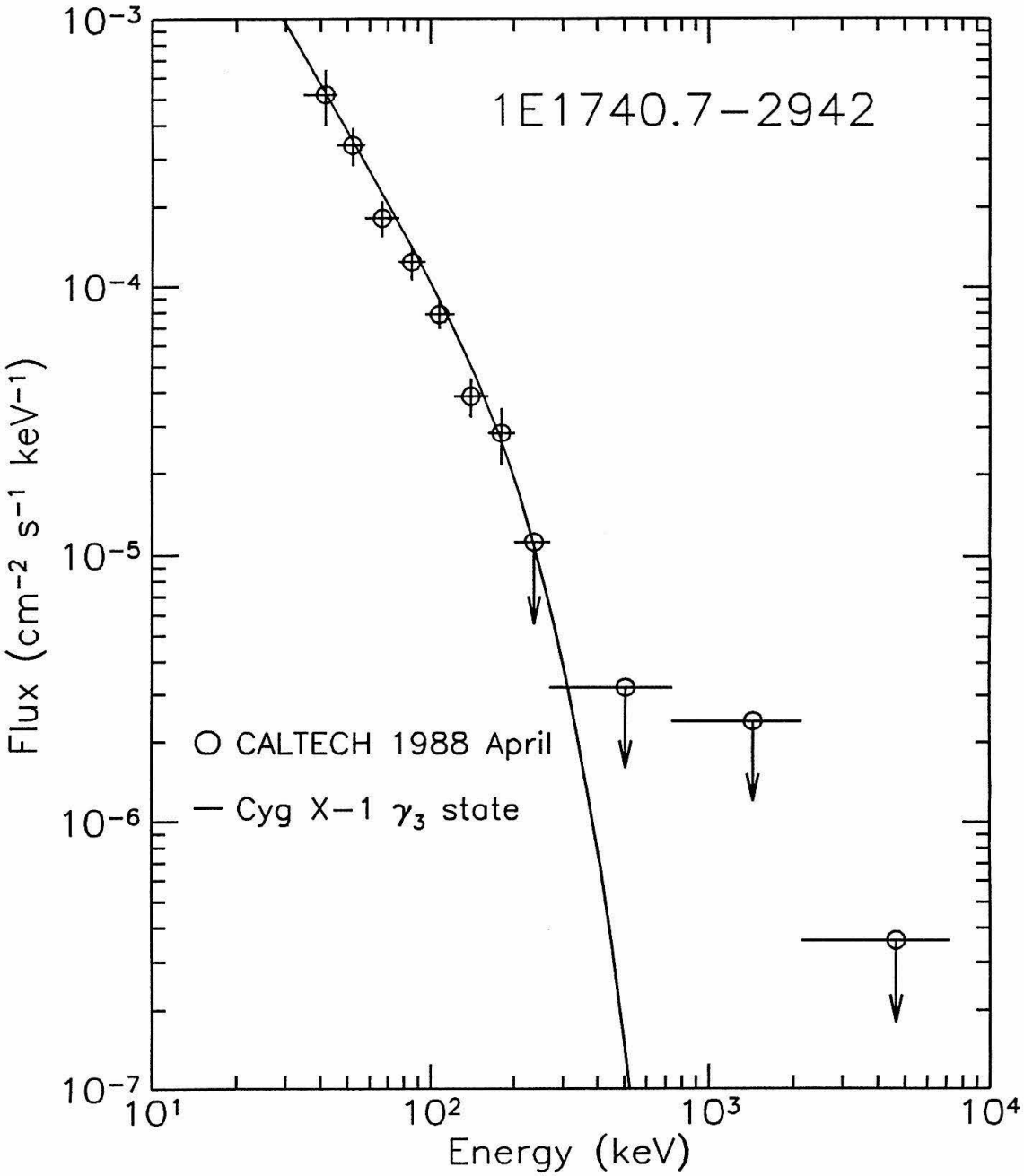

Figure 6.3: The GRIP 1988 spectrum of 1E 1740.7–2942 compared to the γ_3 state of Cyg X-1 (Ling *et al.* 1987) scaled to 8.5 kpc. The spectral fit is a comptonized spectrum with electron temperature, $kT_e = 49.3$ keV and optical depth, $\tau = 2.54$.

one with emission above 200 keV, the other without. The other spectral variations are consistent with changes in luminosity below and above 200 keV. Because of the spectral similarity between the normal, sub-luminous, and low states, and the $<$ 200 keV emission of hard and low-hard states, it seems likely that they are the result of the same physical process occurring at various luminosities.

Because the hard and low-hard states differ from the other states only at energies above 200 keV, their high energy emission is probably caused by an additional, transient phenomena (such as the formation of a pair plasma). The appearance of the hard excess at different flux levels while the Comptonized flux was at the normal level suggests that the two phenomena may be produced independently. The variation of the hard emission between the low and low-hard states can be interpreted similarly. Thus, the hard flux and the $<$ 200 keV emission might result from two separate source components. This fits naturally into a two component emission model, such as that described above. In this case, the five spectral states are more simply categorized in a two state system based on the presence of significant emission above 200 keV. Thus, the low, subluminous, and normal states form one group, while the low-hard and hard states form the second. I will refer to these more basic states as the "Comptonized" and the "hard-excess" states, respectively. If the 1E 1740.7–2942 emission is the result of two components which vary somewhat independently, then this classification more clearly represents the source nature.

The 1E 1740.7–2942 light curve (Figure 6.2) shows no obvious periodicities. It is marked by relatively stable periods in the Comptonized state with brief interruptions by the hard-excess state. The luminosity of the Comptonized state varies from peak to minimum on 6 month or shorter times, while the minimum to peak transitions are more gradual. For example, the simplest interpretation of the fall 1991 through fall 1992 fluxes is that the Comptonized state luminosity gradually increased by a factor of $\sim$5, with the hard-excess state appearing briefly during 1991 fall. The spring 1993 measurements actually seem to show a more rapid, but still smooth, ramping up of flux. In the two component scheme, this variation is interpreted as a continuous luminosity variation of the Comptonized disk component caused, for example, by a variable accretion rate. Because of the more rapid variability of the hard-excess

component, it is likely produced closer to the compact object than the Comptonized component. This is the case in the Cyg X-1 model of Liang and Dermer (1988), where the hard excess is produced by a hot pair plasma surrounding a central, stellar-mass black hole.

Chapter 7

Optical and Infrared Observations

Is 1E 1740.7–2942 in a binary system? There is currently no strong, direct evidence to show that it is. However, its high energy luminosity is almost certainly the result of accretion onto a compact object, and Bondi-Hoyle accretion from the molecular cloud seems an unlikely source of material, as a rather low relative velocity ($\sim$10 km s^{-1}) is required to allow a sufficient mass accretion rate (Mirabel *et al.* 1991; Campana and Mereghetti 1993). In addition, its X–ray and γ-ray emission are very similar to Cyg X-1 (see Chapter 4) which is accreting from its O9.7Iab star companion (Ninkov, Walker, and Yang 1987). Finally, an accretion disk may be necessary to provide collimation for the radio jets, and binary accretion is a natural cause of such a disk. These facts are very suggestive that 1E 1740.7–2942 resides in a binary system.

Detection of a stellar companion to 1E 1740.7–2942 could provide a wealth of new information about its nature. At the most basic level, the type of the companion would show whether this is a high or low mass system. If a bright companion were discovered, Doppler shifts in its spectrum could reveal an orbit, and thus place a limit on the mass of the X–ray source. Other attributes of the spectrum might provide further insight into the X–ray emission. Unfortunately, the location of 1E 1740.7–2942 near the Galactic center – a highly obscured region of the sky – makes chances for the detection of any but the brightest of companions remote and the prospects for spectroscopy even worse.

TABLE 7.1

Limiting magnitudes for companions in optical and infraredwavebands.

Band	Magnitude	Telescope	Date	References
I	21	ESO NTT	10 May 1991	Mereghetti *et al.* (1992)
	21	CFHT	4 June 1991	Leahy *et al.* (1992)
K	17	Hale 5m	21 July 1992	Djorgovsky *et al.* (1992)
	17	ESO 2.2m	16, 17 June 1992	Mirabel and Duc (1992)
L'^1	13*	Hale 5m	21 July 1992	Djorgovsky *et al.* (1992)

Several groups have observed the region surrounding 1E 1740.7–2942 at optical and infrared wavelengths (Prince *et al.* 1991b; Skinner *et al.* 1991; Leahy, Langill, and Kwok 1992; Mereghetti *et al.* 1992; Djorgovski, Thompson, and Mazzarella 1992; Mirabel and Duc 1992). Although several stars appear in the X–ray error circle, none is consistent with the position of the radio source, which has sub-arcsecond accuracy. Nevertheless, the lack of detections provides important constraints on the nature of any companion. Table 7.1 summarizes the observations and current limits on companions in the I, K, and L' bands.

Using these magnitude limits, Chen, Gehrels, and Leventhal (1993) have calculated allowed regions in the H-R diagram for possible companions. For values of the optical extinction, A_v, of 25 and 100, corresponding to column depths of $5 \times 10^{22}\text{cm}^{-2}$ and $2 \times 10^{23}\text{cm}^{-2}$ respectively, they find that, for spectral types later than O, the companion can be no brighter than a giant star of 9 $M_\odot$. The optical/IR limits cannot exclude an O9.7 star as in Cyg X-1; however, such a star located within the molecular cloud, would create an HII region with a λ6 cm flux more than 100 times that of the radio companion to 1E 1740.7–2942. This constrains a companion to later than B2 in the molecular cloud model (Mirabel *et al.* 1991).

While these constraints are useful for constructing models of 1E 1740.7–2942, a wide range of possible companions still exists—including no companion at all.

Chapter 8

Conclusions

8.1 Summary of Past Observations

Through observations made at γ-ray, X–ray, and radio wavelengths, important information has been gained about one of the most luminous hard X–ray sources in our Galaxy. These studies have measured the position, X–ray and γ-ray spectra, and time variability of 1E 1740.7–2942. The most basic results are contributions made to the identification of 1E 1740.7–2942 as a γ-ray and radio source. The discovery that 1E 1740.7–2942, lying $\sim 50'$ from the Galactic center, is a strong high energy emitter is in itself important, because it makes unlikely the theory that Sgr A* was the bright source of hard radiation seen by early instruments. This interpretation of the early observations was favored by those who expected to find a massive black hole at the Galactic nucleus. The radio identification provides an accurate source position for searches at other wavelengths such as optical, infrared, and millimeter.

The GRIP and *ROSAT* observations provided not only positional, but spectral information useful for the interpretation of the source's nature as well. The two GRIP observations helped to define the normal state of 1E 1740.7–2942 and set interesting limits on the variability of the flux on hour time scales. In addition, limits on the strength of the hard state bump and narrow 511 keV emission were set. The *ROSAT* PSPC observation gave new information on the column depth which is important for source models and the interpretation of optical and infrared observations.

TABLE 8.1

Properties of the X–ray source 1E 1740.7–2942

	Property	Chapter(s)
Secure		
	• Association with hard X–ray source	3
	• Association with core of radio jet source	5
	• Association with 200-600 keV outburst source	4,6
	• Celestial coordinates ($\lesssim 1''$)	5
	• Hard X–ray variability on day to month time scales	4,6
	• 30–200 keV spectrum well fit by Comptonized model	3, 4
	• Column depth: $N_H \approx 1 \times 10^{23}\mathrm{cm}^{-2}$	5
Probable		
	• Source of e^+e^-pairs	4, 6
	• Galactic source	5
	• Binary system	4,7
Plausible		
	• Association with molecular cloud	5
	• Source of narrow 511 keV annihilation radiation	4, 6
	• Stellar mass black hole	3, 4, 6

Although extensive (especially at soft γ-ray energies) multiwavelength observations over the last 5 years have shown that the X–ray source 1E 1740.7–2942 is a powerful hard X–ray and γ-ray source, that it may be a source of positron annihilation radiation, that it is a compact radio source at the core of a pair of aligned radio jets, and that it may lie within a dense molecular cloud, the nature of the compact object in 1E 1740.7–2942 remains undetermined. This may well remain the case for some time to come. Since there is no identified optical or infrared counterpart, the most reliable black hole diagnostic — a mass determination — is unavailable. In addition, the prospects for identifying a companion are poor, given the hydrogen column density of $N_H \approx 1 \times 10^{23}$ cm^{-2}, corresponding to an optical extinction of $\sim$45 mag (Gorenstein 1975). Some properties of 1E 1740.7–2942 are listed in Table 8.1 according to the degree to which they are well known. Some properties are quite well determined, others seem likely, but are not confirmed, and others are merely plausible given the current observations.

8.2 Future Observations

An important source of information will soon be lost when the hard X–ray monitoring by SIGMA comes to an end along with the *GRANAT* spacecraft lifetime this spring. However the prospects for new observations are still promising. Two new instruments, GRIP-2 and *ASCA*, as well as BATSE should provide further insights into 1E 1740.7–2942. In addition, monitoring continues at the VLA.

8.2.1 GRIP-2

Since the 1989 balloon flight (see Chapter 4), I have worked with the rest of the GRIP team on the design and construction of a detector system to replace the NaI camera plates and plastic shields in the GRIP gondola (Figure 2.1). The telescope with its new detector is called GRIP-2. The new mask/detector system (shown in Figure 8.1) is optimized for a lower energy range than GRIP (between 30 and 500 keV), but has significant response up to 2 MeV. With a useful area about four times as large as GRIP, GRIP-2 has much better sensitivity over its optimized energy range. It also has a factor of $\sim$2 better angular resolution. Weight reductions achieved through the elimination of the plastic shield along with other structural modifications to the gondola allow GRIP-2 to fly on a larger balloon which reaches higher altitudes. This further improves sensitivity at low energies where the atmosphere is a significant absorber of X–rays. The increased sensitivity will allow GRIP-2 to achieve source detections much more quickly, determine spectra more precisely for a given observation time, and perform variability studies on shorter time scales than GRIP.

These improvements make GRIP-2 a powerful instrument for the study of 1E 1740.7–2942. In particular, GRIP-2 will make high significance spectral measurements, search for variability of the 30-200 keV spectrum on hour and shorter time scales, and be able to rapidly detect the $>$ 200 keV emission from the hard state. GRIP-2 made its first flight in 1993 September from Fort Sumner, New Mexico, USA. During a 40 hr flight, the Galactic center region was observed for $\sim$5 hr. Analysis

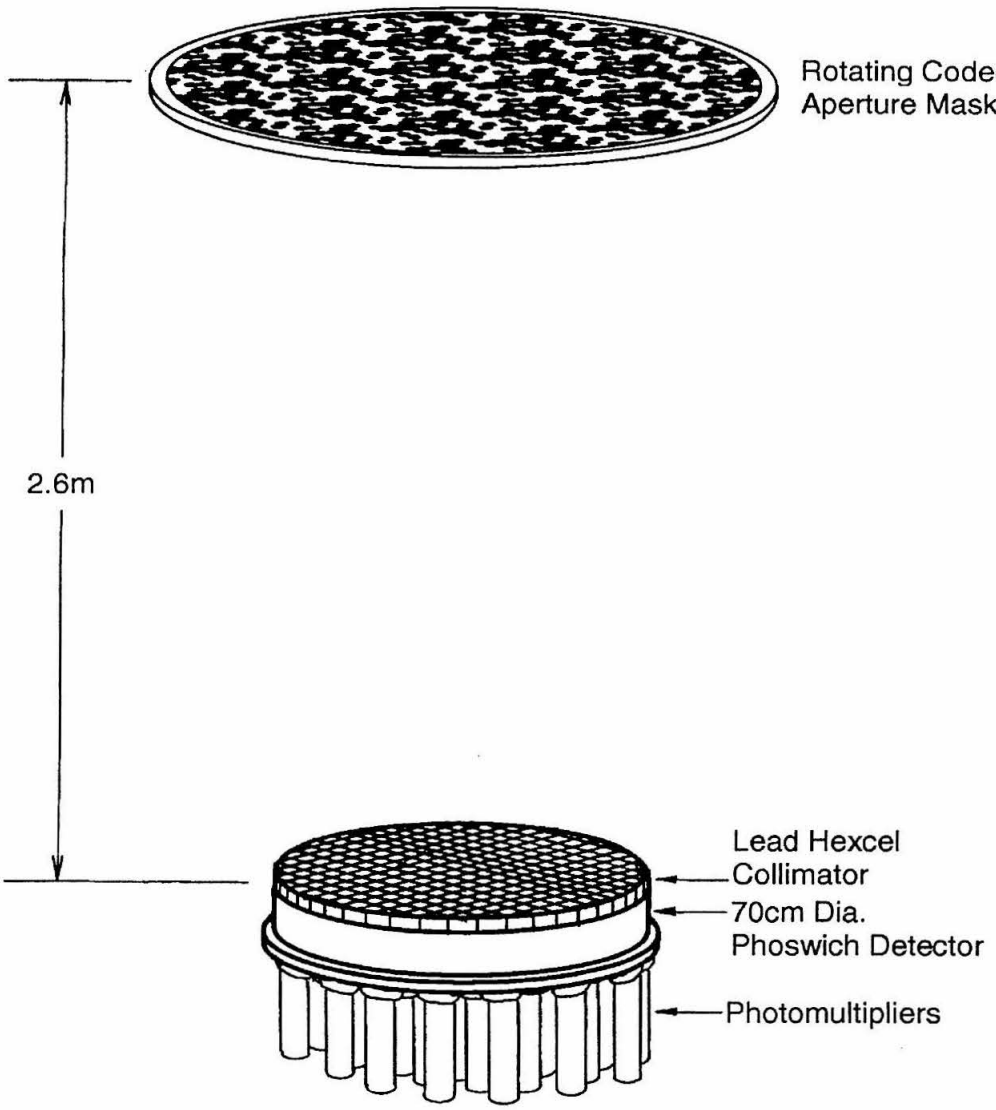

Figure 8.1: Diagram of the GRIP-2 detector system. A new, large area phoswich detector with an integrated CsI(Na) shield has replaced the GRIP primary NaI camera plate, the rear shield, and the bulky plastic shield (see Figure 2.1). The new detector is optimized for observations at and below the 511 keV e^+e^- annihilation line.

of the data from this flight is underway. However, because of the declination of the Galactic center, it is best observed from the southern hemisphere where it transits high in the sky and therefore suffers less atmospheric absorption. For this reason, the data from this flight will not fully show GRIP-2's capabilities for the study of 1E 1740.7–2942.

GRIP-2 will make optimized observations of 1E 1740.7–2942 during a flight from Alice Springs planned for 1995. Based on preflight sensitivity predictions, GRIP-2 will be able to detect the normal state of 1E 1740.7–2942 with $\gtrsim 70\ \sigma$ significance during a single transit ($\sim$8 hr). This will allow for spectral measurements with unprecedented precision on time scales far shorter than those required by SIGMA. One hour of observation will detect 1E 1740.7–2942 at nearly 30 σ significance, so variability studies can be made with shorter time scales and higher precision than those described in Chapter 4. These studies may reveal accretion variability or perhaps orbital modulation which has as yet been undetectable. Finally, GRIP-2 will be capable of detecting the hard state bump at the 3 σ level in $\sim$10 minutes, which could improve the current limits on the size of the emitting region.

8.2.2 *ASCA*

The Japanese/American X–ray telescope *ASCA*, which was launched in 1993 February, has high spectral and time resolution and good sensitivity between 0.5 and 12 keV. It is ideal for new observations of 1E 1740.7–2942, because optimized measurements have not been made in this energy band. *ASCA* will accurately measure the column depth, which is still uncertain (see Chapter 5), and the $\lesssim 12$ keV spectrum. The spectrum in this range is important, as it may show whether 1E 1740.7–2942 exhibits an ultra-soft spectrum and rapid variability ("flickering") similar to other black hole candidates (e.g., Cyg X-1, LMC X-3, and LMC X-1). This energy band also covers the iron K line near 7 keV which has been seen weakly in Cyg X-1 (Marshall *et al.* 1993) and blue-shifted in SS433 (Watson *et al.* 1986), another black hole candidate which produces radio jets. The properties of the iron line are important diagnostics of the emitting region. *ASCA* has already observed 1E 1740.7–2942 in

fall 1993, during the instrument performance verification phase. Results from this observation have not been published at this time. If multiple observations are made, they would provide an X–ray light curve like SIGMA has done in the hard X–rays. Variability of the spectrum in this energy range could also reveal additional similarities to Cyg X-1 which shows both a high X–ray state with an ultrasoft (thermal) spectrum and a low state well fit by a simple power law with a photon index of $\sim$1.7 (Tanaka 1989).

8.2.3 BATSE

The Burst And Transient Source Experiment (BATSE) on the *CGRO* is a powerful instrument for monitoring strong hard X–ray sources. Through earth occultation analysis, BATSE is capable of deriving both images and spectra in the hard X–ray band (Harmon *et al.* 1993; Zhang *et al.* 1993a). BATSE has already imaged the Galactic center and detected 1E 1740.7–2942 during several 50 day integration periods (Zhang *et al.* 1993b). While its one week detection sensitivity of $\sim$50 mCrab is much higher than the $\sim$15 mCrab achieved by SIGMA, BATSE, with its 4π sr FOV, has the advantage of observing the Galactic center region with 1° resolution year round. It is therefore especially useful for monitoring the long term variability and normal hard X–ray state as well as searching for outbursts of 1E 1740.7–2942.

8.2.4 VLA

Finally, monitoring observations are continuing at the VLA. If 1E 1740.7–2942 is Galactic, it is possible that motion of the radio jets will be detected, which would provide new information on their size and properties. These observations could also verify the correlation between the radio and hard X–ray emission.

While the nature of 1E 1740.7–2942 remains a mystery, there are good prospects for new and revealing observations of this enigmatic source.

Bibliography

Althouse, W. E., Cook, W. R., Cummings, A. C., Finger, M. H., Prince, T. A., Schindler, S. M., Starr, C. H., and Stone, E. C. 1985, in *Proc. 19th Intl. Cosmic Ray Conf. (La Jolla)*, volume 3, 299.

Avni, Y. 1976, *ApJ*, **210**, 642.

Bally, J. and Leventhal, M. 1991, *Nature*, **353**, 234.

Basinska, E. M., Lewin, W. H. G., Sztajno, M., Cominsky, L. R., and Marshall, F. J. 1984, *ApJ*, **281**, 337.

Bazzano, A., La Padula, C., Ubertini, P., and Sood, R. K. 1992, *ApJ*, **385**, L17.

Bignami, G. F., Caraveo, P. A., and Mereghetti, S. 1993, *A&AS*, **97**, 229.

Bouchet, L. *et al.* 1991, *ApJ*, **383**, L45.

Bradt, H. V. and McClintock, J. E. 1983, *ARA&A*, **21**, 13.

Bradt, H. V. D., Ohashi, T., and Pounds, K. A. 1992, *ARA&A*, **30**, 391.

Bridle, A. H. 1986, in *Synthesis Imaging*, ed. R. A. Perley, F. R. Schwab, and A. H. Bridle, (Green Bank: NRAO), 253.

Buselli, G., Clancy, M. C., Davison, P. J. N., Edwards, P. J., McCracken, K. G., and Thomas, R. M. 1968, *Nature*, **219**, 1124.

Campana, S. and Mereghetti, S. 1993, *ApJ*, **413**, L89.

Cash, W. 1979, *ApJ*, **228**, 939.

Chapuis, C. G. L. *et al.* 1991, in *AIP Conf. Proc. 232, Gamma-Ray Line Astrophysics (Paris-Saclay)*, ed. P. Durouchoux and N. Prantzos, (New York: AIP), 52.

Chen, W., Gehrels, N., and Leventhal, M. 1993, *ApJ*, **in press**.

Churazov, E. 1993. Private communication.

Churazov, E. *et al.* 1993a, *A&AS*, **97**, 173.

Churazov, E. *et al.* 1993b, in *Proc. 27th ESLAB Symp. (Noordwijk)*, (Paris: ESA), in press.

Churazov, E. *et al.* 1993c, *ApJ*, **407**, 752.

Clark, G. W., Lewin, W. H. G., and Smith, W. B. 1968, *ApJ*, **151**, 21.

Coe, M. J., Engel, A. R., Evans, A. J., and Quenby, J. J. 1981, *ApJ*, **243**, 155.

Cook, W. R., Finger, M., Prince, T. A., and Stone, E. C. 1984, *IEEE Trans. Nucl. Sci.*, **NS-31**, 771.

Cook, W. R., Grunsfeld, J. M., Heindl, W. A., Palmer, D. M., Prince, T. A., Schindler, S. M., Starr, C. H., and Stone, E. C. 1991a, *Adv. Space Res.*, **11**, No. 8, 191.

Cook, W. R., Grunsfeld, J. M., Heindl, W. A., Palmer, D. M., Prince, T. A., Schindler, S. M., and Stone, E. C. 1991b, *ApJ*, **372**, L75.

Cook, W. R., Heindl, W. A., Palmer, D. M., Prince, T. A., Schindler, S. M., Starr, C. H., and Stone, E. C. 1990, in *Proc. 21st Intl. Cosmic Ray Conf. (Adelaide)*, volume 1, 216.

Cook, W. R., Palmer, D. M., Prince, T. A., Schindler, S. M., Starr, C. H., and Stone, E. C. 1989, in *IAU Symp. 136, The Center of the Galaxy*, ed. M. Morris, (Dordrecht:Reidel), 581.

Cordier, B. *et al.* 1993a, *A&AS*, **97**, 177.

Cordier, B. *et al.* 1993b, *A&A*, **275**, L1.

Cordier, B. *et al.* 1993c, *A&A*, **272**, 277.

Cordier, B., Paul, J., and Hameury, J.-M. 1993, in *Integral Workshop*, submitted.

Cordier, B., Roques, J. P., Churazov, E., and Gilfanov, M. 1991, *IAU Circ.*, No. 5377.

Covault, C. E., Manandhar, R. P., and Grindlay, J. E. 1990, in *Proc. 22nd Intl. Cosmic Ray Conf. (Dublin)*, volume 1, 21.

Dennis, B. R., Beall, J. H., Cutler, E. P., Crannell, C. J., Dolan, J. F., Frost, K. J., and Orwig, L. E. 1980, *ApJ*, **236**, L49.

Djorgovski, S., Thompson, D., and Mazzarella, J. 1992, *IAU Circ.*, No. 5596.

Elsner, R. F., Weisskopf, M. C., Apparao, K. M. V., Darbro, W., Ramsay, B. D., Williams, A. C., Grindlay, J. E., and Sutherland, P. G. 1985, *ApJ*, **297**, 288.

Fenimore, E. E., Klebesadel, R. W., and Laros, J. G. 1983, *Adv. Space Res.*, **3**, 207.

Finger, M. H. 1987. Ph.D. dissertation, California Institute of Technology.

Finger, M. H. and Prince, T. A. 1985, in *Proc. 19th Intl. Cosmic Ray Conf. (La Jolla)*, volume 3, 295.

Forman, W., Jones, C., Cominsky, L., Julien, P., Murray, S., Peters, G., Tananbaum, H., and Giacconi, R. 1978, *ApJS*, **38**, 357.

Friedman, H., Byram, E. T., and Chubb, T. A. 1967, *Science*, **156**, 374.

Gehrels, N. 1991, in *AIP Conf. Proc. 232, Gamma-Ray Line Astrophysics (Paris-Saclay)*, ed. P. Durouchoux and N. Prantzos, (New York: AIP), 3.

Gehrels, N., Barthelmy, S. D., Teegarden, B. J., Tueller, J., Leventhal, M., and MacCallum, C. J. 1990, *BAPS*, **35 (4)**, 1081.

Gehrels, N., Barthelmy, S. D., Teegarden, B. J., Tueller, J., Leventhal, M., and MacCallum, C. J. 1991, *ApJ*, **375**, L13.

Gilfanov, M., Churazov, E., Claret, A., and Dezalay, J. P. 1992, *IAU Circ.*, No. 5474.

Gilfanov, M. *et al.* 1989, in *Proc. 23rd ESLAB Symp. (Bologna)*, ed. N. White, volume 1, (Paris: ESA), 71.

Gorenstein, P. 1975, *ApJ*, **198**, 95.

Gray, A. D., Cram, L. E., and Ekers, R. D. 1992, *MNRAS*, **256**, 277.

Grindlay, J. E., Covault, C. E., and Manandhar, R. P. 1993, *A&AS*, **97**, 155.

Grindlay, J. E. and Hertz, P. 1981, *ApJ*, **247**, L17.

Grunsfeld, J., Cook, W., Heindl, W., Palmer, D., Prince, T., and Schindler, S. 1991, in *Proc. 28th Yamada Conf., Frontiers of X-Ray Astronomy (Nagoya)*, ed. Y. Tanaka and K. Koyama, (Tokyo: Universal Academy Press), 417.

Guo, D. D., Webber, W. R., and Damle, S. V. 1973, in *Proc. 13th Intl. Cosmic Ray Conf. (Denver)*, volume 5, 3044.

Harmon, B. A. *et al.* 1993, in *AIP Conf. Proc. No. 280, Compton Gamma-Ray Observatory*, ed. M. Friedlander, N. Gehrels, and D. J. Macomb, (New York: AIP), 314.

Haymes, R. C., Ellis, D. V., Fishman, G. J., Kurfess, J. D., and Tucker, W. H. 1968, *ApJ*, **151**, L9.

Haymes, R. C., Walraven, G. D., Meegan, C. A., Hall, R. D., Djuth, F. T., and Shelton, D. H. 1975, *ApJ*, **201**, 593.

Heindl, W. A., Cook, W. R., Grunsfeld, J. M., Palmer, D. M., Prince, T. A., Schindler, S. M., and Stone, E. C. 1993, *ApJ*, **408**, 507.

Heindl, W. A., Prince, T. A., and Grunsfeld, J. M. 1994, *ApJ*, **in press**.

Hertz, P. and Grindlay, J. E. 1984, *ApJ*, **278**, 137.

Hoffman, J. A., Lewin, W. H. G., and Doty, J. 1977, *MNRAS*, **179**, 57P.

Hoffman, J. A., Lewin, W. H. G., Doty, J., Hearn, D. R., Clark, G. R. W., Jernigan, G., and Li, F. K. 1976, *ApJ*, **210**, L13.

Johnson, W. N., Harnden, Jr., F. R., and Haymes, R. C. 1972, *ApJ*, **172**, L1.

Johnson, W. N. and Haymes, R. C. 1973, *ApJ*, **184**, 103.

Jung, G. V. 1989, *ApJ*, **338**, 972.

Kawai, N., Fenimore, E. E., Middleditch, J., Cruddace, R. G., Fritz, G. G., Snyder, W. A., and Ulmer, M. P. 1988, *ApJ*, **330**, 130.

Kürster, M. and Hasinger, G. 1992. Determination of boresight offsets for ROSAT detectors. Technical Report TN-ROS-ME-ZA00/028, Max Planck Institut für Extraterrestrische Physik.

Knight, F. K., Johnson, W. N., Kurfess, J. D., and Strickman, M. S. 1985, *ApJ*, **290**, 557.

Lampton, M., Margon, B., and Bowyer, S. 1976, *ApJ*, **208**, 177.

Laurent, P. and Paul, J. 1994, *ApJS*, **in press**.

Leahy, D. A., Langill, P., and Kwok, S. 1992, *A&A*, **259**, 209.

Leventhal, M. 1973, *ApJ*, **183**, L147.

Leventhal, M., MacCallum, C. J., Barthelmy, S. D., Gehrels, N., Teegarden, B. J., and Tueller, J. 1989, *Nature*, **339**, 36.

Leventhal, M., MacCallum, C. J., Huters, A. F., and Stang, P. D. 1982, *ApJ*, **260**, L1.

Leventhal, M., MacCallum, C. J., Huters, A. F., and Stang, P. D. 1986, *ApJ*, **302**, 459.

Leventhal, M., MacCallum, C. J., and Stang, P. D. 1978, *ApJ*, **225**, L11.

Levine, A. M. *et al.* 1984, *ApJS*, **54**, 581.

Lewin, W. H. G., Ricker, G. R., and McClintock, J. E. 1971, *ApJ*, **169**, L17.

Liang, E. P. and Dermer, C. D. 1988, *ApJ*, **325**, L39.

Ling, J. C., Mahoney, W. A., Wheaton, W. A., and Jacobson, A. S. 1987, *ApJ*, **321**, L117.

Lingenfelter, R. E. and Ramaty, R. 1982, in *AIP Conf. Proc. No. 83, The Galactic Center*, ed. G. R. Riegler and R. D. Blandford, (New York: AIP), 148.

Lingenfelter, R. E. and Ramaty, R. 1989, *ApJ*, **343**, 686.

Mahoney, W. A. 1988, in *AIP Conf. Proc. No. 170, Nuclear Spectroscopy of Astrophysical Sources*, ed. N. Gehrels and G. H. Share, (New York: AIP), 149.

Makishima, K. *et al.* 1988, *Nature*, **333**, 746.

Manchanda, R. K. 1988, *Ap&SS*, **150**, 31.

Mandrou, P. 1990, *IAU Circ.*, No. 5032.

Mandrou, P. *et al.* 1993, in *Integral Workshop*, submitted.

Mandrou, P., Roques, J. P., Sunyaev, R., Churazov, E., Paul, J., and Cordier, B. 1990, *IAU Circ.*, No. 5140.

Marshall, F. E., Mushotzky, R. F., Petre, R., and Serlemitsos, P. J. 1993, *ApJ*, **419**, 301.

Matteson, J. 1978, in *Proc. AIAA 16th Aerospace Sci. Mtg.*, 78–35, Offprint.

Matteson, J. *et al.* 1989, *IAU Circ.*, No. 4889.

Matteson, J. L. 1982, in *AIP Conf. Proc. No. 83, The Galactic Center*, ed. G. R. Riegler and R. D. Blandford, (New York: AIP), 109.

McClintock, J. E. and Leventhal, M. 1989, *ApJ*, **346**, 143.

Mereghetti, S., Caraveo, P., Bignami, G. F., and Belloni, T. 1992, *A&A*, **259**, 205.

Mirabel, I. F. and Duc, P. A. 1992, *IAU Circ.*, No. 5655.

Mirabel, I. F., Morris, M., Wink, J., Paul, J., and Cordier, B. 1991, *A&A*, **251**, L43.

Mirabel, I. F., Rodriguez, L. F., Cordier, B., Paul, J., and Lebrun, F. 1992, *Nature*, **358**, 215.

Mirabel, I. F., Rodriguez, L. F., Cordier, B., Paul, J., and Lebrun, F. 1993, *A&AS*, **97**, 193.

Mony, B. *et al.* 1989, in *Proc. 23rd ESLAB Symp. (Bologna)*, ed. N. White, volume 1, (Paris: ESA), 541.

Ninkov, Z., Walker, G. A. H., and Yang, S. 1987, *ApJ*, **321**, 425.

Paciesas, W. S., Cline, T. L., Teegarden, B. J., Tueller, J., Durouchoux, P., and Hameury, J. M. 1982, *ApJ*, **260**, L7.

Palmer, D. M. 1992. Ph.D. dissertation, California Institute of Technology.

Palmer, D. M., Schindler, S. M., Cook, W. R., Grunsfeld, J. M., Heindl, W. A., Prince, T. A., and Stone, E. C. 1993, *ApJ*, **412**, 203.

Paul, J. *et al.* 1991, in *AIP Conf. Proc. 232, Gamma-Ray Line Astrophysics (Paris-Saclay)*, ed. P. Durouchoux and N. Prantzos, (New York: AIP), 17.

Peterson, L. E., Jacobson, A. S., Pelling, R. M., and Schwartz, D. A. 1968, *Canadian Journal of Physics*, **46**, S437.

Prince, T., Grunsfeld, J., Gorham, P., Neugebauer, G., Johnson, N., and Skinner, G. 1991a, *BAAS*, **23**, 1392.

Prince, T., Skinner, G., Kulkarni, S., Matthews, K., and Neugebauer, G. 1991b, *IAU Circ.*, No. 5252.

Purcell, W. R., Grabelsky, D. A., Ulmer, M. P., Johnson, W. N., Kinzer, R. L., Kurfess, J. D., Strickman, M. S., and Jung, G. V. 1993, *ApJ*, **413**, L85.

Ricker, G. R., Gerassimenko, M., McClintock, J. E., Ryckman, S. G., and Lewin, W. H. G. 1976, *ApJ*, **207**, 333.

Riegler, G. R., Boldt, E., and Serlemitsos, P. 1968, *ApJ*, **153**, L95.

Riegler, G. R., Ling, J. C., Mahoney, W. A., Wheaton, W. A., and Jacobson, A. S. 1985, *ApJ*, **294**, L13.

Riegler, G. R., Ling, J. C., Mahoney, W. A., Wheaton, W. A., Willett, J. B., Jacobson, A. S., and Prince, T. A. 1981, *ApJ*, **248**, L13.

Rieke, G. H. and Lebofsky, M. J. 1985, *ApJ*, **288**, 618.

Sakao, T. *et al.* 1990, *MNRAS*, **246**, 11P.

Schmitz-Fraysse, M. C., Cordier, B., Gilfanov, M., and Churazov, E. 1992, *IAU Circ.*, No. 5472.

Shafer, R. A., Haberl, F., Arnaud, K. A., and Tennant, A. F. 1990, *XSPEC: An X-Ray Spectral Fitting Package*, (Greenbelt: NASA/GSFC), 2nd edition.

Share, G. H., Kinzer, R. L., Kurfess, J. D., Messina, D. C., Purcell, W. R., Chupp, E. L., Forrest, D. J., and Reppin, C. 1988, *ApJ*, **326**, 717.

Sharma, D. P. *et al.* 1990, in *Proc. 21st Intl. Cosmic Ray Conf. (Adelaide)*, volume 1, 32.

Skinner, G. K. 1984, *NIM*, **221**, 33.

Skinner, G. K. *et al.* 1991, *A&A*, **252**, 172.

Skinner, G. K. *et al.* 1987, *Nature*, **330**, 544.

Skinner, G. K., Willmore, A. P., Foster, A. J., and Eyles, C. J. 1989, in *Gamma-Ray Observatory Science Workshop*, ed. W. N. Johnson, (Greenbelt: NASA/Goddard Space Flight Center), 4–191.

Sunyaev, R. *et al.* 1991a, in *AIP Conf. Proc. 232, Gamma-Ray Line Astrophysics (Paris-Saclay)*, ed. P. Durouchoux and N. Prantzos, (New York: AIP), 29.

Sunyaev, R. and the *GRANAT* team 1990, *IAU Circ.*, No. 5104.

Sunyaev, R. *et al.* 1991b, *ApJ*, **383**, L49.

Sunyaev, R. A. and Titarchuk, L. G. 1980, *A&A*, **86**, 121.

Tanaka, Y. 1989, in *Proc. 23rd ESLAB Symp. (Bologna)*, ed. N. White, volume 1, (Paris: ESA), 3.

Trümper, J. 1984, *Physica Scripta*, **T7**, 209.

Trümper, J. 1992. in the ROSAT calendar, July, (Garching: MPE).

Tueller, J. 1993, in *AIP Conf. Proc. No. 280, Compton Gamma-Ray Observatory*, ed. M. Friedlander, N. Gehrels, and D. J. Macomb, (New York: AIP), 97.

van Paradijs, J. 1993, in *X-ray Binaries*, ed. W. H. G. Lewin, J. van Paradijs, and E. P. J. van den Heuvel, (Cambridge: University Press), in press.

Watson, M. G., Stewart, G. C., Brinkmann, W., and King, A. R. 1986, *MNRAS*, **222**, 261.

Watson, M. G., Willingale, R., Grindlay, J. E., and Hertz, P. 1981, *ApJ*, **250**, 142.

Zhang, S. N., Fishman, G. J., Harmon, B. A., and Paciesas, W. S. 1993a, *Nature.* in press.

Zhang, S. N., Fishman, G. J., Harmon, B. A., Paciesas, W. S., Rubin, B. C., Meegan, C. A., Wilson, R. B., and Finger, M. H. 1993b, in *Proc. Second Compton Symposium*, in press.